An Ensemble Recruited by Alpha$_{2a}$-Adrenergic Receptors is Engaged in a Stressor-Specific Manner in Mice

By

Jordan Brown

Dissertation

Submitted to the Faculty of the

Graduate School of Vanderbilt University

in partial fulfillment of the requirements

for the degree of

DOCTOR IN PHILOSOPHY

In

Pharmacology

December 17, 2022

Nashville, Tennessee

Approved by:

Brad A. Grueter, Ph.D. (Chair)

Lisa Monteggia, Ph.D.

Erin Calipari, Ph.D.

Richard Simerly, Ph.D.

Danny G. Winder, Ph.D. (Thesis Advisor)

DEDICATION

For my mother, my lifelong cheerleader
For my father, for my sense of humor and taste of music
For my sister, the smartest woman I know
For my husband, for being by my side and supporting me every step of the way.
For my dogs Sukie and Izzie (and Paddington)

ACKNOWLEDGEMENTS

This work would not have been possible with our funding sources, especially the Howard Hughes Medical Institute (HHMI). The Gilliam fellowship introduced me to an amazing group of scientists and made me feel like I belonged in science, and I will always be grateful for the opportunity I was awarded. This work was also funded by Dr. Winder's grant from the National Institute on Drugs of Abuse (NIDA).

I would like to thank my mentor, Danny Winder, for his constant support and mentorship. You are one of the kindest and most patient mentors I have ever had. Thank you for your support when I decided that academia was not the path for me. I appreciate the time you took to make sure I was following the path I wanted to take. I want to thank my committee members Dr. Erin Calipari, Dr. Richard Simerly, Dr. Lisa Monteggia, and Dr. Brad Grueter for their advice and support during my thesis work. I am very grateful for all that you have done for my career. Thank you for pushing me to be the best scientist I could be and making me feel like I could accomplish anything. I especially want to thank my chair, Dr. Brad Grueter, for believing in me and convincing me I could accomplish what I set out to do despite the initial bumpy road in my graduate career.

I would like to thank the current and previous Winder lab members. I especially want to thank Dr. Sam Centanni for constantly being someone I could bounce ideas off of or get advice from. I would not have been able to complete my thesis work without your unofficial mentorship. I want to thank Dr. Anel Jaramillo for her constant support and entertainment, I will cherish your jokes forever. I want to thank Kellie Williford for being a constant source of ideas and support, striving to reach your levels of achievements made me a better scientist and person. I want to thank Nick Petersen and Brett Nabit for bringing life and entertainment to our lab, I'll miss being your bay neighbor. I also want to thank the best undergraduate turned friend, Allie Jin, for all your help with my experiments. I enjoyed teaching you science, and I'm so glad our dogs are now best friends. I want to thank my other undergraduates, Grace Rieniets and Benjamin Akande. I want to thank the rest of the Winder lab Dr. Marie Doyle, Danielle Adank, Ritka Raghavan and Anne Taylor. I want to thank previous lab members Dr. Bob Matthews, Dr. James Melchoir, Dr. Oliver Vranjkovic, Dr. Joseph Luchsinger, and Dr. Greg Salimando. I especially want to thank Dr. Tracy Fetterly, Dr. Nick Harris and Dr. Rafael Perez for laying the foundation of my thesis work. I want to thank Bridget Morris, Elana Milano, Megan Altemus and Laith Kayat for their help maintaining the mouse colony and lab. I also want to thank our collaborators Dr. Michelle Bedenbaugh, Dr. Richard Simerly, Stephanie Cajias, Kristine Yoon and Dr. Erin Calipari. Our paper could not have reached such a high level of scientific achievement without your assistance. It has been an absolute pleasure to work with each and every one of you and I wish you all the best in your future endeavors.

I want to thank the Pharmacology department including Dr. Christine Konradi, Dr. Sean Davies, and Bobbi Stidham. I also want to thank our previous coordinator, Karen Gieg for all of her help during my first few years in the department.

Finally, I would like to thank my friends and family. To Bella, Brenna and Danielle, meeting you has been one of the greatest things to happen during graduate school, and I look forward to our lifelong friendship. Thank you to my mom, my lifelong cheerleader, for all your support. Thank you to my dad for always making me laugh and being supportive of everything I chose to do. Thank you for giving me a great taste for music by introducing me to the Beatles and Bob Dylan at a young age. Thank you to my sister for our sisterly rivalry that is always pushing me to be the smartest person I could be. Thank you to my husband, Cameron, I couldn't have made it through graduate school without you. Thank you for being the best dad to our animals and making me laugh all the time (even if it's at my expense). I can't wait to spend the rest of our lives together. Thank you to my dogs, Izzie and Sukie, for always happily greeting me at home and making me feel better when I was stressed. Thank you to my cat, Paddington, for converting me to a cat person.

TABLE OF CONTENTS

LIST OF FIGURES

Chapter 1

Chapter 2

CHAPTER 1

Introduction

Portions of this introductory chapter are adapted from BNST Circuits and Addiction published in The Neurocircuitry of Addiction (Centanni, S.W., Brown, J.A., Williford, K.M., Luchsinger J.R., Flook E.A., Winder D.G., 2022) and Danger and distress: Parabrachial-extended amygdala circuits published in Neurpharmacology (Jaramillo, A.A., Brown, J.A., Winder, DG. 2021)

1.1 The pathophysiology of stress

Stress is an unavoidable part of human existence, and a person's adaptability and resiliency determine the long-term effects of stress on mental health. While stress can occasionally be seen as a challenge and beneficial when overcome, repeated and unpredictable stress has been shown to consistently be detrimental to mental health (Sinha, 2008). How and when is this determined and what makes some individuals more susceptible to the effects of stress?

The human body is primed to respond to physical and mental stress with activation of the hypothalamic-pituitary-adrenal (HPA) axis leading to release of corticosteroid hormones. However, it is unknown when the effects of stress becoming detrimental and result in anxiety or stress disorders. Exposure to stress and the body's ability to respond is conserved across evolution and can be seen across the entire animal kingdom. Whether it is primal such as facing an animal predator or complex such as financial insecurity, various stressors of differing magnitude activate the body's stress response. Variations in stressors do exist and can be acute or chronic, foreseen, or unexpected, mild or severe, and the perception of the level of stress can differ across individuals (Lucassen et al., 2014).

The response to stress is often characterized as two waves dependent on timed response (Lucassen et al., 2014). The immediate response involves activation of the peripheral nervous system including the autonomic nervous system, what is often termed the "fight or flight" response. Activation of this system increases release of adrenaline and noradrenaline from the adrenal medulla and results in downstream increases in metabolic rate, blood pressure, respiration and blood flow to vital organs (Lucassen et al., 2014). The slower neuroendocrine response to stress activates the paraventricular nucleus of the thalamus (PVN) and results in downstream release of adrenocorticotropic

hormone (ACTH) from the anterior pituitary gland and glucocorticoids from the adrenal cortex. Glucocorticoid hormones act in a slower manner and result in alterations of glucocorticoid responsive genes (Lucassen et al., 2014).

Originally it was thought that the pathophysiological responses to stress only occurred in response to chronic stress, while the effects of acute stress were assumed to be transient. In the last few decades, studies have shown that even a single exposure to stress can have lasting effects (Armario et al., 2004; Li and Sawchenko, 1998; Ma and Aguilera, 1999; Schmidt et al., 1995, 2001, 1996; van Dijken et al., 1993; Van Dijken et al., 1992). Various stressors including restraint stress or forced swim are used to study the effects of stress in mouse models. Data has shown that repeated stress results in hindrance of adaptations and resilience, and often leads to heightened stress responses that are dependent on the type of stressor (Armario et al., 2004; Martí and Armario, 1998). Physiological response to stress is heightened or attenuated depending on prior stress exposure. Specifically, repeated exposure to a similar stressor results in habituation and decreased HPA activation. This attenuation was heightened with increased time in between stressors and was correlated with strength of stressor (Armario et al., 2004). Exposure to a second novel stressor resulted in only a slight desensitization in HPA axis activation.

Furthermore, stress is cited as a common risk factor for the development of substance use disorder (SUD) as well as a major cause of relapse to drug seeking behavior (Sinha, 2008, 2007, 2001). For example, adolescents with exposure to stressful life events, including childhood sexual and physical abuse or even parental divorce, have increased likelihood of developing SUDs (Barrett and Turner, 2006; Clark, 2003; Clark et al., 1997; Dembo et al., 1988; Douglas et al., 2010; Harrison et al., 1997; Khoury et al., 2010; Mingione et al., 2012; Perkins, 1999; Sher et al., 1997; Wills et al., 1992). Anxiety and mood disorders, including post-traumatic stress disorder (PTSD) have also been shown to increase chances of developing SUDs (Brady and Sinha, 2005; Grant et al., 2015; Kandel et al., 1997; Kessler et al., 1996; King et al., 1996).

1.2 The interplay of stress and addiction

Drug addiction is a highly prevalent chronic relapsing brain disorder, often described in three cycles or stages including preoccupation/anticipation, binge/intoxication, and withdrawal/negative affect (Koob, 2008; Zorrilla et al., 2014; Koob and Volkow, 2010). The cyclic nature of addiction is one of the large barriers for treatment. Additionally,

each cycle is increased in intensity often resulting in a shift from impulsive to compulsive and positive to negative reinforcement of drug seeking behavior. There are at least three major triggers for reinstating drug seeking behavior: exposure to the drug (drug-induced reinstatement), drug associated cues (cue-induced reinstatement) and exposure to stressors (stress-induced reinstatement) (McReynolds et al., 2014a; Silberman and Winder, 2013). Efforts can be taken to minimize exposure to the previously taken drug or drug associated cues, unlike stress, which is an often unavoidable part of human life, making it an ideal target for drug relapse prevention therapy. Stress and addiction are very intertwined and can affect predisposition and treatment of drug addiction. Early life or chronic stress increases the risk of addiction many drugs of abuse (Sinha, 2008). The precise mechanisms involved in stress-induced relapse are not well understood and targeting these mechanisms presents a potential intervention to prevent drug relapse. In comparison to cue- and drug-induced reinstatement, the neuromodulators underlying stress-induced reinstatement can be targeted pharmacologically without the side effects or abuse potential seen with the neuromodulators underlying cue- and drug-induced reinstatement (Silberman and Winder, 2013). Currently there are no approved medical therapies addressing stress-induced craving or relapse. A group of brain regions identified as the extended amygdala play a critical role in stress-induced reinstatement of drug seeking behavior (Koob and Volkow, 2010; Shaham et al., 2003).

1.3 The Extended Amygdala

The extended amygdala (EA) is the anatomical structure encompassing the BNST, central and medial amygdales (CeA and MeA), nucleus accumbens shell (NAcSh) and the areas in between (Alheid, 2006; Alheid and Heimer, 1988). These areas of the brain have been associated with states of fear, anxiety, and substance use disorders (Brown et al., 2011; Centanni et al., 2019a; Hyytiä and Koob, 1995; Jennings et al., 2013; Lange et al., 2017; Rinker et al., 2017; Shackman and Fox, 2016; Walker and Davis, 2008). Accumulation of sensory, contextual and evaluative cues from thalamic prefrontal/insular cortical, hippocampal inputs, the EA coordinates responses to internal and external stimuli and evaluates threat potential onto downstream outputs (Davis and Whalen, 2001; Fox et al., 2015; Shackman and Fox, 2016). Previous studies postulated the CeA and the BNST play distinct roles in response to different classes of stimuli, with the CeA primarily involved in the acute fear response while the BNST plays a role in anxiety as a long-term response (Walker and Davis, 2008). However, recent studies show that this original hypothesis was a simplified map of a more

interconnected circuit (Kovner et al., 2019; Shackman and Fox, 2016), as both regions appear to overlap in their contribution to threat responses. This is in part due to the GABAergic neurons of the CeA and the BNST that project locally within each structure to form inhibitory microcircuits.

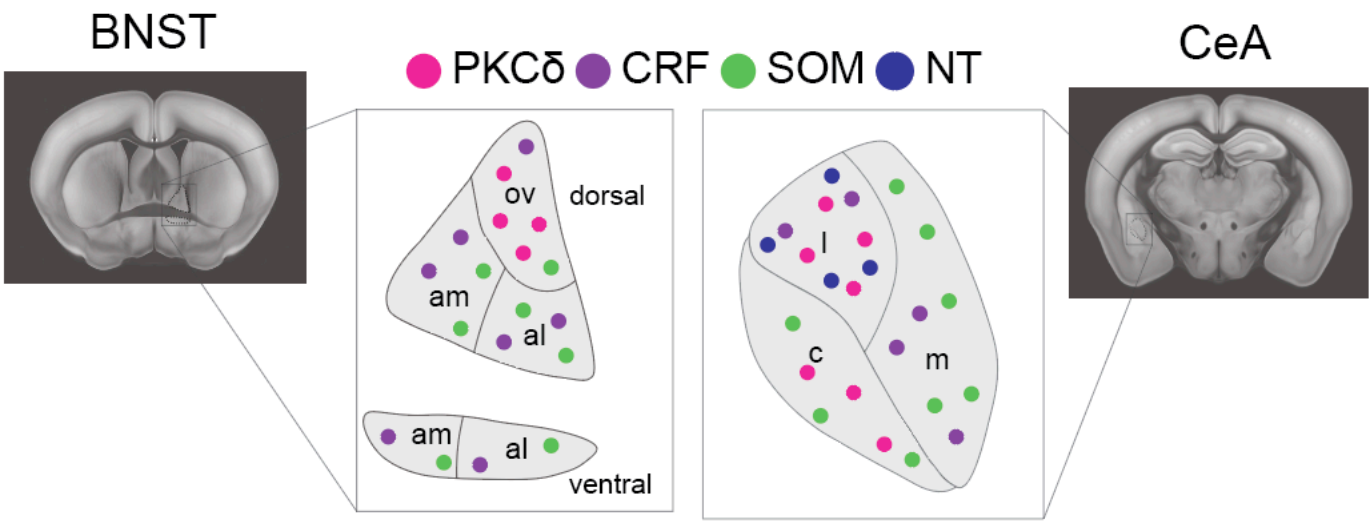

Figure 1. Distribution of major cell types in the Extended Amygdala.

Representative image of the distribution of various cell markers across the CeA and BNST and PBN involved in the reciprocal connections of the PBN to the EA. Somatostatin (SOM), Protein Kinase C delta (PKC δ), Corticotrophin Releasing Factor (CRF), and Neurotensin (NT).

1.3.1 CeA circuitry

The CeA is subdivided into three main sections: the capsular (CeC), medial (CeM), and the lateral (CeL) (Kovner et al., 2019). The CeM is the major output region of the CeA that projects to downstream regions such as the brainstem. The CeL projects locally to the CeM and to the BNST and regulates output from the CeM. The majority of the nociceptive PBN inputs into the CeA synapses onto neurons in the CeL and the CeC and respond strongly to noxious stimuli. This region of the CeA is often referred to as the "nociceptive amygdala" (Han, 2005; Li and Sheets, 2020; Neugebauer, 2020). The majority of the GABAergic neurons in the CeL and CeC that form local inhibitory circuits. These interneurons express somatostatin (SOM), CRF or PKCδ and are often synapsed onto by the PBN (Neugebauer, 2020; Ye and Veinante,

2019). While a population of CRF and PKCδ neurons in the CeA express other neuropeptides including Dyn and Enk, respectively, the majority of these neuronal types are mostly non-overlapping and underlie fear learning, anxiety and feeding (Campos et al., 2016; Fadok et al., 2017; H. Li et al., 2013; Ye and Veinante, 2019). Similarly, PKCδ and SOM expressing neurons are primarily non-overlapping. CeC and the CeL are densely populated with PKCδ and SOM positive neurons, while CRF neurons are found primarily in the CeM and CeL (Cai, 2014). CRF neurons form local synapses onto both SOM and PKCδ neurons in the CeL but mainly receive input from SOM neurons (Fadok et al., 2017). PKCδ and SOM neurons are involved as input and output cells in the reciprocal local circuitry within the CeA and the connection of the CeA to the BNST.

1.3.1.1 PBN to CeA circuitry

Using CGRP and CGRP-R expression and viral tracing as confirmation, it was found that inputs from the PBN project onto neurons expressing CRF, PKCδ, and SOM in the CeA (Li and Sheets, 2020; Neugebauer, 2020; Ye and Veinante, 2019). Anterograde tracing, optogenetics and immunofluorescence revealed CGRP expressing inputs from the PBN favor PKCδ expressing neurons in the CeL/CeC while a non-CGRP, potentially PACAP, expressing input from the lPBN favored SOM-positive neurons in the CeA (Li and Sheets, 2020; Ye and Veinante, 2019). With the studies showing SOM-positive and PKCδ-positive cells as the input and output cells of the CeA, this provides evidence that the differential innervation of CGRP and PACAP could bidirectionally regulate the CeA synaptic transmission. With approximately 50% of CRF neurons in the CeA receive inputs from the PBN determined by CGRP expression and optogenetic whole-cell recordings (Kozicz and Arimura, 2001; Li and Sheets, 2020). CGRP expression only accounting for 50% of the PBN innervation of the CeA suggests differential innervation of CRF cells by another neuropeptide, potentially through PACAP-expressing terminals from the PBN. PACAP containing fibers from the PBN in the CeC have been shown to regulate nociceptive response in the CeA (Missig et al., 2017, 2014). These fibers mostly colocalize with CGRP containing fibers in the CeC but the role of each neuropeptide in nociceptive signaling is yet to be determined. It is possible that PACAP expressing fibers provide a stronger input onto SOM positive neurons in the CeL/CeC. SOM and PKCδ neurons in the CeA often act in bidirectional manner and are thought to have opposing roles in pain-related behaviors. PKCδ neurons in the CeA have been shown to modulate pronociceptive or increased pain states while SOM positive neurons

are linked to decreased pain response or antinociceptive states (X. Li et al., 2013). The opposing roles of SOM and PKCδ positive neurons could result from their differential innervation by PACAP or CGRP expressing PBN projections, respectively. Overall PBN projections modulate CRF, PKCδ and SOM expressing neurons in the CeL/CeC and thus provide distinct control of the CeA.

1.3.2 BNST circuitry

The BNST is a nexus of the stress and reward pathways and contains a multitude of inputs and outputs from various region involved in both pathways. The efferents and afferents of the BNST have been heavily associated with drugs of abuse (Briand et al., 2010, 2010; Dumont et al., 2005; Grueter, 2006; Kash et al., 2008; Pleil et al., 2015; Reisiger et al., 2014; Sartor and Aston-Jones, 2012; Silberman et al., 2013; Vranjkovic et al., 2014). Two major fiber tracts connect the BNST to downstream brain regions including the stria terminalis/dorsal bundle and the ansa peduncularis/ventral bundle, or the amygdalofugal pathway (Dong et al., 2001a). The majority of inputs and outputs from the BNST are GABAergic or glutamatergic. The ovBNST is pivotal to the efferent and afferent projections of the BNST. The oval BNST modulates anxiety and assigns valence through the convergence of multiple neuromodulators including SOM, PKCδ, PACAP, CRF, dopamine, and GABA (Lebow and Chen, 2016). It is hypothesized that the BNST contains an inhibitory parallel circuit of SOM and PKCδ positive neurons similar to the CeL/CeC (Ye and Veinante, 2019). While PKCδ positive neurons in the dBNST project to the CeM, SOM positive neurons in the BNST are involved in more long-range projections including to the PBN and periaqueductal gray (PAG).

1.3.2.1 BNST efferents

Circuit mapping approaches have revealed that the BNST projects to several brain regions such as the PBN, LH, medial preoptic area, substantia nigra, dorsal raphe, NTS, PVN, PAG, CeA, and the VTA (Ch'ng et al., 2018; Jennings et al., 2013; Kim et al., 2013; Mahler and Aston-Jones, 2012). The connections between the BNST and the CeA, PVN, PAG and VTA are reciprocal and have been well-studied (Dong and Swanson, 2004; Georges and Aston-Jones, 2002; Jalabert et al., 2009; Kim et al., 2013; Kudo et al., 2012; Silberman and Winder, 2013). Glutamatergic and GABAergic neurons in the BNST synapse onto dopaminergic and non-dopaminergic neurons in the VTA influencing multiple pathways (Dong and

Swanson, 2006; Geisler and Zahm, 2005; Kudo et al., 2012). The majority of BNST efferents to the VTA are GABAergic and are associated with anxiolytic-like behavioral effects, however a small portion of glutamatergic efferents from the BNST to VTA have been associated with anxiogenic-like and aversive effects (Jennings et al., 2013). Activation of glutamatergic inputs from the BNST to VTA produce conditioned place aversion, reduce reward-seeking behavior, and increase anxiety-like behavior in mice (Jennings et al., 2013). Conversely, activation of GABAergic vBNST efferents to the VTA increase reward-seeking behavior, produce conditioned place preference, and reduce anxiety-like behavior (Jennings et al., 2013). It is through these pathways that the BNST modulates activity of dopamine neurons in the VTA (Georges and Aston-Jones, 2002; Jalabert et al., 2009). BNST efferents synapse onto dopamine and GABA cells in the VTA . Application of noradrenaline in the BNST increases spontaneous inhibitory transmission in VTA-projecting BNST neurons, and this effect is dependent on alpha1-ARs (Dumont, 2004). Future studies will need to parse the individual effects of each on stress- and addiction-related outcomes.

The BNST sends dense projections to the PAG in the midbrain; specifically these are CRF-containing projections originating in the BNSTov (Dong and Swanson, 2004). Activation of the BNST-PAG pathway results in CRF release from BNST terminals onto dopaminergic neurons in the PAG, depolarizing them and resulting in downstream DA release from PAG terminals in the BNST. Dopamine activates D1R on CRF-positive neurons in the BNST resulting in release of CRF and downstream modulation of glutamatergic synaptic transmission in the BNST via actions at CRFR1 (Bowers et al., 2003; Kash et al., 2008; Silberman and Winder, 2013).

The BNST acts as a relay between the IL and VTA dopamine neurons (Massi et al., 2008). The IL provides phasic glutamatergic control of BNST neurons through AMPAR, NMDAR and $GABA_AR$ activity(Massi et al., 2008). Similarly, the BNST relays information between the prelimbic area of the mPFC (PL) and the PVN (Radley et al., 2009). As described in a previous section, the BNST receives glutamatergic input from regions of the prefrontal cortex, including the orbital, infralimbic and prelimbic cortices. The PL modulates activity of the HPA axis through PVN neurons and this pathway is involved in acute emotional responses (Radley et al., 2009). However, there is only a weak projection from the PL to the PVN that seems unlikely to mediate this response to stress. Therefore, it was hypothesized the PL acts through a relay brain region to exert its effects on the PVN, and the BNST has been investigated as the potential relay between the PL and PVN. Specifically, projections from BNST to PVN and from PL to BNST were confirmed using anterograde and

retrograde tracing techniques (Radley et al., 2009). Predominantly GABAergic projections from the vBNST synapse onto CRF-positive neurons in the PVN, although some sparse projections are glutamatergic and CRF-expressing(Ch'ng et al., 2018). This pathway allows the BNST to drive HPA axis activation and modulate the production of stress hormones such as CRF. Ablation of GABAergic neurons in the BNST results in an enhanced stress response in the PVN, evidenced by stress-induced increases in nuclear expression of cfos protein, and CRF mRNA (Radley et al., 2009). This suggests the GABAergic projection from the BNST to the PVN is necessary for the stress response initiated by the mPFC. This response is similar to enhanced stress-induced activation of PVN neurons that is observed following mPFC ablation (Radley et al., 2009). Furthermore, exposure to stress results in a switch from LTD to LTP in the BNST following mPFC stimulation(Glangetas et al., 2013). This effect is due to CB1R actions on glutamatergic terminals in the BNST and is absent in CB1R knockout animals (Glangetas et al., 2013). These results, in addition to evidence showing that CB1R activation on mPFC glutamatergic terminals in the BNST control neuronal response to cortical stimulation, suggest a CB1R-sensitive di-synaptic circuit from the mPFC to the PVN through the BNST that is necessary for generating stress responses.

The lateral hypothalamus receives two non-overlapping projections from the BNST that express either CRF or cholecystokinin (CCK)(Giardino et al., 2018). These pathways respond differently to various emotional states. For example, CRF-positive cells respond more to predator odor, while CCK-positive cells respond more to odor of the opposite sex. Both CRF and CCK cells in the BNST receive intra-BNST projections, with CRF-positive cells receiving projections from the BNSTal and CCK-positive cells receiving inputs from the BNSTam and the medial pBNST. Both CRF-positive and CCK-positive neurons in the BNST receive inputs from the MeA and the medial preoptic area.

1.3.2.2. BNST Afferents

The BNST receives various afferents from regions across the entire brain. The main afferents are glutamatergic and GABAergic, but also include neuropeptidergic, dopaminergic, serotonergic, and noradrenergic. These afferents will be described in detail below.

1.3.2.2.1 Glutamatergic afferents

The BNST receives glutamatergic input from various brain regions including the basolateral amygdala (BLA), entorhinal cortex (EC), lateral hypothalamus (LH), olfactory bulb, parabrachial nucleus (PBN), insular cortex (insula), the ventral subiculum of the hippocampus (HPC) and the paraventricular thalamus (PVT) (Canteras and Swanson, 1992; Ch'ng et al., 2018; Cullinan et al., 1993; Dong et al., 2001a; McDonald, 1998; Myers et al., 2014). The BNST also receives glutamatergic inputs from regions of the prefrontal cortex, including the orbital, infralimbic and prelimbic cortices. The majority of prior research on glutamatergic afferents in the BNST have focused on the BLA, PVN, PBN, mPFC, and insula, and these studies will be described below. While anatomical studies have revealed synaptic inputs from other areas, the function of these inputs has not been thoroughly characterized.

Basolateral Amygdala (BLA): BLA projections to the BNST are divided into two parallel circuits that project to specific regions of the BNST (Ch'ng et al., 2018). The medial BLA projects to the BNSTam while the lateral BLA projects to the BNSTal (Krettek and Price, 1978). Interestingly, the BLA projection is absent in the BNSTov, a portion of the BNST that receives various other inputs. Optogenetic activation of BNST-projecting BLA afferents is anxiolytic and decreases respiratory rate (Kim et al., 2013).

Paraventricular Nucleus (PVN): The PVN, a nucleus in the hypothalamus involved in hormonal regulation, sends a glutamatergic onto the BNSTal that contribute to regulating the stress-response hormone corticotrophin releasing factor (CRF, CRH) (Berk and Finkelstein, 1982; Myers et al., 2014). Additionally, the PVN sends an excitatory orexin/dynorphin co-expressing projection to the BNST(Peyron et al., 1998).

Medial prefrontal cortex (mPFC): The BNST receives glutamatergic input from the mPFC, a brain region involved in cognitive control and decision making. This input is endocannabinoid (eCB) sensitive (Massi et al., 2008; Radley et al., 2009). One study showed that mPFC inputs from the prelimbic area of the mPFC synapse onto cells in the BNSTov that themselves project onto PVN neurons (Radley et al., 2009). The other study demonstrated that projections from the infralimbic subregion of the mPFC synapse onto VTA-projecting BNST neurons (Massi et al., 2008), potentially outlining a role for the BNST in relaying cortical information to downstream regions to regulate the reward behavior.

Insular cortex (insula): The BNST receives glutamatergic input from the insula, a brain area involved in interoception. These inputs are modulated by eCB signaling (Centanni et al., 2019b; Reichard et al., 2017), but not

noradrenergic signaling (Fetterly et al., 2019). Increased activity in CRF-positive cells in the BNST following optogenetic insular input activation was diminished with application of a cannabinoid 1 receptor (CB1R) agonist (Centanni et al., 2019b) . Moreover, neuronal activity in the insula-BNST circuit (measured by *in vivo* activity sensors for calcium, glutamate, and GABA) is positively correlated with active escape behavior during restraint stress (Luchsinger et al., 2021), suggesting a distinct role for this circuit in regulating behavioral response during a stressor.

Parabrachial Nucleus (PBN): The PBN provides a glutamatergic input onto cells in the BNST. The majority of neurons projecting from the PBN, specifically the lPBN, to the BNST culminate in the oval BNST (ovBNST) (Palmiter, 2018). This synapse has been associated with increased arousal and food-seeking/consummatory behavior in a stressed state (Carter et al., 2013; Palmiter, 2018). Optogenetic stimulation of PBN synapses in the BNST reveals two BNST cell populations that are either activated or inhibited by PBN stimulation. Activation of PBN inputs to BNST increases phasic calcium activity and anxiety-like behavior (Jaramillo et al., 2020). Moreover, PBN projections specifically onto BNST CRF cells are sensitive to noradrenaline, as washing on noradrenaline decreases spontaneous glutamatergic activity (Fetterly et al., 2019), outlining a strong role for this specific input in regulating reward and arousal. The CeA and the BNST are reciprocally connected and include a CRF projection from the CeL that innervates non-CRF cells in the BNST (Salmaso et al., 2001). Using viral tracing and immunofluorescence, it has been shown that the PBN synapses onto PKCδ neurons in the BNST, with the majority of PKCδ neurons located in the ovBNST (Jaramillo et al., 2020; Ye and Veinante, 2019). PKCδ-positive neurons in the ovBNST receive the majority of the signal from the PBN through CGRP expressing cells originating in the lPBN (Ye and Veinante, 2019). Conversely, SOM positive neurons are dispersed across the BNST and comprise the majority of cells in the BNST that convey signals to the PBN (Ye and Veinante, 2019). CRF is expressed across the BNST with around 50% of cells innervated by the PBN (Fetterly et al., 2019; Kozicz and Arimura, 2001; Sink et al., 2013). CRF positive cells in the BNST are surrounded by CGRP and PACAP positive terminals suggesting multiple parallel pathways from the PBN synapsing onto the BNST (Kozicz et al., 1997; Kozicz and Arimura, 2001). Thus, PBN projections distinctly innervate PKCδ, CRF, and SOM expressing BNST neurons. Anterograde tracing revealed a non-CGRP input onto SOM and PKCδ positive neurons in the BNST suggesting similar PACAP innervation of SOM positive neurons but potential CGRP and PACAP innervation of PKCδ positive neurons in the BNST (Ye and Veinante, 2019). It is the plethora of different neuronal cell types across these brain regions that result in the bidirectional modulation of various emotional,

psychological and physical states. Overall, the PBN→EA circuit is ideally positioned to encompass an animal's response to threat-inducing stimuli from the initial sensory stimuli to the resulting acute or chronic physical and emotional response. In this review, we focus on the incorporation of a PBN "alarm" response to nociceptive signals and the modulation of stress responses through its reciprocal connections to the EA. Overall, the various cell populations and interconnectedness of the EA allows cells in the PBN to exert influence over the multitude of aspects that culminate in an animal's response to noxious stimuli.

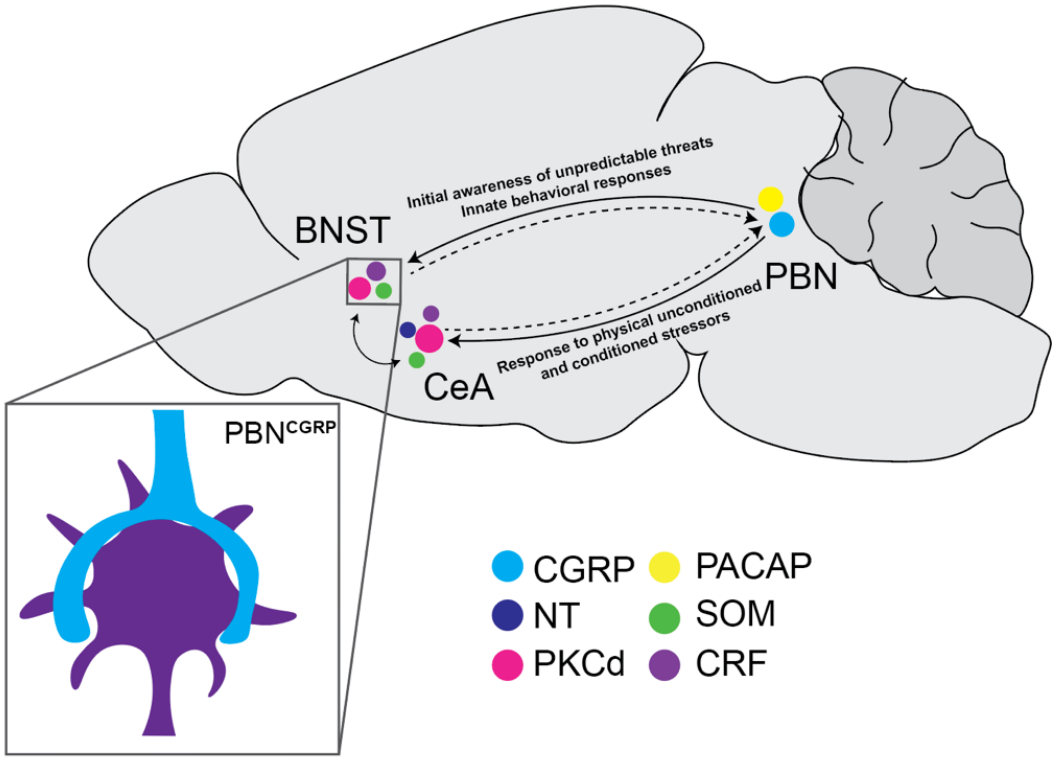

Figure 2. Reciprocal connections between the parabrachial nucleus and the extended amygdala.

Representative image depicting dense basket-like axosomatic PBN projections (inset) onto the BNST and CeA. Hypothesized overall function of reciprocal connection described above projection. Somatostatin (SOM), Protein Kinase C delta (PKC δ), Corticotrophin Releasing Factor (CRF), Pituitary Adenylate Cyclase-Activating Polypeptide (PACAP), calcitonin gene related peptide (CGRP), Neurotensin (NT).

1.3.2.2.2 GABAergic Afferents

The primary GABAergic input into the BNST originates in the central amygdala (CeA) (Vranjkovic et al., 2017) . The CeA to BNST circuit expresses various neuropeptides including ENK, substance P, and/or neurotensin (Ch'ng et al., 2018). Less predominant GABAergic inputs to the BNST originate from the striatum, lateral septum, and nucleus accumbens (NAcc) shell (Cullinan et al., 1993; Dong et al., 2001b; Hurley et al., 1991; McDonald, 1998; Myers et al., 2014; Takagishi and Chiba, 1991; Vertes, 2004).

1.3.2.2.3 Neuropeptide afferents

Neurons in the BNST receive and send neuropeptide-expressing projections from and to several brain regions. Neuropeptide signaling is prominent and interconnected in the BNST with cells often expressing multiple peptides. CRF-positive neurons from the CeA and PVN, and CRF-positive interneurons, synapse onto cell bodies in the BNST and regulate cell excitability (Vranjkovic et al., 2017). CRF signaling has been linked to excitation and inhibition in the BNST via actions on distinct presynaptic or postsynaptic receptors (Kash and Winder, 2006; Silberman and Winder, 2013) . Inhibitory drive onto CRF-positive neurons in the BNST is enhanced through NPY activation (Pleil et al., 2015) , further showing the interconnectedness of neuropeptide signaling in the BNST. While each of these neuropeptides modulates BNST activity, to date very few studies have examined their roles in addiction. As better pharmacological targets emerge, research may uncover new BNST-centric targets for treating addiction.

1.3.2.2.4 Dopaminergic afferents

The BNST receives dopaminergic input from the VTA and PAG (Freedman and Cassell, 1994; Meloni, 2006). The VTA and PAG are heavily implicated in reward and arousal, highlighting the involvement of the BNST in reward-mediated circuitry. Additionally, a D2R-expressing inhibitory input projects from the CeA onto GABAergic and non-GABAergic neurons in the BNST (Kim et al., 2018). Dopaminergic innervation is diffuse across the dlBNST with dense localization of fibers in the BNSTov, and the BNSTjx (Freedman and Cassell, 1994; Krawczyk et al., 2011; Meloni, 2006; Phelix et al., 1992). D1Rs and D2Rs are expressed throughout the anterior BNST, with only D2Rs localized to the BNSTov (Krawczyk et al., 2011). Drugs of abuse such as cocaine, alcohol, morphine, and nicotine increase extracellular dopamine release in

the BNST in a dose-dependent manner (Carboni et al., 2000), decreasing inhibitory and excitatory transmission in the BNSTov through activation of presynaptic D2R or alpha2-AR, respectively (Krawczyk et al., 2011) . Projections from the VTA and PAG synapse primarily onto CRF-positive neurons in the dBNST (Meloni, 2006).

1.3.2.2.5 Serotonergic afferents

The caudal regions of the dorsal raphe nucleus have reciprocal 5HT connections with the dBNST (Block and Hoffman, 1987; Commons et al., 2003; Lowry et al., 2008). It is hypothesized that CRF release during stress activates serotonergic neurons in the dorsal raphe through CRFR2 activation (Hammack et al., 2003). It is hypothesized that BNST projections to the dorsal raphe influences 5HT signaling in that region via effects on CRF signaling. 5HT acts on presynaptic receptors to alter glutamatergic transmission in the BNST and serotonergic input to the BNST is linked with anxiety (Guo and Rainnie, 2010). It is also hypothesized that 5HT modulates release of neuropeptides, such as CRF, through activation of presynaptic 5HTRs , but the precise mechanism underlying this effect is not fully characterized. The BNST-dorsal raphe reciprocal circuits are hypothesized to function as a negative feedback loop in response to stress or anxiety-provoking stimuli (Hammack et al., 2007) .

1.3.2.2.6 Noradrenergic afferents

The BNST receives one of the densest noradrenergic projections originating from the nucleus tractus solitarius (NTS) of the ventral noradrenergic bundle (Banihashemi and Rinaman, 2006; Egli et al., 2005; Flavin et al., 2014a; Forray and Gysling, 2004; Ricardo and Tongju Koh, 1978; Shields et al., 2009a). Additionally, the BNST receives a sparse noradrenergic input from the locus coeruleus. The vBNST is densely innervated by alpha1-AR- and alpha2-AR-expressing noradrenergic cells, which can influence both excitatory and inhibitory transmission. Stimulation of the ventral noradrenergic bundle results in noradrenaline release in the BNST as measured by *in vivo* fast-scan cyclic voltammetry (Park et al., 2009). Noradrenergic and non-noradrenergic inputs to the BNST are altered by several pharmacological agents that target adrenergic receptors (Flavin et al., 2014a; Harris et al., 2018; Perez et al., 2020a). In addition, axons from the PBN form peri-somatic connections with BNST neurons and these synapses are regulated by noradrenergic signaling. Guanfacine inhibits glutamatergic input from the PBN onto CRF-positive neurons in the BNST (Fetterly et al.,

2019; Flavin et al., 2014a). Both noradrenaline and guanfacine reduce glutamatergic transmission from the PBN onto CRF-positive neurons in the BNST (Fetterly et al., 2019). Conversely, guanfacine has no effect on glutamatergic transmission from the BLA or insula, suggesting input-dependent effects of noradrenergic modulation (Fetterly et al., 2019; Flavin et al., 2014a).

1.3.2.3 Endocannabinoid modulation of BNST afferents

Endocannabinoids act through their endogenous receptors, CB1R or CB2R, to influence the activity of GABAergic and non-GABAergic cells in the BNST. Specifically, eCB regulation of BNST inputs from the mPFC, insula, CeA, BLA, and ventral subiculum have been investigated in rodent models. Glutamatergic inputs from the infralimbic cortex (IL, a subregion of the mPFC) and ventral subiculum onto the BNST directly affect the excitatory BNST projections to the VTA through an eCB-sensitive pathway (Caillé et al., 2009; Georges and Aston-Jones, 2002; Jalabert et al., 2009; Massi et al., 2008). Furthermore, infusion of CB1R agonist into the BNST blunts the excitatory drive of IL onto downstream VTA DA neurons (Massi et al., 2008) . This study provides the framework of an IL--> BNST --> VTA circuit originating from the IL onto DA neurons in the VTA that requires CB1R activity in the BNST. Similarly, infusion of a CB1R antagonist into the BNST prevented stimulation-induced LTP in the mPFC of stressed mice (Glangetas et al., 2013). *Ex vivo* extracellular field recordings revealed that CB1R agonism inhibits evoked excitation and inhibition in the BNST, and these effects were reversed by CB1R antagonism (Puente et al., 2010). CB1R agonism decreases excitatory responses in CRF-positive cells in the BNST following optical stimulation of the insular terminals (Centanni et al., 2019b). Presynaptic CB1R activation inhibits inputs from the CeA and BLA onto BNST neurons (Lange et al., 2017). Conversely, inputs from the MeA are not affected by CB1R activation (Lange et al., 2017). While a majority of endocannabinoid work has focused on CB1Rs, recent studies also show a role for CB2R activation in the BNST in negative affective behaviors (Gomes-de-Souza et al., 2021): this study found that CB1Rs and CB2Rs are located in the anterior and posterior portions of the BNST.

1.4 The effects of drugs of abuse on the BNST

1.4.1 Alcohol

Alcohol directly modulates BNST neurotransmission, as bath application of alcohol onto an acute slice containing the BNST results in decreased amplitude of NMDAR-dependent currents and long-term potentiation (Kash et al., 2009; Weitlauf, 2004; Wills et al., 2012). A large portion of research on the role of the BNST in addiction has focused on alcohol use disorder. The BNST has been linked to the both alcohol consumption and alcohol withdrawal-induced anxiety and depression.

Commonly used methods to evaluate the underlying mechanisms of alcohol use disorder is to use a binge-drinking and/or intoxication model using continuous or limited access to alcohol, systemic administration, or contingent access(Holleran et al., 2016). Acute exposure to alcohol increases cfos expression in the BNST suggesting that the BNST directly responds to alcohol via increased neuronal activation (Saalfield and Spear, 2019; Sharko et al., 2016) . A single acute exposure to alcohol decreased expression of DNA methyltransferase (DNMT), an enzyme linked to epigenetic regulation of gene expression, in the BNST that was increased following a second systemic alcohol injection (Sakharkar et al., 2014). Stress and alcohol modulate phosphorylated CREB (pCREB) expression in the BNST and this effect can be blocked by NMDAR antagonism (Blundell and Adamec, 2007) . A moderate-dose alcohol exposure that produces conditioned place aversion (CPA) is blunted by previous stress exposure and results in a reduction in pCREB expression in the BNST (Schreiber et al., 2019). Alcohol increases noradrenaline release (Jadzic et al., 2021) dopamine release in the BNST as measured by *in vivo* voltammetry (Carboni et al., 2000). Alcohol-induced conditioned place preference (CPP) results in increased intrinsic excitability of neurons in the vBNST. This effect was not seen following alcohol-induced CPA or alcohol exposure in home cage, suggesting specific effects on the rewarding properties of alcohol in the BNST.

Neuromodulators such as CRF and NPY have also been linked to alcohol use. Persistent alcohol drinking in stressed mice compared to non-stressed mice is correlated with increased CRF mRNA levels in the BNST (Albrechet-Souza et al., 2017). Administration of a CRFR2 antagonist dose-dependently increases alcohol consumption, regardless of exposure to stress while a CRFR1 antagonist directly infused into the BNST reduces alcohol intake in unstressed mice(Albrechet-Souza et al., 2017). Activation of NPY1R results in enhanced inhibitory neurotransmission onto CRF

neurons in the BNST, an effect that has been associated with decreased alcohol drinking (Pleil et al., 2015). Alpha-melanocyte stimulating hormone (alpha-MSH), a key component of the melanocortin system, is reduced in rats exposed to chronic alcohol (Navarro et al., 2008) . Alpha-MSH has been associated with regulation of dopamine release in the VTA to NAcc pathway, a circuit heavily involved in drugs of abuse, further implicating the BNST to VTA circuit in alcohol consumption.

Non-contingent methods, such as chronic intermittent ethanol (CIE), that allow for precise measurements of exposure and result in high blood alcohol levels are often used to study alcohol use disorder in animal models (Holleran et al., 2016). This method produces alcohol dependence in animals and can be used to measure effects on alcohol drinking. Alterations in synaptic plasticity of glutamatergic inputs to the BNST have been associated with response-contingent and non-response-contingent alcohol exposure effects. Specifically, exposure to acute and chronic non-response-contingent alcohol administration resulted in alterations in expression and function of the NMDAR subunit GluN2B (Kash et al., 2009, 2008; Wills et al., 2012). Additionally, CIE produces an increase in expression of GluN2B in the BNST (Kash et al., 2009). CIE results in increased basal activity of CRF-positive neurons in the BNST in a manner similar to stress exposure (Snyder et al., 2019), and this effect requires noradrenergic signaling through beta-ARs. CIE enhances basal activity in VTA-projecting neurons in the BNST via a CRFR1-dependent mechanism, and moreover, binge-like alcohol drinking is reduced following inhibition of BNST CRF projections onto the VTA (Rinker et al., 2017). *Ex vivo* application of alcohol attenuates the beginning phase of high frequency LTP in the dBNST through depression of NMDAR function that requires GABAergic inhibition (Weitlauf, 2004). This effect on NMDAR synaptic transmission is dependent on GluN2B expressing NMDARs (Kash et al., 2009, 2008; Wills et al., 2012). Interestingly, CIE increases the expression of GluN2B expressing NMDARs in the BNST and increases excitatory postsynaptic currents and enhances LTP induction through a GluN2B-dependent mechanism (Kash et al., 2009, 2008; Wills et al., 2012). Alcohol produces a greater effect on NMDAR-evoked excitatory and GABAergic inhibitory postsynaptic currents in BNST neurons in adolescent mice relative to adults(Wills and Winder, 2013), highlighting unique effects of alcohol on BNST circuitry during adolescence. Chronic alcohol drinking can also impact downstream signaling molecules in the BNST. Chronic alcohol drinking increases protein levels of Homer, an mGluR5-scaffolding protein, and activated extracellular signal-related kinase (ERK) in the BNST, suggesting mGluR5 phosphorylation as a potential adaptive response to alcohol consumption(Campbell et al.,

2019). To further this observation, transgenic animals with a point mutation in mGluR5 preventing phosphorylation by ERK exhibited increased alcohol-drinking (Campbell et al., 2019). These transgenic animals were determined to be insensitive to alcohol aversion and this effect is mimicked by ERK inhibition in the BNST.

Alcohol results in increased activation of GABAergic and non-GABAergic neurons in the BNSTal (Crankshaw et al., 2003; Leriche et al., 2008). Disruption of GABAergic signaling (Hyytiä and Koob, 1995) or dopaminergic signaling (Eiler et al., 2003) results in decreased alcohol-seeking behaviors. Inhibition of GABA signaling in the BNST decreases alcohol self-administration in rats (Hyytiä and Koob, 1995). This supports the proposed role of reciprocal VTA-BNST circuits in mediating the rewarding effects of alcohol. Binge alcohol intake is decreased following silencing of GABAergic BNST neurons that project to the VTA. Similarly, self-administration of alcohol is decreased following injection of a dopamine D1R antagonist into the BNST in a dose-dependent manner (Eiler et al., 2003).

1.4.2 Cannabinoids

Cannabinoids have been studied for their strong anxiolytic properties (and anxiogenic properties in certain individuals and/or at higher doses), suggesting BNST circuitry may play a central role in its effects. Cannabinoids inhibit glutamatergic transmission from the IL to the BNST through activation of presynaptic CB1Rs (Massi et al., 2008). Delta (9)-tetrahydrocannabinol (THC) is the major psychoactive component of marijuana and acts as an agonist at CB1Rs. Chronic exposure to THC can have interesting effects on subsequent drug exposure. Chronic THC before heroin injection results in a suppression of heroin-induced increase in locomotion (Singh et al., 2005), and the BNST may play a role in this effect, as chronic THC attenuates heroin-induced increases in cfos expression in the BNST. This effect of THC exposure on heroin response was also seen following perinatal exposure to THC and adolescent exposure to heroin (Singh et al., 2006).

Another cannabinoid, cannabidiol (CBD) has gained popularity recently for its ability to treat certain forms of epilepsy and is an intriguing compound for several affective disorders for its perceived lack of psychoactive properties and low abuse potential. The role of CBD in emotional regulation and its effects on BNST circuitry have not been fully elucidated, however research suggests an interaction with 5HT, as CBD injected directly into the BNST decreases anxiety-like behavior and contextual fear conditioning mediated through $5HT_{1A}$Rs (Gomes et al., 2012, 2011). Moreover,

systemic injection of CBD activates $5HT_{1A}$Rs to decrease cardiovascular responses to acute restraint stress (Gomes et al., 2013). Microinjection of CBD into the BNST can also attenuate contextual fear behavior (Gomes et al., 2012), and this effect is blocked by pre-treatment with a $5HT_{1A}$R antagonist. While much work remains to be done to understand the direct actions of CBD on the BNST and the brain as a whole, these initial studies provide intriguing rationale for further exploring its role in negative affective disorders.

1.4.3 Opioids

Mice that have undergone morphine CPP have increased levels of phosphorylated CREB, a marker of neuronal activity, in the BNST (García-Carmona et al., 2013), and acute heroin exposure increases cfos expression in the BNST (Singh et al., 2005). After morphine CPP, there is an increase in pCREB co-expression in CRF-positive neurons in the BNST. Acute opioid withdrawal results in increased GABAergic synaptic activity in the BNST potentially through a noradrenergic-sensitive pathway. This effect potentially modulates downstream inhibitory projections onto VTA neurons (Dumont, 2004). Pharmacologically targeting the BNST opioid system has been shown to impact opioid-seeking behavior. Injection of an opiate receptor antagonist, methylnaloxonium, into the BNST dose-dependently decreases heroin-seeking behavior in heroin-dependent rats (Walker et al., 2000) , while having no effect on heroin-seeking behavior in non-heroin-dependent animals. During acute withdrawal, injection of a CRFR1 antagonist into the BNST decreases fentanyl-associated cue-conditioned reinforcement (Gyawali et al., 2020). Injection of an opiate receptor antagonist, methylnaloxonium, into the BNST dose-dependently decreased heroin seeking behavior in dependent rats (Walker et al., 2000). The antagonist had no effect on non-dependent animals. Morphine withdrawal increases noradrenaline release in the BNST (Fuentealba et al., 2002). Antagonism of alpha2 presynaptic receptors resulted in attenuated the decrease in food responses seen in opioid withdrawal, suggesting reversal of withdrawal-induced decreased motivation (Sparber and Meyer, 1978). Beta-adrenergic receptor antagonists, propranolol and atenolol, blocked increase anxiety behavior during cocaine and morphine withdrawal (Harris and Aston-Jones, 1993). Direct infusion of beta2 antagonist or alpha2 agonist into the BNST blocked opiate withdrawal-induced place aversions (Delfs et al., 2000). Prazosin, the alpha1 antagonist, reduced self-administration of heroin, decreased motivation to self-administer cocaine, and attenuated increased drinking linked with acute withdrawal of alcohol (Greenwell et al., 2009;

Walker et al., 2008; Wee et al., 2008). These studies underscore the importance of noradrenaline signaling in the BNST and the role this signaling plays in addiction. This interaction will be the focus of the next sections.

1.5 Peripheral and central effects of noradrenaline

The autonomic nervous system (ANS) is an extensive system that governs most organ systems within the body. The ANS can be divided into the central and peripheral autonomic nervous systems. The peripheral autonomic nervous system comprises the sympathetic nervous system (SNS), the parasympathetic nervous system (PNS) and the enteric nervous system. The main function of the SNS is to prepare the body for a physical activity (referred to as the "fight or flight" response). The main function of the PNS is to calm the body and recover from physical activity or "rest and digest" (Gibbons, 2019; Mulkey and du Plessis, 2019). Groups of neuronal cell bodies in the ANS are termed ganglions and can be divided into preganglionic and postganglionic depending on the location of their synapses. Preganglionic and postganglionic neurons of the PNS and SNS communicate with each other or their target organs through release of neurotransmitters at the synapse that act upon receptors located at the post-synapse.

Ganglionic neurons of the peripheral autonomic nervous system connect the central nervous system to the organs of the cardiac, exocrine and endocrine systems. In the PNS, both preganglionic and postganglionic neurons release acetylcholine as a neurotransmitter. Preganglionic neurons contain nicotinic receptors while postganglionic neurons contain muscarinic receptors. The preganglionic neurons of the SNS act through acetylcholine and contain nicotinic receptors located on postganglionic neurons. On organs, the postganglionic neurotransmitter is norepinephrine that act upon noradrenergic receptors located on peripheral tissues (Gibbons, 2019).

Throughout the autonomic nervous system, noradrenaline is involved in various bodily functions. Increased noradrenaline release through activation of the sympathetic nervous system causes increased blood pressure and cardiac output, relaxation of smooth muscles including bronchial and intestinal, increased pupil size, increased levels of blood glucose and free fatty acids (William Tank and Lee Wong, 2014). The central ANS comprises of the forebrain, upper and lower brainstem, and spinal cord. The forebrain includes the hypothalamus that controls homeostasis of the body and the limbic system that comprise of the insula, extended amygdala, and anterior cingulate cortex. The forebrain is involved in higher order functioning including integration of internal responses, emotions, and behaviors with the

external world. The interaction of the brainstem and the limbic system control how the emotional and physical experiences one has molds behavior and physical and mental health (Mulkey and du Plessis, 2019). This connection is heavily involved in the pathogenesis of neuropsychiatric disorders. The lower brainstem controls automatic functions that are required for life including circulation and respiration while the upper brainstem is involved in responses to pain or stressors (Gibbons, 2019). Noradrenergic activity has been linked to several physiological and psychological states including arousal, attention, learning and memory, anxiety and pain (Weinshenker and Schroeder, 2007). Altered levels of noradrenaline can lead to physiological or psychological conditions including cardiac heart failure, anxiety, attention deficit/hyperactivity disorder or posttraumatic stress disorder.

1.6 Noradrenaline pathways in the brain

Early studies in rats and monkeys using radioisotopes, anterograde tracers, and staining for dopamine-beta-hydroxylase, the enzyme responsible for production of noradrenaline, mapped the pathways from the locus coeruleus (LC). It was discovered that the LC projects ubiquitously in the cerebral cortex (Morrison et al., 1982, 1978; Rho et al., 2018). The noradrenergic neurons of the LC project extensively in the brain. These areas include the midbrain, hypothalamus, majority of telencephalic areas, all neocortices, and contralaterally to basal forebrain areas including the amygdala, hippocampus, frontal cortex and cingulate cortex (Moore and Bloom, 1979). There are two main noradrenergic circuits in the brain: the dorsal and ventral noradrenergic bundles pathways (Moore and Bloom, 1979; Weinshenker and Schroeder, 2007). The dorsal noradrenergic bundle originates in the LC and projects to the hippocampus, forebrain and cerebellum. The ventral noradrenergic bundle originates in the nuclei of the pons and medulla and projects to the extended amygdala, midbrain and hypothalamus. The extensive distribution of noradrenergic projections through the brain underlies its ability to modulate various behaviors. Specifically, adrenergic projections to the prefrontal cortex have been heavily linked to working memory (Lapiz and Morilak, 2006; Tronel, 2004; Usher, 1999), focused attention, and attentional set shifting.

1.6.1 Molecular components of NA signaling

As mentioned previously, the locus coeruleus is the major production source of noradrenaline in the brain. The majority of cells in the locus coeruleus are noradrenaline producing cells, accounting for over 40% of noradrenaline cells in rats. Synthesis of noradrenaline begins with the amino acid tyrosine (Figure 3). Tyrosine is converted to DOPA by tyrosine hydroxylase, the rate limiting step, and then further synthesized to dopamine by L-DOPA decarboxylase. Dopamine is oxidized to noradrenaline by dopamine-β-hydroxylase (DBH) in storage vesicles. Noradrenaline is stored in synaptic vesicles along with ATP and DBH for release into the synapse (Blaschko et al., 1972; Glavin, 1985). The production of noradrenaline contains an internal feedback mechanism by which the enzymatic activity of tyrosine hydroxylase is inhibited by DOPA and noradrenaline. Additionally, noradrenaline is metabolized by monoamine oxidase to noradrenaline aldehyde. This aldehyde is further reduced by aldehyde reductase to 3-dihydroxyphenylglycol, and then further degraded by catechol-O-methyltransferase (COMT) to 3-methoxy-4-hydroxy-phenylethylene glycol (MHPG), the major metabolite of noradrenaline in the brain (Glavin, 1985; Szabadi, 2013).

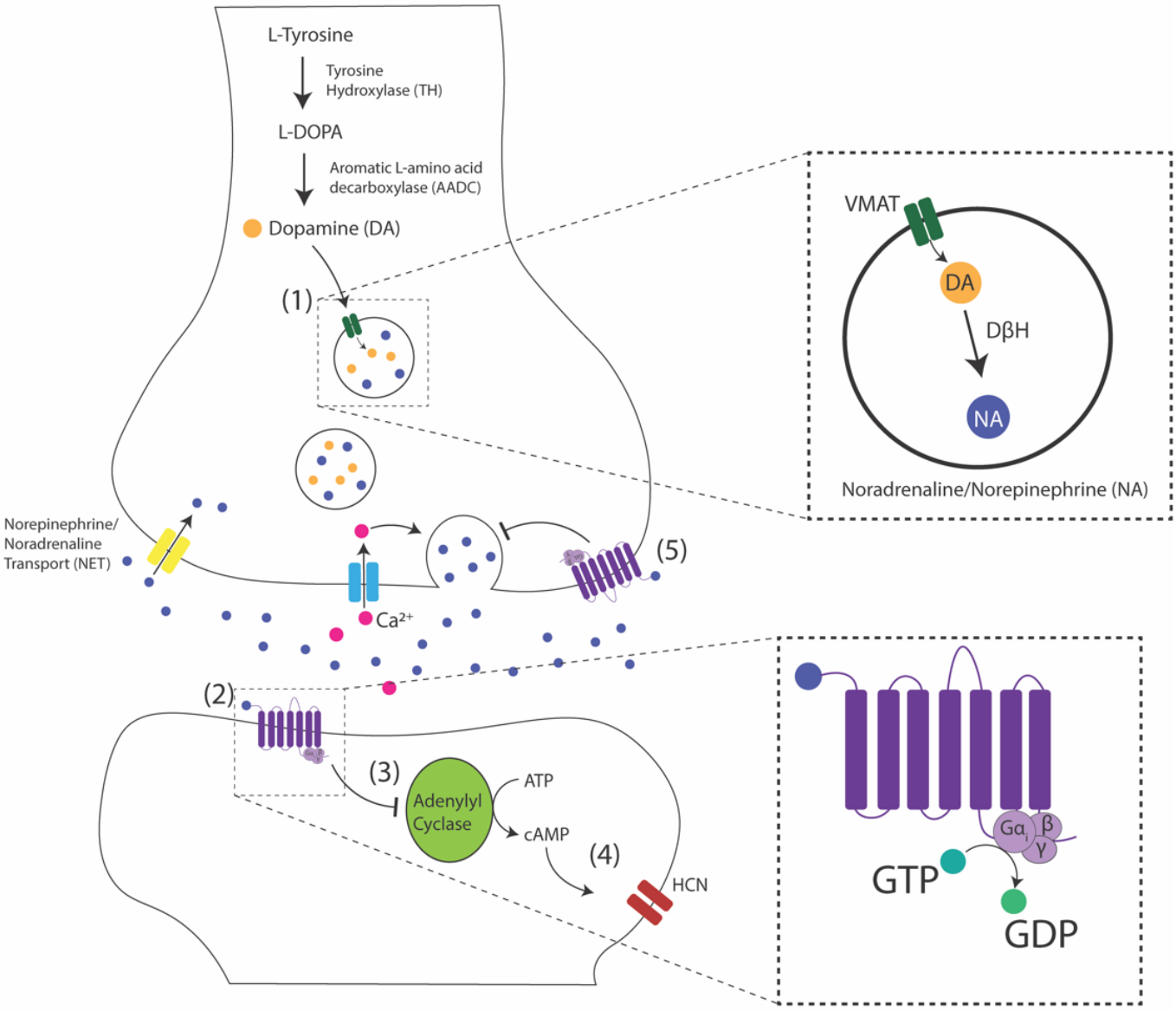

Figure 3. Noradrenergic signaling and the role of α2a-AR activation.

(1) Noradrenaline is produced from Dopamine by Dopamine Beta-hydroxylase (DBH) and is stored in synaptic vesicles. (2) Noradrenaline release following calcium influx into the cell results in activation of post-synaptic alpha2a-adrenergic receptors (α2a-AR). (3) α2a-AR are Gi-GPCRs which inhibit the activity of adenylyl cyclase. This results in a decrease in the production of cAMP from ATP. (4) It has been shown that a decrease in cAMP inhibits the opening of HCN channels, increasing the membrane potential and increasing functional connectivity of the post-synapse. (5) Activation of pre-synaptic α2a-ARs results in a decrease in neurotransmitter release from the pre-synapse.

Noradrenaline acts on three types of adrenergic receptors: α_2-, α_1-, and β-adrenergic receptors. Within each of these types, they are further delineated into subtypes. α_1-adrenergic receptors contain subtypes α_{1A}-, α_{1B}-, and α_{1D}-adrenergic receptors while α_2-adrenergic receptors contain subtypes $\alpha_{2A/D}$-, α_{2B}-, α_{2C}-adrenergic receptors. β-adrenergic receptors contain subtypes β_1-, β_2- and β_3-adrenergic receptors. All three classes are located in the CNS and have been linked to individual roles in various behaviors and neurological disorders. Specifically, $\alpha_{2A/D}$- adrenergic receptors have been linked heavily to working memory involving the noradrenergic innervation of the prefrontal cortex. In the prefrontal cortex, expression of α_{2A}-adrenergic receptors (α_{2A}-ARs) are most abundant (Huss et al., 2016; Jäkälä, 1999).

The first α_2-AR receptor was cloned from purified human platelet α_2-AR receptor and expressed in Xenopus oocytes (Kobilka et al., n.d.). The membrane spanning domain sequence for this receptor was similar to the β_1- and β_2-adrenergic receptors previously cloned. Functional analysis of the cytoplasm regions revealed similarities to muscarinic receptors in inhibition of adenylyl cyclase, as opposed to activation of adenylyl cyclase by β-adrenergic receptors. Interestingly, it was determined that the coding region of the α_2-AR is contained within a single exon similar to other G-protein coupled receptors. Binding of [^{3}H]-yohimbine from membranes prepared from oocytes confirmed α_{2A}-AR binding properties. This binding was saturable and was competed for by other α_2-AR antagonists and agonists. Southern blot analysis resulted in an additional two bands sharing significant homology for the human platelet gene cloned. These fragments were localized on separate chromosomes, with the human platelet gene on chromosome 10, and the other genes located on 2 and 4. Altogether, this evidence suggests multiple α_2-AR subtypes (Kobilka et al., n.d.). A subtype of the α_2-AR, located on chromosome 4, was first cloned in 1989 from a human kidney cDNA library (Regan et al., n.d.). The cDNA using the gene for the human platelet α_2-AR was expressed in a mammalian cell line (COS-7) and the α_2-AR ligand [^{3}H]-rauwolscine was used to confirm binding. The two subtypes differed in terms of ligand binding for α_2-AR antagonists, antagonists or endogenous catecholamines (Regan et al., n.d.), Finally, in 1990, the last subtype of α_2-ARs located on chromosome 2 was cloned from a human kidney cDNA library (Lomasney et al., n.d.). Transfection of COS-cells with the receptor sequence and radioligand binding of [^{3}H]-yohimbine confirmed α_2-AR activity. Additionally, differential responses to α_2-AR agonists and antagonists were confirmed across receptor subtypes.

α_2-ARs are located pre-synaptically and post-synaptically and act through Gi signaling to inhibit noradrenaline release or inhibit neuronal firing, respectively (Szabadi, 2013). Noradrenaline is released into the synaptic cleft following

calcium release due to increased neuronal activity. Noradrenaline binding to α_2-ARs results in receptor conformation changes allowing associations of G-proteins, including Gαi and G$\beta\gamma$. The Gαi subunit associate and inhibits adenylyl cyclase, resulting in a decrease in cAMP production.

1.7 Alpha2a-receptor signaling and noradrenaline release

α_{2A}-AR signaling is required for presynaptic modulation of noradrenaline release (Hein et al., 1999). Activation of pre-synaptic α_{2A}-AR results in decreases in noradrenaline release from the pre-synaptic neuron. This effect is seen in cardiac and cortical noradrenergic neurons. Following knockout (KO) of the α_{2A}-AR gene subtype in atria and brain cortex slices, the maximal inhibitory effect of α_2-AR agonist UK-14304 was reduced to around 70%. This differed from KO of α_{2B}- and α_{2C}-AR reduction to 95%. Crossing the KO of α_{2C}- and α_{2A}-AR subtype completely abolished the inhibitory effect of UK-14304, suggesting both subtypes are involved in regulating noradrenaline release. α_{2A}-AR mediated autoinhibition was most effective at higher frequencies, equating to higher noradrenaline concentrations. This is hypothesized to be due to lower affinity of noradrenaline to α_{2C}-AR as compared to α_{2a}-AR, that were most effective at inhibition with lower frequencies. Coupling of α_2-AR activation and inhibition of noradrenaline release was faster for the α_{2A}-AR than the α_{2C}-AR.

Additionally, α_{2A}-AR are located on adrenergic and non-adrenergic pre-synaptic neurons, termed autoreceptors and heteroreceptors, respectively (Perez et al., 2020a; Szabadi, 2013). α_2 receptors have been found on serotonergic, dopaminergic, and glutamatergic synapses (Millan et al., 2000; Szabadi, 2013). α_{2A} receptors agonists have been shown to decrease noradrenaline release from frontal cortex. These receptors were originally believed to be inhibitory, but recently have been shown to differ in action depending on their neuronal type (Perez et al., 2020a).

Intracellular recordings following noradrenaline application or stimulation of the locus coeruleus revealed a particular hyperpolarization with no change in membrane resistance in several brain areas known to be downstream of the locus coeruleus (Moore and Bloom, 1979). This hyperpolarization effect was unique to noradrenaline and contrasted to the effects of classic inhibitory actions of pharmacological compounds like GABA. This effect was potentiated with administration of phosphodiesterase inhibitors and was mimicked with application of cAMP (Moore and Bloom, 1979), suggesting a role for the cAMP second messenger system underlying the effects of noradrenaline. It was later found that

α_{2A}-receptor activation influences neuronal activity through effects on hyperpolarization-activated cyclic nucleotide gated (HCN) channels located on pyramidal neurons in the PFC (Wang et al., 2007). HCN channels are dependent on cAMP and their activation results in efflux of potassium and other cations. Opening HCN channels increases I_h current that lowers the membrane potential of the neuron, moving it farther away from the action potential threshold, thus decreasing its ability to fire. Therefore, closing HCN channels is linked to increased neuronal activation.

1.8 Noradrenergic signaling and working memory

Cognition and increases in working memory have been linked to activation of the prefrontal cortex, a brain region involved in executive functions including working memory and attentional set-shifting (Jäkälä, 1999). Noradrenergic innervation of the prefrontal cortex is necessary for the functional role of the PFC (Jäkälä, 1999). Noradrenaline enhances PFC function through activation of α_{2A}-AR in mice, rats, monkeys, and humans (Ramos et al., 2006). It is thought that this is through noradrenaline acting upon α_{2A}-receptors results in closing of HCN channels increasing efficiency of synaptic connections in the PFC and improving working memory (Arnsten and Jin, 2012).

Catecholamine deficiency induced by infusion of 6-hydroxydopamine resulted in impaired accuracy on a delayed response tasks in monkeys. This impairment was improved with administration of α_{2A}-AR agonists, clonidine or guanfacine (Jäkälä, 1999). Decreased levels of noradrenaline in aged monkeys are hypothesized to underlie defects in working memory. Guanfacine was shown to improve memory of aged monkeys without the negative effects such as sedation often seen with other α-receptor agonists including clonidine. The effects of guanfacine on delayed response tasks often lasted for several days following a single injection. This improvement is prevented with prior administration of α_2-AR antagonist, providing support for α_2-ARs underlying the effects of guanfacine (Arnsten et al., 1988). Similarly, studies in humans have provided evidence for guanfacine's ability to improve working memory. Using various tasks to measure spatial working memory, planning and attentional set-shifting, guanfacine was shown to enhance performance on spatial working memory and planning tests with no effects on attentional set-shifting performance tasks (Jäkälä, 1999). These results differed from the effects of clonidine on the tasks potentially due to guanfacine's greater selectivity for α_{2A}-receptors over other α_2-receptors.

1.9 Noradrenergic signaling and addiction

A role for noradrenergic signaling during acute and protracted withdrawal of drugs of abuse has been well documented (Aston-Jones et al., 1999; Buffalari et al., 2012; Delfs et al., 2000; Fuentealba et al., 2002; Harris and Aston-Jones, 1993; Trzaskowska and Kostowski, 1983). Brain levels of noradrenaline originate from the brain stem and the locus coeruleus of the dorsal pons. Noradrenaline acts upon three types of receptors, alpha1-, alpha2- and beta-adrenergic receptors, with further delineation into subtypes of each. Pharmacological inhibition or activation of these receptors has been heavily studied for their effects on withdrawal of various drugs of abuse including morphine, nicotine, and alcohol.

Clonidine, an alpha2-AR agonist, has been heavily studied as a modifier of stress-induced reinstatement of drug seeking behavior. Its actions include decreased reinstatement of cocaine, opiate, alcohol and nicotine (Erb et al., 2000; L et al., 2005; Shaham et al., 2000; Zislis et al., 2007). Alternatively, the alpha2 antagonist, yohimbine, reinstates drug seeking behavior. Yohimbine also exacerbates withdrawal symptoms (Trzaskowska and Kostowski, 1983).

1.9.1 Noradrenergic signaling in the BNST and addiction

The BNST receives one of the densest noradrenergic projections originating from the nucleus tractus solitarius (NTS) of the ventral noradrenergic bundle (Banihashemi and Rinaman, 2006; Egli et al., 2005; Flavin et al., 2014a; Forray and Gysling, 2004; Ricardo and Tongju Koh, 1978; Shields et al., 2009a). Additionally, the BNST receives a sparse noradrenergic input from the locus coeruleus. The vBNST is densely innervated by alpha1-AR- and alpha2-AR-expressing noradrenergic cells, which can influence both excitatory and inhibitory transmission. Stimulation of the ventral noradrenergic bundle results in noradrenaline release in the BNST as measured by *in vivo* fast-scan cyclic voltammetry (Park et al., 2019) . Noradrenergic and non-noradrenergic inputs to the BNST are altered by several pharmacological agents that target adrenergic receptors (Flavin et al., 2014a; Harris et al., 2018; Perez et al., 2020a). In addition, axons from the PBN form peri-somatic connections with BNST neurons and these synapses are regulated by noradrenergic signaling (Fetterly et al., 2019; Flavin et al., 2014a).

Interestingly, adrenergic signaling through alpha1- and alpha2-adrenergic receptors has been shown to both decrease excitatory (Dumont, 2004; Egli et al., 2005; Fetterly et al., 2019; McElligott and Winder, 2008; Shields et al.,

2009a) and inhibitory drive onto the BNST (Shields et al., 2009a). Specifically, alpha2-adrenergic receptor inhibition of glutamatergic synaptic transmission in the BNST occurs through alpha2a-activation (Egli et al., 2005). Conversely, signaling through beta-adrenergic receptors enhances both excitatory (Egli et al., 2005; Nobis et al., 2011) and inhibitory (Dumont, 2004) drive onto neurons in the BNST. Noradrenergic signaling has been shown to modulate CRF and glutamate signaling in the BNST (Nobis et al., 2011; Shields et al., 2009a; Silberman et al., 2013). Isoproterenol, a beta-AR agonist, results in increased excitability of BNST neurons through increased spontaneous (Nobis et al., 2011) and evoked excitatory synaptic events (Egli et al., 2005).

Guanfacine, an alpha2a-adrenergic receptor partial agonist, inhibits glutamatergic input from the PBN onto CRF+ neurons in the BNST (Fetterly et al., 2019; Flavin et al., 2014a). Both noradrenaline and guanfacine reduce glutamatergic transmission from the PBN onto CRF-positive neurons in the BNST (Fetterly et al., 2019). Conversely, guanfacine has no effect on glutamatergic transmission from the BLA or insula, suggesting input-specific effects of noradrenergic modulation (Fetterly et al., 2019; Flavin et al., 2014a).

Noradrenergic inputs onto BNST neurons are activated during drug withdrawal (Aston-Jones et al., 1999; Delfs et al., 2000). Activation of these inputs during withdrawal or stress results in noradrenaline release in the BNST that has been associated with changes in behavior. Ethanol dose-dependently increases norepinephrine release from the BNST (Jadzic et al., 2021). Isoproterenol increases spontaneous glutamatergic transmission in the BNST through activation of beta1-adrenergic receptors in a CRFR1-dependent mechanism (Nobis et al., 2011). This effect occurs through activation of glutamatergic synapses not affected by dopamine and is occluded by repeated *in vivo* exposure to cocaine. This and several other studies have shown a role for noradrenergic signaling in the BNST and the effects of drugs of abuse. Inhibition of beta-adrenergic signaling in the BNST prevented stress-induced reinstatement of conditioned place preference (CPP) while activation of beta-adrenergic signaling caused reinstatement of CPP (Vranjkovic et al., 2012). It was later shown that beta-receptor adrenergic signaling modulates CRF signaling in the BNST onto downstream VTA neurons and is critical for stress-induced cocaine seeking behavior (Vranjkovic et al., 2014). Stress and chronic alcohol exposure act similarly upon beta-adrenergic receptors to increase neuronal excitability of CRF neurons in the BNST (Snyder et al., 2019). Inhibition of alpha-adrenergic receptor signaling blocks stress-induced reinstatement of heroin seeking behavior (Erb et al., 2000). Signaling through alpha2a heteroreceptors, receptors located on non-noradrenergic

neurons, is necessary for stress-induced reinstatement of drug seeking behavior (Perez et al., 2020a). A low dose of guanfacine, that does not recruit activation of BNST, was shown to block stress induced reinstatement of cocaine conditioned place preference (cCPP) while mimicking activation of alpha2a heterorceptors through Gi-DREADDs (Designer Receptors Exclusively Activated by Designer Drugs) resulted in reinstatement of cCPP (Perez et al., 2020a). Furthermore, post-synaptic alpha2-AR function is decreased in patients during acute and late withdrawal of alcohol (Berggren, 2000). These experiments and others (Brown et al., 2011; McReynolds et al., 2014b, 2014a) provide evidence of a BNST circuit involving neuropeptide and monoamine signaling that underlies stress-induced reinstatement of drug-seeking behavior. BNST activity can directly influence stress responses through direct and indirect connections to the PVN. Noradrenergic signaling in the BNST has been linked to HPA activation and anxiogenic behaviors (Cecchi et al., 2002; Harris et al., 2018).

1.10 Development of Guanfacine, an alpha2a-AR partial agonist

Guanfacine (brand name Tenex) was originally developed by Promius Pharma as an antihypertensive agent. It was approved by the FDA in 1986. Preclinical studies using anesthetized dogs showed that arterial or intravenous infusion of guanfacine reduced blood pressure within 40 minutes of infusion (Scholtysik, 1986). Reduced sympathetic nerve activity was seen following guanfacine administration in anesthetized cats (Scholtysik, 1986; Sorkin and Heel, 1986). Sympathetic nerve activity has been attributed specifically to central inhibition of sympathetic tone providing evidence that guanfacine acts through this mechanism. Intracerebroventricular injection reduced blood pressure and heart rate but was not effective when giving intravenously. This effect was blocked by pretreatment with α_2-AR antagonist (Sorkin and Heel, 1986). Guanfacine has been shown to alter norepinephrine turnover, a result of central α-AR stimulation, providing evidence that the effects of guanfacine are due to activation of central α-AR. Additionally, studies in cat, rat, rabbit and dog confirmed guanfacine's effects on peripheral α-AR resulting in prolonged decrease in blood pressure (Scholtysik, 1986). In 1982, the antihypertensive effects of guanfacine were studied in a two-month trial with 25 male patients with hypertension. Ten of the 25 patients developed normalized blood pressure within 15 days of guanfacine treatment, while 12 patients required higher doses to normalize blood pressure within the two months(Safar et al., 1982). In 1980, a long-term clinical study was performed that involved 580 and 169 patients treated with

guanfacine for one year or two years, respectively. The main side effect of guanfacine treatment was dryness of the mouth and slight sedation at the beginning of treatment (Jerie, n.d.). These effects were less likely at lower doses of guanfacine.

In vitro experiments using isolated rabbit hearts and atria from guinea pigs also confirmed guanfacine's effects on central and peripheral α-AR. Studies using pithed rats and isolated dog blood vessels provided evidence to support the selectivity of guanfacine on pre-synaptic α_2-AR (Scholtysik, 1986). It was shown in several human clinical trials that guanfacine decreased blood pressure in patients suffering from mild to moderate hypertension. It was shown to decrease peripheral resistance and slight reduction in heart rate without altering cardiac output at rest or during physical activity. To determine the affinity of guanfacine to each α_{2A}-AR, radioligand binding with [^{3}H]-guanfacine was used to characterize α_{2A}-AR binding sites in dissociated rat cerebral cortex membranes (Jarroit et al., n.d., p. 3). The resulting scatchard plot is linear suggesting a single population of binding sites with average B_{max} of 118.2 ± 8.4 [^{3}H]-guanfacine fmol/mg protein and an average K_d of 1.77 ±0.24 nM (Jarroit et al., n.d., p.). Hill plot analysis did not indicate cooperativity in binding. Binding of [^{3}H]-guanfacine was measured across various areas of the brain. In order of binding the cerebral cortex had the highest amount of binding followed by hippocampus, thalamus, hypothalamus, medulla/pons, spinal cord, striatum, and cerebellum having the least amount of binding (Jarroit et al., n.d., p.).

To investigate the affinity of guanfacine for α-AR, a competition binding assay was used to measure the effects of α-AR antagonists and agonists on displacement of [^{3}H]-guanfacine binding. The most potent α-AR agonists were naphazoline and clonidine. In terms of antagonists, those specific to α_2-AR receptors were most effective further confirming guanfacine's specificity to α_2-AR. The most potent antagonists were phentolamine and dihydroergocryptine. Drugs targeting other adrenergic receptors including β_1- and β_2-AR antagonists and agonists were ineffective at displacing [^{3}H]-guanfacine, similar to drugs targeting other neuronal receptors including cholinergic, opioid, or histamine. Monoamine oxidase (MAO), catechol-O-methyl transferase (COMT) or neuronal uptake inhibitors were also unable to remove [^{3}H]-guanfacine. Finally, adrenergic neuron blockers guanethidine and debrisoquine that reduce noradrenaline release did not have an effect on [^{3}H]-guanfacine binding.

Guanfacine HCl or INTUNIV was approved by the FDA in 2009 for childhood and adolescent ADHD. It is currently not a treatment for adults with ADHD. The exact mechanisms underlying the mechanism with which guanfacine helps

ADHD is unknown. It is hypothesized that guanfacine activation of α_{2A}-receptors in the prefrontal cortex (PFC) underlie its effects on ADHD. cAMP analogs, used to mimic the effect of cAMP, blocked the ability of guanfacine to improve PFC cognitive function using delayed alternation performance in aged rats. Similarly in monkeys, administration of rolipram, a PDE4 inhibitor that results in increased levels of cAMP, prevented guanfacine from improving working memory(Ramos et al., 2006). These studies provide evidence that the ability of guanfacine to improve working memory relies on decreases in cAMP signaling in the PFC. Guanfacine or INTUNIV target the α_{2A}-AR with a 15-20 times higher selectivity for α_{2A}-AR over α_{2B}- or α_{2C}-AR. It is hypothesized that its actions on α_{2A}-AR in the prefrontal cortex underlie the therapeutic effect on those with ADHD (Huss et al., 2016). In neuroimaging studies, guanfacine was shown to increase blood flow in the PFC while improving working memory (Alamo et al., 2016).

1.10.1 Pharmacokinetics

In vitro studies using rabbit isolated hearts produced evidence that guanfacine reduced norepinephrine release following sympathetic nerve stimulation(Pacha et al., 1975). The effects of guanfacine on sympathetic nerve activation was investigated using anesthetized cats. Guanfacine resulted in a decrease in preganglionic sympathetic nerve activity supporting its role in central inhibition of sympathetic tone. Guanfacine does not result in altered levels of norepinephrine levels specifically. However, following blockade of norepinephrine synthesis with diethyldithiocarbamate, guanfacine prevents the diethyldithiocarbamate-induced decrease in norepinephrine synthesis (Scholtysik, 1986). Further supporting that guanfacine acts upon central α-AR to decrease sympathetic tone.

The efficacy of guanfacine at treatment for ADHD in children was investigated through several clinical trials, including placebo-controlled monotherapy trials and adjunctive trial with psychostimulants in the United States, Europe, and Canada (J. Biederman et al., 2008; Joseph Biederman et al., 2008; Connor et al., 2010; Hervas et al., 2014; Huss et al., 2016; Newcorn et al., 2013; Sallee et al., 2009b, 2009a; Wayne, 2010; Wilens et al., 2017, 2012). The monotherapy trials researched the effects of fixed-doses or dose-ranging for dose-optimization studies on children and adolescents diagnosed with ADHD whose ages ranged from 6-17 or 6-12 years (J. Biederman et al., 2008; Joseph Biederman et al., 2008; Connor et al., 2010; Hervas et al., 2014; Huss et al., 2016; Newcorn et al., 2013; Sallee et al., 2009b, 2009a; Wayne, 2010). Similarly, the adjunctive therapy trials investigated the effects of ranges of doses for dose-optimization

on children and adolescents ages 6-17 years diagnosed with ADHD and a suboptimal response to stimulants alone (Childress, 2012; Wilens et al., 2017, 2012). ADHD signs and symptoms were determined based on ADHD Rating Scale (ADHD-RS-IV) administered and scored by a clinician on a weekly basis. The efficacy outcome used was change from baseline to endpoint on the ADHD-RS-IV scale where endpoint was defined as the score for the last post-randomization treatment week obtained before dose tapering. These trials resulted in statistically significant mean reductions in ADHD-RS-IV scores at end point compared to baseline in the guanfacine treated groups compared to placebo. Overall, these clinical trials show that guanfacine is effective as a potential treatment for ADHD in children and adolescents as a sole therapy or in conjunction with stimulants (J. Biederman et al., 2008; Joseph Biederman et al., 2008; Connor et al., 2010; Hervas et al., 2014; Huss et al., 2016; Newcorn et al., 2013; Sallee et al., 2009b, 2009a; Wayne, 2010; Wilens et al., 2017, 2012).

1.10.2 Absorption

A schematic overview for the absorption, distribution, metabolism, and elimination of guanfacine is shown in Figure 4. The oral bioavailability of guanfacine is about 80%. Plasma concentrations reach their peak around 1-4 hours (average 2.6 hours) after single dose or at steady state (Sorkin and Heel, 1986). Liquid chromatography-tandem mass spectrometry (LC-MS/MS) was used to quantify plasma concentrations in plasma of beagle dogs following administration of 4 mg oral dose of guanfacine(X. Li et al., 2013). The maximum concentration of guanfacine (C_{max}) was calculated as 5.72 ±1.78ng/mL occurring at a time (T_{max}) of 3.08 ±1.63 hours following administration. The AUC was measured as 44.14 ±17.19 ng/mL h with a half-life around 2.6 ±17.19 hrs. The apparent volume of distribution was 395.52 ± 302.96 L and an oral clearance of 100.84 ± 33.62 L/hr. As compared to human trials, the T_{max} was shorter and the C_{max} was higher.

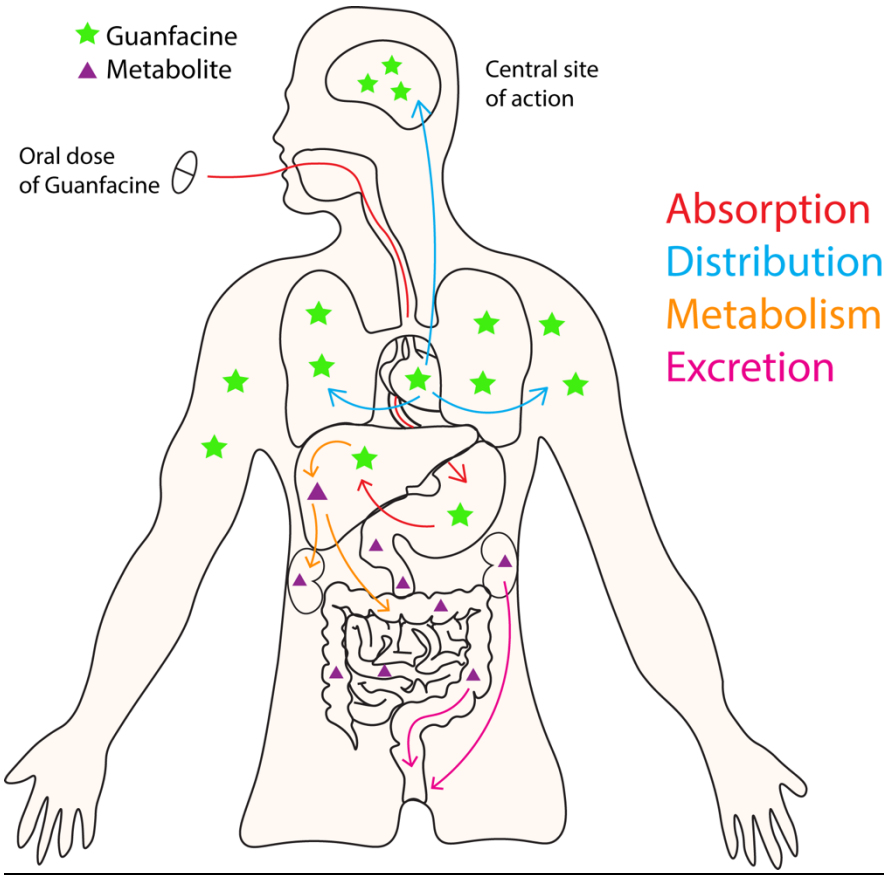

Figure 4. Absorption, distribution, metabolism, and excretion (ADME) of Guanfacine.

Following oral dose of guanfacine, it undergoes first pass metabolism by the liver. It is highly distributed to tissues with a high volume of distribution and low plasma binding. Guanfacine is distributed to its central site of action is the brain. It is metabolized in the liver around 50% by CYP3A4. It is primarily excreted in urine.

Exposure to guanfacine was measured in children ages 6-12 and adolescents 13-17. Administration of a single 2 mg dose of guanfacine extended release revealed higher levels of plasma concentration levels, C_{max} and AUC in children compared to adolescents (Boellner et al., 2007). Similar T_{max} was calculated for children and adolescents, 4.98 and 4.96 hours respectively. After multiple daily doses of 2 mg, the AUC was calculated as 70.0 ± 28.3 and 48.2 ± 16.1 ng•hour/ml in children and adolescents, respectively. The C_{max} was calculated as 4.39 ± 1.66 ng/ml in children and 2.86 ± 0.77 ng/ml in adolescents. After dosing with 4 mg, the C_{max} and AUC were doubled. The C_{max} was 10 ng/mL with AUC of 162 ng/mL and 7 ng/mL with an AUC of 116 ng/mL in children and adolescents respectively (Boellner et al., 2007; Cruz, n.d.; Wayne, 2010).

1.10.3 Distribution

In preclinical studies using animals, equilibrium dialysis was used to measure protein binding following guanfacine administration. Low levels of plasma protein binding were found. Oral and intravenous doses of [^{14}C]-guanfacine in animals revealed significant distribution to highly perfused organs and a large volume of distribution (300L). The highest levels of plasma concentration of guanfacine were measured 1.5-2 hours following oral administration with minimal levels detected 24 hours after administration. Interestingly, the highest levels of [^{14}C]-guanfacine in the brain were measured 4 hours after administration. Absolute bioavailability was close to 100%. In pregnant animals, [^{14}C]-guanfacine crossed the placental barrier and was found in the fetus's intestines. Additionally, low levels were measured in the mother's milk.

Clinical studies revealed around 70% of guanfacine is bound to plasma proteins regardless of drug concentration. More [^{14}C]-guanfacine was bound to red blood cells than plasma proteins in human and rat studies. Guanfacine has a high volume of distribution with a mean of 6.3 L/kg. Wide distribution was seen in healthy subjects and in hypertensive patients (Sorkin and Heel, 1986).

1.10.4 Metabolism

Guanfacine is mainly metabolized by the liver. The majority of metabolism occurs through oxidative metabolism of the aromatic ring. [^{14}C]-guanfacine was given to rats and dogs orally and intravenously to investigate metabolism of guanfacine. Unmetabolized drug was measured by gas chromatography-mass spectrometry. Drug metabolites were measured by high pressure liquid chromatography from urine samples. In rats and dogs, 15 metabolites of guanfacine were identified. One of the first human studies to measure metabolism of guanfacine administered a 3 mg oral dose or 2.3 mg intravenous dose of [^{14}C]-guanfacine to fourteen men with an average age of 73 and a mean body weight of 130 pounds (Kiechel, 1980). Radioactivity of parent drug plus metabolites was measured in urine, erythrocytes, and plasma samples. Parent drug was also measured using gas chromatography-mass spectrometry. Metabolites were measured using high pressure liquid chromatography. Absolute bioavailability in man was ~100%, similar to results in animals. The kinetics of guanfacine metabolism was determined to be modeled by two-compartment. Guanfacine is a substrate of CYP3A4 and CYP3A5, and fifty percent of the drug is metabolized by the cytochrome P-450 3A4 (Bridgewater, 2006;

Wayne, 2010). In vitro studies using isolated human liver microsomes and recombinant CYP enzymes found that guanfacine did not inhibit the activity of the major cytochrome P450s including CYP1A2, CYP2C8, CYP2C9, CYP2C19, CYP2D6, or CYP3A4/5 (Wayne, 2010). Therefore, dosing with inducers and inhibitors of these enzymes will alter drug exposure and should be considered.

1.10.5 Elimination

In animals, the major route of excretion was through urine. Regardless of route of administration, around 75% of original dose in dog was found in urine. The elimination half-life was around 17 hours (Kiechel, 1980; Saameli et al., 1982; Strange, 2008). Minimal levels of [^{14}C]-guanfacine was found in dogs or rats 24 hours after administration.

In the previously described study in humans, the half-life was estimated around 17.1-21.4 hours with a clearance of 11 L/h with around 33-35% through renal elimination (Kiechel, 1980). The half-life of guanfacine increases with age of patients. Steady state levels of guanfacine are often obtained within 4 days of dosing. Guanfacine is mainly excreted in the urine with 50% of the dose eliminated as unchanged drug. The drug is poorly dialyzed and is not affected by patients on dialysis (Bridgewater, 2006; Cruz, n.d.; Wayne, 2010).

1.11 Alpha2a agonists as treatment for stress induced reinstatement of drug seeking behavior

α_{2a}-adrenergic receptor (α_{2a}-AR) agonists are candidate substance use disorder therapeutics in part due to their ability to recruit noradrenergic autoreceptors to dampen stress system recruitment. However, α_{2a}-ARs postsynaptic to the noradrenergic terminal are required for stress-induced reinstatement of cocaine-conditioned behavior. Understanding the cells recruited by these postsynaptic receptors is necessary to understand reinstatement biology and develop more effective therapeutics. This led to the hypothesis that the cells activated by guanfacine through post-synaptic α_{2a}-AR had pro-reinstatement effects and were dynamically regulated by stress. This topic is investigated in the next chapter adapted from *Brown et al. 2022*, titled "An ensemble recruited by α_{2a}-adrenergic receptors is engaged in a stressor-specific manner in mice."

CHAPTER 2

An ensemble recruited by α_{2a}-adrenergic receptors is engaged in a stressor-specific manner in mice.

Adapted from: Brown et al. 2022 Neuropsychopharmacology

2.1 Introduction

G-protein coupled receptors (GPCRs) sculpt the activity of neural circuits to shape organism behavior. Systemic administration of GPCR ligands is a commonly considered therapeutic strategy, yet this approach often suffers from side effects brought on by recruitment of receptor populations ectopic to the targeted receptor. Identifying specific cell populations involved in receptor actions is needed to drive improved therapeutic targeting and increase understanding of the relevant biology. Ligands targeting adrenergic receptor signaling, including α_{2a}-adrenergic receptor (α_{2a}-AR/*adra2a*) agonists and antagonists, are clinically utilized in a variety of contexts including substance use disorder (SUD) therapeutics and stress disorders(Buffalari et al., 2012; Gowing et al., 2004; Harmon and Riggs, 1996; Milivojevic et al., 2020; Pergolizzi et al., 2019; Simpson et al., 2018, p., 2015). Stress is cited as a common risk factor for development and relapse of SUDs(Sinha, 2008, 2007, 2001) and is thought to play a role in exacerbating and/or initiating other psychiatric conditions. In rodent models α_{2a}-AR agonist administration blocks stress-induced reinstatement to cocaine seeking behavior(Erb and Stewart, 1999; Mantsch et al., 2010; Sinha, 2007). Guanfacine, an α_{2a}-AR partial agonist, has been clinically investigated as a potential treatment for prevention of stress-induced relapse to cocaine and opiates and post-traumatic stress-disorder (PTSD) (Fox and Sinha, 2014; Fox et al., 2014, 2012; Krupitsky et al., 2013). Guanfacine has been shown to decrease symptoms associated with PTSD in children and adolescents(Anderson et al., 2020; Horrigan, 1996). However, the trials for adults have been less positive(Connor et al., 2010; Davis et al., 2008). Recent evidence suggests this effect of guanfacine may be due to differential expression of presynaptic and postsynaptic α_{2a}-AR receptor expression in the bed nucleus/nuclei of the stria terminalis (BNST/BST)(Harris et al., 2018; Perez et al., 2020b), warranting further investigation.

The BNST receives one of the densest noradrenergic inputs in the CNS and this transmitter's signaling has been shown to be critical for stress-induced reinstatement of drug-seeking behavior(McElligott and Winder, 2009; Pina et al.,

2015; Shields et al., 2009b; Vranjkovic et al., 2017; Wenzel et al., 2014). We recently observed that while a low dose of guanfacine blocks stress-induced reinstatement of cocaine conditioned place preference (cCPP) in mice, it does not elicit cFos expression in the BNST while a higher dose produces neuronal activation via postsynaptic α_{2a}-AR heteroceptors(Harris et al., 2018; Perez et al., 2020b). Mimicking postsynaptic heteroceptor activation in the BNST, via Gi-DREADD (Designer Receptor Exclusively Activated by Designer Drugs), resulted in increased cFos expression in the BNST and reinstatement of cCPP(Harris et al., 2018; Perez et al., 2020b). Our previous data highlight a population of α_{2a}-AR expressing cells in the BNST that are recruited by guanfacine and play a role in reinstatement of stress-induced reinstatement of cCPP.

Here, we utilize a pharmacogenetic strategy to isolate and study this guanfacine-activated neuronal ensemble in the BNST using a tamoxifen-inducible, activity-driven Cre line (FosTRAP, Targeted Recombination in Active Populations) in conjunction with Cre-dependent viruses(DeNardo et al., 2019; Guenthner et al., 2013). To simplify the verbiage to describe this guanfacine-recruited ensemble, we here shorten the term to “Guansemble”. This experimental paradigm allows us to study TRAPed cells activated by guanfacine but removes the off-target effects of systemic injection of pharmacological compounds. We use convergent approaches to characterize this guanfacine-recruited ensemble or Guansemble, demonstrating competing roles of guanfacine and stress in the regulation of cAMP-dependent kinase signaling as well as neuronal activity. We show afferent circuit inputs to these cells and demonstrate task-specific anxiety-like behavior produced by optogenetic stimulation. Our investigation into these cells known to underlie a reinstating effect of drug seeking behavior will inform the field about how we can modify current pharmacotherapies to modulate the interplay of stress and reinstatement.

2.2 Methods

Subjects

$Fos^{CreERT2}$ mice were obtained from Jackson Laboratory [line #021882] and maintained as heterozygous on a C57BL/6J background. Homozygous $Fos^{iCreERT2}$ mice were obtained from Jackson Laboratory [line # 030323] and were backcrossed at least 3 generations to C57BL/6J mice before being crossed to homozygosity. Heterozygous CRF-Rosa mice were bred in house by crossing CRH-IRES-Cre mice (Jax, line #012704) with Rosa-tdTomato Ai14 mice (Jax, line

#007914). Homozygous SOM-Rosas, bred from SOM-IRES-Cre mice (Jax, line #013044) crossed with Rosa-tdTomato Ai14 mice (Jax, line #007914), were generously donated by Dr. Sachin Patel. Heterozygous BAC transgenic mice expressing Cre recombinase under the promotor Drd1a (FK150, GENSAT) were generously donated from Dr. Jeffrey Conn for experiments(Gong et al., 2007; Joffe et al., 2018, 2017). C57BL/6J mice were obtained from Jackson Laboratory and acclimated for at least one week before experimental procedures. All transgenic mouse lines were bred in house and genotyped using primers designed by Jackson Laboratories or lab designed primers targeting Cre recombinase (Fwd: GGTCGATGCAACGAGTGA, Rev: CCCTGATCCTGGCAATTT). All mice were group housed with 2-5 mouse per cage and maintained on 12-hour light/dark cycle (lights on from 0600 to 1800 h) under controlled temperature (20 –25°C) and humidity (30–50%) levels. Water and food were provided ad libitum except for experiments requiring deprivation. Male and female mice, >8 weeks of age, were used in all experiments to minimize animal numbers. There were no sex differences found in the initial amounts of TRAPed cells following guanfacine injection (Figure 6F), therefore males and females were combined for the rest of experiments. Additionally, there were no sex differences found across *in vivo* calcium activity responses to guanfacine or restraint stress (Figure 10B-C).

Reagents

Guanfacine hydrochloride (Tocris) was made fresh before use at 0.5 mg/mL in 0.9% saline and delivered intraperitoneally at a dose of 1 mg/kg. SKF81297 (Tocris) was made in 0.9% saline and delivered intraperitoneally at a dose of 3 mg/kg. 4OHT was purchased from Sigma Aldrich or Tocris Pharmaceuticals. 4OHT was diluted with 100% EtOH at 10 mg/mL at 37˚C shaking in water bath overnight. 4OHT was either aliquoted into 50µl aliquots for further use or diluted with a dilution ratio of 1:4 with corn oil, warmed to 37˚C in shaking water bath. Diluted 4OHT was returned to the shaker for at least 30 minutes until completely mixed. 4OHT was loaded into syringe with a 25- or 26-gauge needle, kept warm and out of light, and administered at 50 mg/kg. For GCaMP imaging, Guanfacine stock solutions were prepared at a concentration of 10mM in water and diluted to 10µM in aCSF the day of recording.

Stereotaxic surgeries

Virus injections

Mice that were at least 8 weeks of age were used for virus injection studies. Mice were anesthetized with isoflurane (initial dose 3%; maintenance dose 1.5%) and injected with viral constructs using Leica Angle Two Small Animal Stereotaxic Instrument. 300nL of virus were injected unilaterally or bilaterally into the dBNST (AP:0.14, ML: 0.88 DV: -4.18; 15.03° angle) or Striatum (AP:0.26, ML:1.76, DV: -3.15) at a rate of 50 nL/min (Fetterly et al., 2019; Harris et al., 2018; Luchsinger et al., 2021; Perez et al., 2020b).. The syringe remained in place for five minutes after injection to increase viral uptake. Mice were treated with 5 mg/kg Ketoprofen or 2.5 mg/kg Metacam for 48-hour post-surgery. Except for rabies injections, mice were allowed to recover for at least 3 weeks prior to the start of experimentation to allow for optimal viral expression. It should be noted that while our initial experiments confirmed the stability of Guansembles over 1-2 weeks, this response to guanfacine was measured 4 weeks after initial TRAPing to ensure sufficient viral expression. However, our results showing an excitatory effect of guanfacine on calcium activity, similar to increase in activity measured by initial cFos expression, supports the stability of the Guansemble.

Implant surgeries

Mice were injected with 300nL of virus unilaterally as described above, proceeded by implantation of a fiber implant, described previously(Jaramillo et al., 2020; Luchsinger et al., 2021). The corresponding implant (opto: 400 μm ceramic fiber implant (RWD Life Science, Ø1.25 mm, 200μm Core, 0.50NA, 4 mm); photometry: 400 μm mono fiberoptic cannula, (Doric lenses, MFC_400/430-0.66_4.1mm_MF2.5_FLT)) was placed 0.1mm above the virus D/V coordinates. The implant was secured using Optibond primer and Optibond adhesive followed by Herculite enamel.

Rabies injections

Following unilateral dBNST injection of rabies helper viruses (TREtight-mTagBFP2-B19G and syn-FLEX-splitTVA-EGFP-tTA), mice were allowed to recover from surgery for three days before beginning the five-day handling protocol and subsequent TRAP procedure. Ten days after the TRAP procedure (described below), EnvA-deleted-rabies-mCherry was injected into the same BNST coordinates as the helper viruses. One week later, mice were transcardially perfused following SHIELD (Stabilization under Harsh conditions via Intramolecular Epoxide Linkages to prevent Degradation) protocol(Park et al., 2019).

Viruses

For guanfacine trapping, we injected 300 nL of AAV-hSyn-DIO-mCherry (Addgene) bilaterally into the dBNST. For *in vivo* recordings of PKA activity using FLIM, we injected 300nL of Cre-dependent AAV1-CAG-FLEX-FLIM-AKAR (AKAR3.4, Dr. Sabatini) unilaterally into the striatum of D1-cre or rBNST of FosTRAP mice. For GCaMP *in vivo* fiber photometry, we did 300nL unilateral injections of AAV9-syn-FLEX-jGCaMP7f-WPRE (Addgene) into the rBNST. For rabies injections, helper viruses, TREtight-mTagBFP2-B19G and syn-FLEX-splitTVA-EGFP-tTA (Addgene), were diluted 1:20 and 1:200(Lavin et al., 2020; Luchsinger et al., 2021), respectively, in sterile, filtered PBS, and subsequently mixed 1:1 and 300nL were injected unilaterally into the rBNST. Following helper virus injection and guanfacine TRAPing, EnvA-G-deleted-rabies-mCherry (300nL, Salk) was injected into the rBNST. For *in vivo* optogenetic experiments, 300nL of AAV5-Ef1a-DIO-eYFP (Addgene) or AAV5-Ef1a-DIO-hChR2(H134R)-EYFP-WPRE-pA (UNC) was injected unilaterally into the rBNST.

Viral targeting validation

Following experiments, mice were assessed for virus and implant verification using standard immunohistochemistry (IHC) procedures or BLAQ. If virus or implant placement was incorrect or if there was no virus, often due to a poor 4-OHT injection, the animal was excluded from analysis.

Fluorescent immunohistochemistry

Mice were anesthetized using isoflurane and perfused transcardially with at least 10 mL cold 1X PBS followed by 15 mL 4% paraformaldehyde (PFA). Brains were extracted and incubated in 4% PFA for 24 hours at 4°C and cryoprotected in 30% sucrose in PBS for a minimum of two days. Coronal slices were obtained at 40μM on a cryostat (Leica, CM3050S) in Optimal Cutting Temperature (OCT) solution. Slices were stored in PBS at 4°C until immunohistochemistry was performed. Fluorescent immunohistochemistry was performed as previously described(Fetterly et al., 2019; Harris et al., 2018; Perez et al., 2020b). Briefly, slices were incubated for 30 minutes in 0.5% PBST (0.5% Triton X-100 in PBS) followed by blocking for 1 hour in 0.1% PBST (0.1% Triton X-100 in PBS) and 10% Normal Donkey Serum (NDS). Slices were then incubated in fresh blocking solution with primary antibodies for 3-4 days at 4°C. Primary antibodies used in these studies were rabbit anti-cFos at 1:1000 dilution, chicken anti-GFP at 1:1000 dilution, and mouse anti-PKCd at 1:1000 dilution. Following primary antibody incubation, slices were washed four times in PBS and incubated in 0.1% PBST containing secondary antibodies. Secondary antibodies used in these studies were

Cy5 donkey anti-mouse (Jackson ImmunoResearch), Alexa Fluor Plus 647 donkey anti-rabbit (Thermo Scientific), Cy2 donkey anti-rabbit (Jackson ImmunoResearch), Cy2 donkey anti-chicken (Jackson ImmunoResearch) and Cy5 donkey anti-chicken (Jackson ImmunoResearch), at a dilution of 1:400 in 0.1% PBST. Following secondary antibody incubation, slices were washed three times in PBS followed by an incubation of DAPI (1:10,000) in PBS for 10 minutes. Slices were moved to PBS before mounting on Fisher plus slides (Fisher Scientific) and coverslipped with PolyAquamount when dry. All images were obtained with a Zeiss LSM 710 scanning confocal microscope using a 20X/0.80 N.A. Plan-Apochromat objective lens.

Brain Blocking of Lipids and Aldehyde Quenching (BLAQ)

For validation of virus expression and targeting following *ex vivo* GCaMP imaging and optogenetic electrophysiology, the Brain Blocking of Lipids and Aldehyde Quenching (BLAQ) procedure was used as described previously(Harris et al., 2018; Kupferschmidt et al., 2015; Perez et al., 2020b). Following *ex vivo* imaging or electrophysiology, slices were incubated in 4% PFA for 30 minutes at room temperature followed by overnight incubation at 4˚C. The following day, slices were transferred to PBS at 4˚C before undergoing BLAQ staining for validation and targeting. Sections were washed for 1 hour in 0.2% PBST (0.2% Triton X-100 in PBS), rinsed twice for 1 minute in diH2O, and quenched in freshly prepared sodium borohydride (NaBH4; 5 mg/mL in diH2O; Sigma-Aldrich, #213462, 99%). Following this incubation, slices were rinsed again in diH2O (twice for 1 minute each), incubated for 15 minutes in Sudan Black B solution (0.2% in 70% ethanol), washed twice for 30 minutes each in PBS, and incubated for 4 hours in 5% BSA in 0.2% PBST. Slices were incubated in primary antibody (chicken anti-GFP 1:1000 dilution, Abcam Ab13970) for 96 hours at 4°C, washed 4 times in 0.2% PBST for a total of 24 hours at 4°C, and then incubated in secondary antibody (Cy5 donkey anti-chicken 1:400 dilution, Jackson ImmunoResearch) for 48 hours at 4°C. Finally, slices were washed 4 times in 0.2% PBST for a total of 24 hours at 4°C, including a 10 minute DAPI incubation (1:10,000 in PBS), moved to PBS and then mounted on Fisher Plus slides and coverslipped with PolyAquaMount when dry. All images were obtained with a Zeiss LSM 710 scanning confocal microscope using a 10x/0.50 N.A. Plan-Apochromat objective lens. The same acquisition parameters and alterations to brightness and contrast in Zeiss were used across all images within an experiment.

Guanfacine TRAPing

TRAP protocol

Mice were handled for at least 5 days prior to injection as described previously(Olsen and Winder, 2010). To habituate the mice to i.p. injections, mice were given an i.p. injection of saline with a syringe with a 29-gauge needle on day 4 and 25- or 26-gauge needle on day 5 of handling. Following this habituation protocol, mice were administered 50 mg/kg dose of 4OHT and immediately returned to their home cage and corresponding rack in the mouse facility (DeNardo et al., 2019; Guenthner et al., 2013). One hour later, mice received a 0.5 mL/kg saline or 1 mg/kg dose of guanfacine. Mice were then left undisturbed for at least a week.

Restraint stress for cFos quantification

Mice were acclimated in their home cage for an hour in a sound- and light-attenuating box (Med Associates) to habituate to the procedure room. Mice were then placed in 50 mL conical tubes (Falcon) modified with holes to ensure mice were able to breathe during restraint. Conical tubes were then placed in a clean cage containing bedding placed in a separate sound- and light-attenuating box for 1 hour. Mice were then removed from the conical tubes and placed back in their home cage for an additional 30 minutes before being sacrificed for cFos expression(Fetterly et al., 2019).

Fiber photometry

Fluorescence lifetime imaging microscopy (FLIM) setup

Fluorescence lifetime imaging microscopy (FLIM) was recorded using the ChiSquare dual-probe system (ChiSquare Bioimaging, Brookline, MA) as described previously(Harris et al., 2018; Jaramillo et al., 2020). Briefly, blue light from a 473-nm picosecond-pulsed laser (at 50 MHz; pulse width ~80 ps FWHM) was directed through a single mode fiber. Fluorescence emission from the sample was collected by a multimode fiber. The single mode and multimode fibers were arranged side by side in a ferrule connected to a detachable multimode fiber implant(Cui et al., 2013). The emitted photons collected through the multimode fibers are passed through a bandpass filter (FF01-550/88, Semrock) into a single-photon detector. Photons were recorded by the time-correlated single photon counting (TCSPC) model (SPC-130EM, Becker and Hickl, GmbH, Berlin, Germany) in the ChiSquare dual-probe system.

The principle of fluorescence lifetime determination using time-correlated single photon counting (TCSPC), as described previously(Becker, 2021, 2005; O'Connor, 2014), is implemented in the ChiSquare system using pico-second pulsed laser technology. Fluorescence lifetime of FLIM-AKAR was determined using a time-domain and outputted through SPCM software (Becker and Hickl). Data was acquired using a 473 pico-second pulsed laser at a frequency of 50 MHz, and emitted photons of the FRET-donor was detected on an average at a rate of $1.4x10^{10}$ kHz. Each decay curve is an accumulation of around 17 nanoseconds of photons and decay curves are acquired at an interval of 60 seconds. Fluorescence decay kinetics were analyzed using SPC Image (Becker&Hickl) where an incomplete multiexponential decay model was fitted to the data, yielding the lifetime of the donor. Before beginning each experiment, a standard fluorescence decay curve of 5 µM fluorescein solution (Thermo Fisher Scientific, Fluorescein – NIST – Traceable Standard) was acquired and its lifetime was used as reference.

GCaMP fiber Photometry setup

A TDT RZ5P fiber photometry system and Synapse software were used for GCaMP fiber photometry as described previously(Jaramillo et al., 2020; Luchsinger et al., 2021; Salimando et al., 2020). Briefly, light from a 470nm and 405nm fiber-coupled LED were modulated at 210 Hz and 530 Hz, respectively, and power output was maintained at 40mA with a DC offset of 10mA. A power output of 80-100 µW was maintained at the tip of a 400µm mono fiberoptic cannula in the BNST (Doric Lenses) connected to low-autofluorescence 0.57NA mono fiberoptic patch cord with a 400µm diameter core (Doric Lenses). Signal was collected at 1 kHz and low pass filtered at 6 Hz. The 405nm channel was used as an isosbestic, calcium-independent control wavelength for GCaMP to offset any bleaching or movement artifacts as compared to the calcium-dependent 470 nm channel. Videos were obtained at 10 frames per second through a Logitech HD Pro Webcam (Logitech, C920).

Guanfacine injections

Mice were attached to the recoding system as described above and placed in a small open field chamber for 5-10 minutes, during which baseline recording was obtained. Following baseline measurements, mice were injected with 1 mg/kg dose of guanfacine or 0.1mL saline and returned to the open field chamber an additional 50-60 minutes. If cage mates were run, mice were placed into a fresh cage until all mice in the cage were run.

Stress exposures

To evaluate the effect of Guansemble recruitment with various stressors, we chose to investigate calium activity in Guansembles during exposure to a novel object, restraint stress, and unpredictable foot shocks. We ranked these stressors loosely based on previous papers' reported CORT levels following novelty, restraint stress, and foot shock exposures. Novel object/environment exposure: 100-150 ng/ml (Beerling et al., 2011; Gould et al., 2014; Hennessy, 1991; Moore et al., 2013); Shock exposure: 300 ng/ml (Hajós-Korcsok et al., 2003; Shanks et al., 1990; Wu et al., 2020); Restraint stress: 150-250 ng/ml (Sallinen et al., 1999; Shoji and Miyakawa, 2020) 300 with chronic stress

Novel object exposure

For Novel Object Exposure, mice were attached to the recording system as described above and placed in a small open field arena and allowed to acclimate for 10 minutes, during which baseline recordings were obtained. Following the acclimation period, a novel object (clean AA battery) was placed in the center of the open field. Mice were allowed to interact with the object for 50 minutes following placement. If cage mates were run, mice were placed into a fresh cage until all mice in the cage were run.

Restraint stress

For GCaMP and FLIM *in vivo* recording studies, mice were acclimated to the testing room for at least one hour before testing. Restraint stress were performed using a restraint device designed by our lab and created by Vanderbilt Kennedy Center Scientific Instrumentation Core, details and specifications described previously(Luchsinger et al., 2021). Fibers were attached to animal's implant using a ceramic mating sleeve (Precision Fiber Products) of 2.5mm diameter, 11.4mm length for GCaMP recordings or 1.25mm diameter, 6.80mm length for FLIM. Mice were acclimated to attached cable in an empty cage for at least three days for at least 10 minutes each prior to actual recordings. On day of recordings, mice were attached and acclimated for 5-10 minutes in an empty cage or small open field arena before being placed in restraint device. Restraint stress exposure was recorded for at least 30 minutes and videos were captured with a webcam from above and analyzed via DeepLabCut.

Shock exposure

For shock experiments, mice were placed in individual Med Associates (St. Albans, Vermont) operant conditioning chambers. A total of 10 footshocks were delivered in a non-contingent and inescapable fashion over a 5 minute period. Shocks were delivered at 0.5mA with an interstimulus interval of 30 seconds. All shocks were presented in the same session and were repeated for a second day.

***Ex vivo* GCaMP imaging**

Mice were anesthetized using isoflurane, and transcardially perfused with ice-cold cutting solution, oxygenated for at least 15 minutes, consisting of (in mM): 92 N-Methyl-D-glucamine (NMDG), 2.5 KCl, 20 HEPES, 10 MgSO47H2O, 1.2 NaH2PO4, 0.5 CaCl2-2H2O, 25 glucose, 3 Na^+-pyruvate, 5 Na^+-ascorbate, 2 Thiourea, 30 NaHCO3 and 5 N-acetylcysteine. Coronal brain slices were prepared at 200μm thickness on a vibrating Leica VT1000S microtome. The brain slices were then transferred to a 34˚C chamber containing oxygenated cutting solution for a 10–15-minute recovery period. Slices were then transferred to a holding chamber containing oxygenated artificial cerebrospinal fluid (aCSF) solution consisting of (in mM): 124 NaCl, 2.5 KCl, 2.5 CaCl2-2H2O, 5 HEPES, 2 Mg2SO4, 1.2 NaH2PO4, 12.5 glucose, 24 NaHCO3, 0.4 -L-ascorbic acid and were allowed to recover for at least 1 hour at room temperature. For recording, slices were placed in a perfusion chamber (Warner Instruments) and perfused with oxygenated aCSF (30˚C), at a flow rate of 3mL/min.

Optical excitation from 470nm LED (Thorlabs, M470L3-C1) was driven by a T-Cube LED Driver (LEDD1B, Thorlabs) and passed through two Neutral Density Filters, U-25ND25 and U-25ND50, (Olympus), and an EN-GFP filter cube (Olympus, U-N410107, C26986) to emit blue light and record green fluorescence. Using a 20X/0.5W water immersion objective (Olympus), slices were exposed to constant light at 75-100% power for at least 10 minutes before recordings. Following acclimation, visual recordings were obtained using Hamamatsu ORCA-Spark camera and HCimageLive software. High speed streaming imaging parameters were set at a gain of 240, 200ms exposure, binning of 2x2, and rate of 5 frames per second (fps). Recordings lasted 15 minutes in total with 5 minutes of baseline, 5 minutes of guanfacine (10μM) wash on, and 5 minutes of wash out for a total of 4500 frames. Concentration of 10μM based on previous data using guanfacine wash ons for voltammetry(Harris et al., 2018).

SHIELD clearing

SHIELD (Stabilization under Harsh conditions via Intramolecular Epoxide Linkages to prevent Degradation). Mouse brain tissue was prepared according to the LifeCanvas SHIELD protocol(Park et al., 2019). Mice were anesthetized with isoflurane and transcardially perfused with 20 mL cold PBS followed by 20 mL of cold SHIELD perfusion solution at a rate of 5 mL/min. Brains were dissected and incubated in 20 mL of SHIELD perfusion solution shaking at 4°C for 48 hours. Brains were then transferred to 20 mL of SHIELD-OFF solution and shaken for 24 hours at 4°C. Brains were then transferred to passive SDS clearing solution and shaken for 3-4 weeks until fully transparent, with solution replaced every week. SHIELD perfusion and SHIELD-OFF solutions was prepared fresh before all perfusions, as described previously(Luchsinger et al., 2021). After clearing, brains were shaken in PBS at 37°C for 12 h. The samples were then shaken in 50% EasyIndex (LifeCanvas Technologies) refractive index (RI) matching solution in diH20 for at least 48 hours at room temperature. Samples were then transferred to 100% EasyIndex solution for two days before being mounted. Sample holders (LifeCanvas Technologies) were rinsed with diH_2O, followed by 70% ethanol. Once the sample holder was dry, it was filled with 1.1% agarose (Sigma-Aldrich, A9539) made in Easy Index. The brains were then placed in a sample holder and allowed to congeal at 4°C for around 5-10 minutes. Brains were returned to conical tube of EasyIndex and shaken overnight at 37°C and then allowed to equilibrate in the imaging chamber overnight before imaging.

Light Sheet Microscopy

Whole-brain images were obtained using a light sheet microscope (SmartSpim, LifeCanvas Technologies)(Dean et al., 2015; Hedde and Gratton, 2018), and a 3.6x objective (NA = 0.2). Light with excitation wavelengths of 488nm and 561nm were illuminated through the sample with emission detection filters of 525/50 and 600/52, respectively. Laser power was set to 30–55% for each channel, with a 2 µm step size. Images were destriped and stitched to generate composite TIFF images with codes provided by SmartAnalytics that utilized a modified version of Terastitcher(Bria et al., 2019). Destriped and stitched TIFF images were converted to Imaris files using Imaris File Converter 9.2.1 for visualization, using Imaris 9.5.1. Processed images were run through SmartAnalytics (LifeCanvas Technologies) workstation and software. Briefly, scans were downsampled and aligned to the Allen Brain Atlas through manual registration. A cell detection model designed to detect fluorescently tagged cells was run to quantify rabies-infected cells across all brain regions listed in the Allen Brain Atlas.

***In vivo* optogenetics**

Optogenetic parameters

Optogenetic setup and stimulation were administered as described previously(Folkes et al., 2020). At least four weeks following TRAPing, mice were habituated to false patch cables in 10-20-minute bins for 3 consecutive days. Mice were acclimated to the testing room for at least one hour before testing, and all tests occurred during the light phase. On test days, stimulation patterns were delivered from the PlexBright 4 Channel Optogenetic Controller and controlled by Radiant v2 software (Plexon). The optogenetics controller box was attached to the Plex- Bright Dual LED rotatable commutator, in which a blue (465 nm) LED light and a 0.5NA PlexBright Optical patch cable were affixed (Plexon). For real time place preference, mice received constant 20-Hz blue light stimulation immediately upon entering stimulation side of the two-sided chamber. For open field, elevated plus maze, novel suppressed feeding task (NSFT), light/dark, and restraint recordings, animals received 20-Hz blue light stimulation (Plexon) in 5 seconds on, 5 seconds off, pattern at 10–13 mW. Both mice that received intra-BNST infusion of ChR2 or control EYFP received the same stimulation protocols. If cage mates were to be recorded from, mice were placed into a fresh cage until all mice in the cage were run. Videos were recorded and analyzed using ANY-maze Behavioral tracking software (Stoelting Co) from a camera (The imaging source, DMK) located above the behavioral apparatus.

Realtime Place Preference (RTPP)

Optogenetic stimulation was delivered when animals entered a randomly assigned chamber and ended when animals left the stimulation chamber. Mice were tested for 20 minutes. Time in stimulated/unstimulated sides, entries to sides, distance traveled per side and time immobile per side were calculated using ANY-maze. Time in each side was used to calculate time spent per side as a percentage of total time using [(total time – time per side)/total time *100].

Elevated Plus Maze (EPM)

Mice were attached to fiber cables before being placed in the center of EPM (San Diego Instruments) arena. Mice were tested for 10 minutes. Time spent in each arm, total distance, and entries to each arm was calculated using ANY-maze.

Open Field Test (OFT)

Mice were attached to fiber cables and placed in brightly lit open field box (50 × 50 cm, San Diego Instruments) filled with bedding. Mice were allowed to explore open field arena for 10 minutes before being removed. Time spent in outer and inner portions of the box were calculated using ANY-maze.

Novelty Suppressed Feeding Task (NSFT)

The 3-day novelty-suppressed feeding task (NSFT) was performed as previously described(Britton and Britton, 1981; Centanni et al., 2019b; Holleran et al., 2016; Jaramillo et al., 2020). Briefly, mice were food restricted in their home cage for 48 hours with only 2-hour access to food ad libitum 22-24 hours before testing. On test day, a 5g food pellet was placed in the middle of a brightly lit open field arena with fresh bedding. A new pellet and refreshed bedding were used for each test. Mice were attached to the optic cable and placed in a corner of the arena. Initial bite was determined as the first time the mouse interacted with the food pellet. The first 5-second bite was determined as the first time the mouse interacted with the food pellet for at least 5 seconds. Following the 5-second bite, mice were immediately removed from the arena and returned to a new cage with the pellet from the test, which was then weighed after 10 min. Mice that did not eat within the first 20 minutes of the test and/or 10 minutes of the post-test were omitted from analysis. Following the test, the mice were returned to ad libitum access to chow.

Light/Dark test

Mice were placed in the light side of a two-sided chamber that was made in house containing an unlit, closed off "dark" side and a brightly lit, open "light" side, as described previously(Luchsinger et al., 2021; Salimando et al., 2020). Mice were allowed to explore both sides for 20 minutes while receiving constant stimulation. ANY-maze software (Stoelting Co) was used to track mice entering and exiting each side. Since the dark side is closed and hidden, any time that the camera could not detect a mouse in the light side was automatically assigned as in the "dark" side. Time spent in light and dark side and entries to each side were calculated using ANY-maze.

Restraint stress

Mice were connected to fiber cables before being placed in previously described custom RESTRAINT device. Mice received constant 20Hz stimulation during the 30-minute restraint stress. Videos were analyzed using DeepLabCut as described below.

***Ex vivo* optogenetic validation**

Coronal slices of 300μM were obtained as described above for *ex vivo* GCaMP Imaging. Whole-cell voltage-clamp recordings were performed as previously described(Fetterly et al., 2019; Flavin et al., 2014a). Electrodes (2.5-5.0 MΩ) were filled with internal aCSF (in mM: 117 D-gluconic acid, 59 CsOH, 20 HEPES, 5 Triethylamine (TEA), 2 MgCl2, 4 Na2ATP, 0.3 Na2GTP). Optical stimulation was under the control of a T-Cube LED Driver (LEDD1B, Thorlabs) and passed through an EN-GFP filter cube (Olympus, U-N41017) to produce blue wavelength light. To confirm channelrhodopsin activity, cells were stimulated with a brief 5ms pulse of light while being held at -70mV. Following confirmation, slices used for electrophysiology underwent BLAQ staining.

QUANTIFICATION AND STATISTICAL ANALYSIS

IHC cell quantification

Cell counts were performed manually using ImageJ by two researchers blinded to experimental groups. No differences were observed between sub-nuclei of the dBNST, so all numbers are reported as a single summed value for each dBNST. The cell counts for left and right BNST across a single section per animal (Bregma=0.145mm) were averaged across animals. Colabeling was determined as overlap of cFos immunohistochemical staining, which is defined as a circular, nuclear stain with ~90% overlap with mCherry labeling that should denote the entire soma in addition to processes.

Restraint bout analysis

Restraint bout behavioral scoring was performed as described previously using DeepLabCut (DLC)(Luchsinger et al., 2021). A single piece of green tape on the fiberoptic cable and the tip of the tail were used to manually locate points in a training dataset of 20-30 images per video. DLC was trained for at least 5 iterations to confirm accurate and precise

labeling. Once a model was trained sufficiently, it was used to analyze videos in batches, markers were confirmed across videos. Outputs from DLC were further analyzed using custom R and MATLAB scripts that allow for time locking of calcium signal to the onset of active coping bouts. Specifically, whole body bouts were identified across frames where the tail and the fiber were moving at the same time, while smaller bouts were designated with only one of the two moving. The bout duration was calculated as continuous until all tracked points were immobile for >0.7s.

Fiber Photometry analysis

A fluorescence intensity trace was made by plotting the number of photons recorded in 30 or 60 ms intervals against time. Photons were recorded in 30 or 60ms intervals and plotted against time to make a fluorescence intensity trace. Fluorescence decay kinetics were used to confirm in vivo GCaMP7f expression. Average fluorescence values were calculated across baseline for 10 minutes for guanfacine and novel object exposure or 5 minutes for restraint stress and were used as initial fluorescence. Change in fluorescence lifetime was calculated as [(Recorded Fluorescence -Initial Fluorescence)/Initial fluorescence].

For GCaMP studies, linear regression MATLAB scripts from TDT were used to fit the 405 nm signal to the 470 nm signal. Change in GCaMP-mediated signal was calculated as $\frac{(Change\ in\ 470\ nm\ signal - Change\ in\ 405nm\ signal)}{Change\ in\ 405nm\ induced\ signal}$. Time-locked Z-scores were calculated using $Z = \frac{\frac{instantaneous \frac{\Delta F}{F}}{mean \frac{\Delta F}{F}}(from -5\ to -3\ seconds)}{standard\ deviation\ of \frac{\Delta F}{F}(from -5\ to -3\ seconds)}$. Peaks per minute and average Z-scores were calculated using a custom MATLAB script that incorporated adaptive iteratively reweighted Penalized Least Square (airPLS) code to account for baseline noise or signal drift and comparison of transients across mice(Martianova et al., 2019; Zhang et al., 2010). The signal was then calculated using a Z-score transformation and fit to the 405nm reference signal. Data points with a Z-score ≥ 2 ($p<0.05$) were considered statistically significant. Average Z-score and number of peaks was calculated in 10-minute bins or five-minute bins for restraint stress. Peaks per minute were calculated as number of transients with Z-score >2 averaged across time.

***Ex vivo* GCaMP analysis**

Ex vivo GCaMP imaging was analyzed a combination of open-source analysis tools and custom MATLAB and ImageJ scripts. To preprocess the videos, ImageJ was used to combine individual TIFF images and spatially downsample

the frames. A modified NoRMCorre algorithm was used in MATLAB for motion correction(Pnevmatikakis and Giovannucci, 2017; Zhou et al., 2018). Data is then extracted using automated ROI detection with signal deconvolution, denoising, and demixing using constrained nonnegative matrix factorization for microendoscopic data (CNMF-E) analysis(Zhou et al., 2018). CNMF-E analysis allows for Z-score calculation and detection of calcium events in single cells using custom MATLAB scripts. The change in spikes per minute of each cell was calculated by subtracting the instantaneous spikes/minute by the average spikes/minute during baseline (minutes 1-5). Percent change from baseline was calculated by dividing the change in spikes/minute of each cell by the average spikes/minute of the population baseline. A threshold of 20% was selected to determine cells that responded when the drug was on, allowing for grouping analysis based on increases or decreases in cell responses.

Light sheet cell quantification

To create a less exhaustive list, cell counts were combined across brain regions with a granularity set to 6, meaning all subregions beyond the first six levels of hierarchically organized taxonomy based on the Allen Brain Atlas were combined within its parent structure, using custom Python scripts provided by SmartAnalytics. Average counts across all brain regions were calculated across all guanfacine-trapped animals and top ten counts based on these averages were plotted.

Statistics

All statistics were run using Prism. All values are plotted as mean ± SEM. For analysis of two groups, an unpaired students t-test was used. For analysis of three or more groups, a two-way ANOVA was used. For analysis of two or more groups with at least two treatments or time points, a two-way ANOVA with Holm-Sidak post hoc correction was used. For analysis across time or over days, corresponding test with repeated measures analysis was used. For all analyses, significance of $p<0.05$ was used.

2.3 Results

Guanfacine recruits an ensemble of molecularly heterogeneous neurons in the BNST.

Guanfacine (1 mg/kg) increases cFos expression in the BNST in *adra2a*-expressing cells(Harris et al., 2018; Perez et al., 2020b). The BNST is comprised of numerous cell populations(Ch'ng et al., 2018; Giardino and Pomrenze, 2021; Vranjkovic et al., 2017). To elucidate cell populations activated by guanfacine, we used immunohistochemistry and transgenic reporter lines to examine colocalization of guanfacine-induced cFos with well-characterized BNST neuropeptide/kinase cell population markers, including corticotrophin releasing factor (CRF), somatostatin (SOM), and protein kinase C delta (PKCδ). cFos partially colocalized with each of these cell populations (Figure 5A, 5B). These data are consistent with our previous work indicating partial *adra2a* colocalization with several BNST cellular markers(Harris et al., 2018), suggesting a heterogenous population of cells is activated by guanfacine, analogous to previous studies examining CGRP receptor distribution in the central nucleus of the amygdala (CeA)(Han et al., 2015; Palmiter, 2018). To gain access to guanfacine-activated cells, we utilized a genetic FosTRAP approach that uses a tamoxifen-inducible activity-driven Cre mouse model combined with stereotaxic injection of hSyn-DIO-mCherry bilaterally into the BNST (Figure 5C, 5D). The advantage of this approach is our ability to achieve precise spatially- and temporally-limited targeting of cell populations, though it should be noted that viral delivery of Cre-dependent constructs constrains us to a subpopulation of the total ensemble. Utilizing this approach, we were able to successfully TRAP guanfacine-activated cells by administering an i.p. injection of guanfacine (1 mg/kg) an hour after i.p. injection of 4-hydroxytamoxifen (4-OHT, 50 mg/kg) (Figure 6A-C). To assess the stability of guanfacine-recruited ensembles (Guansembles) in the BNST, we performed TRAP experiments in which we included a second injection of guanfacine (guanfacine-guanfacine [Guan Guan]) (Figure 5E-5H). To test whether Guansembles overlapped with cells activated by injection stress, we injected two additional cohorts to compare saline injection-activated neurons to Guansembles (guanfacine-saline [Guan Sal], saline-saline [Sal Sal], Figure 5E-5H). We found a significantly greater number of total cells reactivated by guanfacine (Guan Guan) quantified as mCherry+cFos+ cells when compared to saline injections (Guan Sal or Sal Sal) (Figure 5F). It is important to note that this co-expression likely reflects an under-reported fidelity, as viral expression of CRE-dependent mCherry rather than a Rosa transgenic line was utilized to restrict expression. We found approximately 45% of cells colabeled with mCherry fluorescence and cFos immunohistochemistry in the group that received two injections of

guanfacine (guanfacine-guanfacine), confirming the stability of BNST Guansembles, similar to published FosTRAP results with different stimuli(DeNardo et al., 2019; Girasole et al., 2018; Guenthner et al., 2013; Xing et al., 2021) (Figure 5H). Within the saline-saline and guanfacine-saline groups, there were significantly greater numbers of mCherry+ only when compared to mCherry+cFos+ cells in the same treatment (Figure 5H).

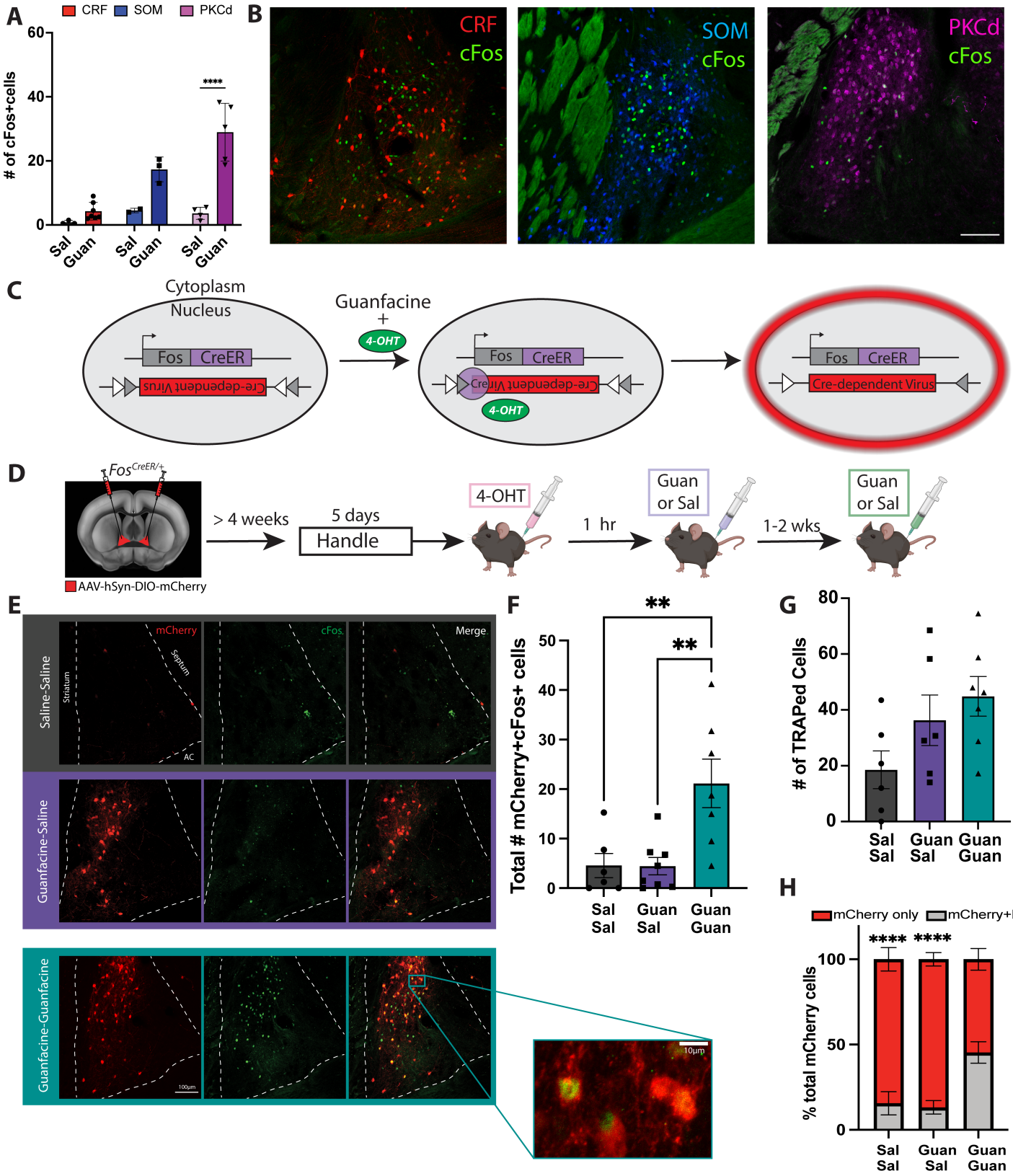
A
CRF
SOM
PKCd
# of cFos+cells
60
40
20
0
****
Sal
Guan
Sal
Guan
Sal
Guan
B
CRF
cFos
SOM
cFos
PKCd
cFos
C
Cytoplasm
Nucleus
Fos
CreER
Cre-dependent Virus
Guanfacine
+
4-OHT
Fos
CreER
Cre-dependent Virus
4-OHT
Fos
CreER
Cre-dependent Virus
D
Fos CreER/+
AAV-hSyn-DIO-mCherry
> 4 weeks
5 days
Handle
4-OHT
1 hr
Guan
or Sal
1-2 wks
Guan
or Sal
E
Saline-Saline
mCherry
Septum
Striatum
AC
cFos
Merge
Guanfacine-Saline
Guanfacine-Guanfacine
100µm
10µm
F
**
**
Total # mCherry+cFos+ cells
50
40
30
20
10
0
Sal
Sal
Guan
Sal
Guan
Guan
G
# of TRAPed Cells
80
60
40
20
0
Sal
Sal
Guan
Sal
Guan
Guan
H
mCherry only
mCherry+Fos+
% total mCherry cells
****
****
100
50
0
Sal
Sal
Guan
Sal
Guan
Guan

Figure 5. Guanfacine activates a heterogeneous cell population in the BNST

(A) cFos colocalization with corticotrophin releasing factor (CRF), somatostatin (SOM), and protein kinase C delta (PKCδ, p<0.0001) in the BNST following saline (n=2-4) or guanfacine (n=3-7) injection. **(B)** Immunohistochemistry results showing cFos colocalization with cell markers including corticotrophin (CRF), Somatostatin (SOM) and Protein Kinase C delta (PKCδ). **(C)** Schematic of tamoxifen-inducible activity-driven expression of Cre-dependent viruses in FosTRAP mouse model. **(D)** Experimental design to investigate reproducibility and specificity of Guansembles by comparing repeated exposure to guanfacine (guanfacine-guanfacine) or guanfacine- and saline-activated cells (saline-saline, guanfacine-saline). **(E)** Representative images of mCherry and cFos labeled cells in the BNST from saline-saline, guanfacine-saline, and guanfacine-guanfacine experimental groups. AC=anterior commissure **(F)** Quantification of cells colabeled with mCherry and cFos after saline-saline (n=6, p=0.0081), guanfacine-saline (n=8, p=0.0043), and guanfacine-guanfacine (n=7) injections (Averaged left and right BNST of single section). **(G)** Total number of TRAPed (mCherry+) calls in saline-saline (n=6, p=0.0081), guanfacine-saline (n=8, p=0.0043), and guanfacine-guanfacine (n=7) injections. **(H)** Dual labeled cells as percentage of total mCherry cells after saline-saline (n=6, p<0.0001), guanfacine-saline (n=8, p<0.0001), and guanfacine-guanfacine (n=7) injections. All error bars are mean ± SEM. Post-hoc p values derived from ordinary two-way ANOVA followed by Šídák's multiple comparisons test (A, F) or ordinary one way ANOVA followed by Tukey's multiple comparison test (E). *p<0.05, **p<0.01, ***p<0.001, ****p<0.0001. Statistical tests and results can be found in Table 1.

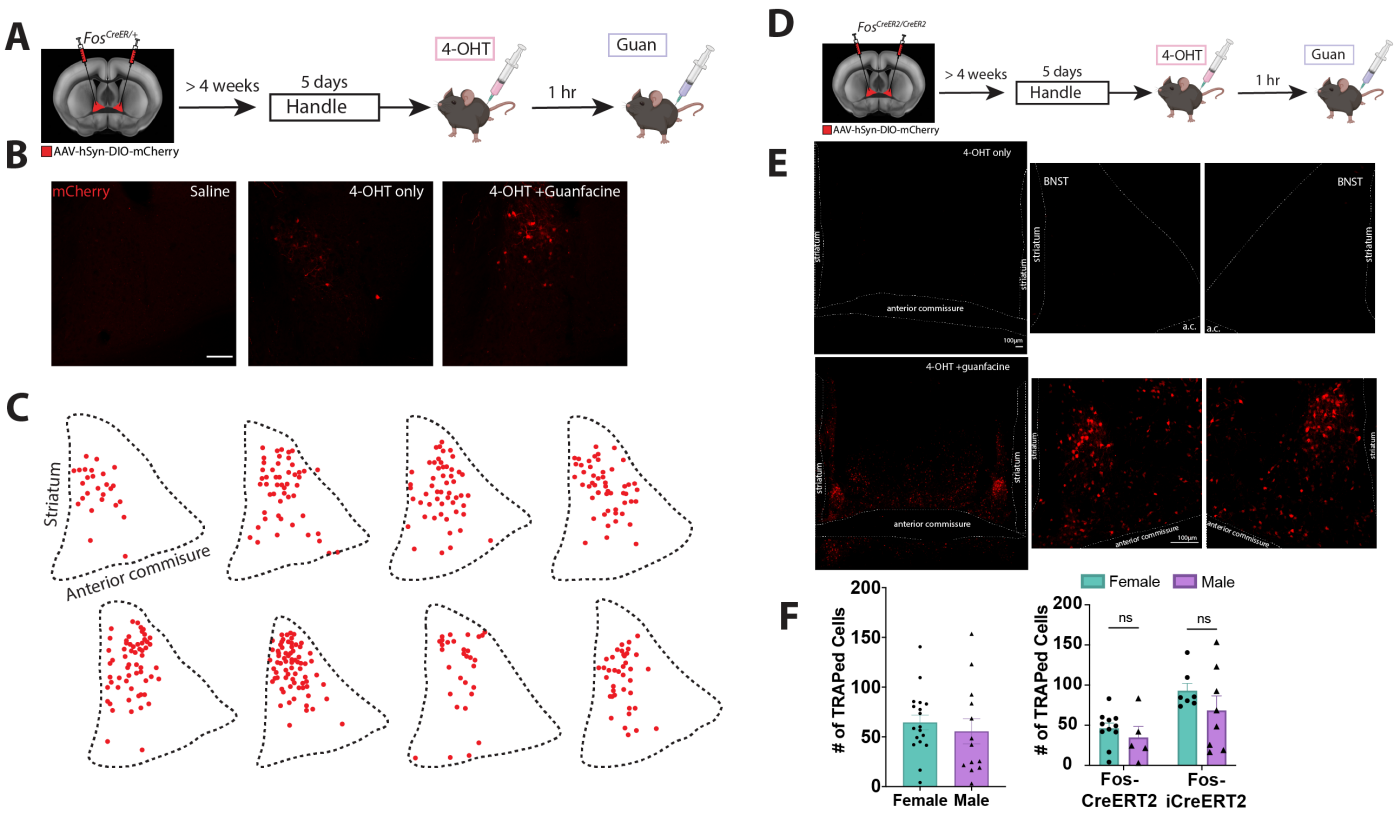

Figure 6. FosTRAP can be used to capture heterogenous cell population in the BNST activated by Guanfacine.

(A) Experimental timeline using FosTRAP to capture guanfacine-activated neurons in the BNST. **(B)** Representative images of using FosTRAP to capture guanfacine-activated neurons in the BNST. **(C)** Representative maps showing distribution of Guansembles across the BNST. **(D)** Experimental timeline using FosTRAP2 to capture guanfacine-activated neurons in the BNST. **(E)** Representative images validating the use of FosTRAP2 to capture guanfacine-activated neurons in the BNST. **(F)** Comparison of number of Guanfacine TRAPed cells in females vs. males in Fos-CreERT2 and Fos-iCreERT2 mouse lines combined (left) or separate (right).

cAMP-dependent protein kinase (PKA) activity in Guansembles is inhibited by guanfacine.

Previous studies suggest a cell autonomous action of α_{2a}-AR signaling in producing neuronal activation in BNST(Harris et al., 2018). The canonical signaling pathway of G_i-coupled GPCRs, such as α_{2a}-ARs, is inhibition of cAMP signaling. Thus, we used a Cre-dependent viral cAMP-dependent protein kinase A (PKA) sensor, FLEX-FLIM-AKAR, and fluorescence lifetime imaging microscopy (FLIM)(Chen et al., 2014; Lee et al., 2019) to record *in vivo* PKA activity in BNST Guansembles (Figure 7A). We measured the lifetime changes of the donor fluorophore with decreased donor lifetime indicative of increased PKA activity(Chen et al., 2014; Lee et al., 2019) (Figure 8A). Repeating previously published studies of this sensor(Gong et al., 2007; Joffe et al., 2018; Lemberger et al., 2007), we found injection of the D1 agonist SKF81297 (3 mg/kg) produced a decrease in observed fluorescent lifetime in D1-Cre mouse line expressing FLIM-AKAR in the striatum (Figure 8B-E). We then expressed FLIM-AKAR in BNST Guansembles using the guanfacine-FosTRAP approach (Figure 7A, 7B). We found an increase in fluorescence lifetime measured within the BNST in FLIM-AKAR expressing mice, consistent with a decrease in PKA activity in Guansembles after injection of guanfacine (Figure 7C, 7D). These results extend our previous study(Harris et al., 2018) to strongly suggest that Guansembles are recruited via guanfacine action at α_{2a}-ARs on Guansemble neurons.

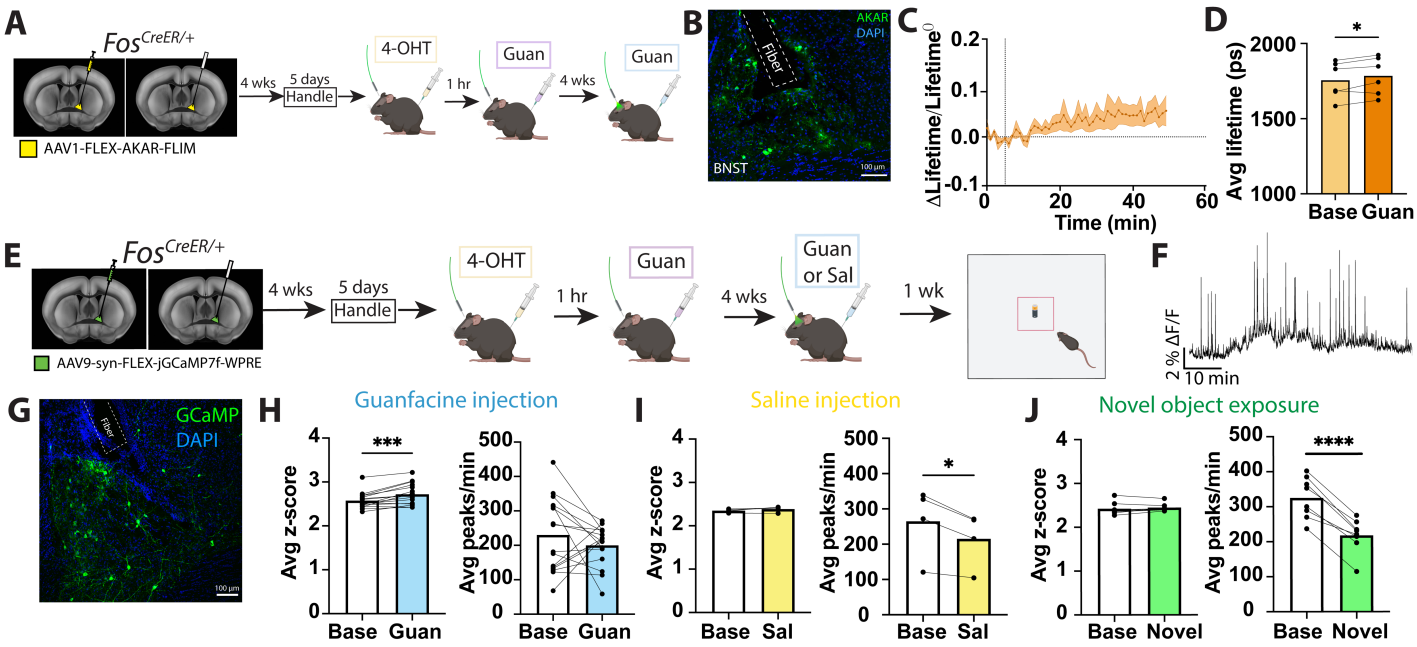

Figure 7. Guanfacine decreases PKA and increases calcium activity in BNST Guansembles.

(A) Experimental design and timeline for recording PKA activity in Guansembles in the BNST using FosTRAP. **(B)** Representative image of Guansembles in the BNST expressing FLIM-AKAR. **(C)** Decrease in PKA activity recorded in Guansembles following guanfacine injection (1 mg/kg, n=6). **(D)** Quantification of average fluorescence lifetime of PKA sensor in Guansembles following guanfacine injection (p=0.0459, n=6). **(E)** Experimental design and timeline for recording calcium activity in Guansembles in the BNST using FosTRAP. **(F)** Representative trace of calcium transients in Guansembles following guanfacine injection. **(G)** Representative image of FLEX-GCaMP7f expression in Guansembles in the BNST. **(H)** Average Z-scores (p=0.0002) and peaks per minute (p=0.2996) in BNST Guansembles following guanfacine injection (1 mg/kg, n=16). **(I)** Average Z-score and peaks per minute recorded in Guansembles following saline injection (n=4, p=0.0221). **(J)** Average Z-score and peaks per minute recorded in Guansembles following novel object exposure (n=8, p<0.0001). All error bars are mean ± SEM. Post-hoc p-values derived from two-tailed paired t-test (D, H, I, J). *p<0.05, **p<0.01, ***p<0.001, ****p<0.0001.

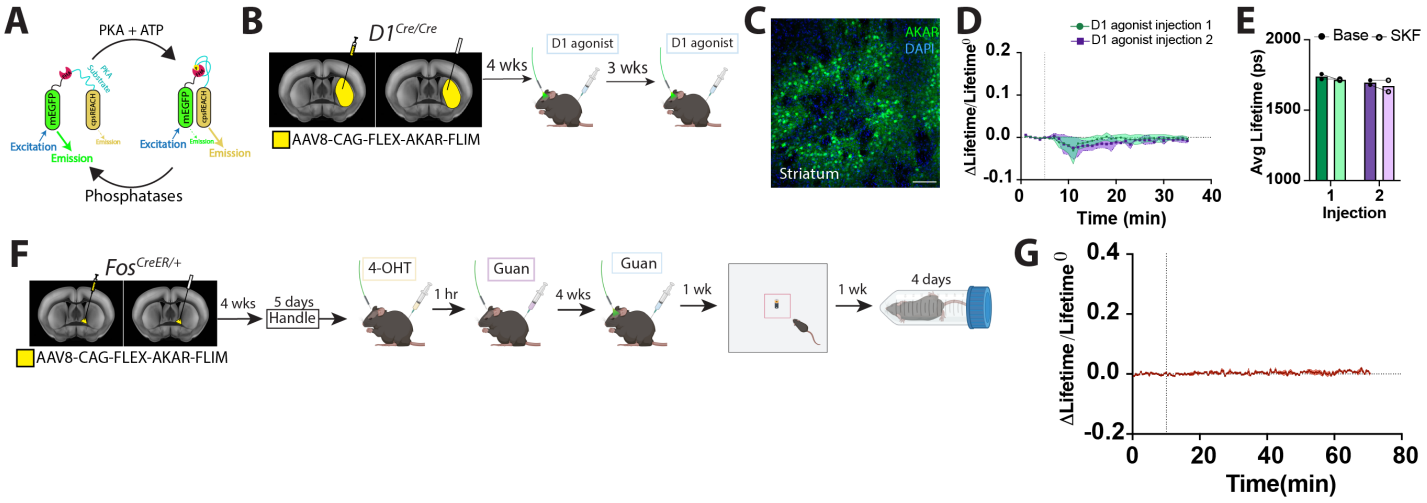

Figure 8. PKA activity in BNST Guansembles during novel object exposure.

(A) Diagram portraying how PKA activity induces fluorescence resonance energy transfer (FRET) activity of FLEX-FLIM-AKAR virus. With increased PKA activity and phosphorylation of PKA substrate, the substrate binds to the FHA domain, bringing the donor (modified GFP) and acceptor (dark YFP) together resulting in decreased fluorescence. **(B)** Experimental design and timeline for recording PKA activity in D1-receptor expressing dopamine neurons in the striatum. **(C)** Representative image of FLIM-AKAR expression in the striatum of D1-cre mouse. **(D)** PKA activity recording following repeated injections of D1-agonist, SKF81297 (3 mg/kg, n=2). **(E)** Quantification of PKA activity in D1-cre mouse following injections of D1-agonist, SKF8127. **(F)** Experimental timeline for measuring PKA activity in BNST Guansembles. **(G)** PKA activity of BNST Guansembles during novel object exposure.

Guansemble activity is dynamically regulated by guanfacine.

To extend the fixed measure analysis of activity provided by Fos recruitment, we combined the FosTRAP model with *in vivo* fiber photometry using FLEX-GCaMP7f to measure dynamic calcium activity of BNST Guansembles (Figure 7E-7G). We recorded calcium transients in Guansembles after an i.p. injection of guanfacine (Figure 7F), normalized the signal using a Z-score transformation, and calculated changes in fluorescence across these transients over time. We found a consistent significant increase in average transient Z-scores following guanfacine injection compared to baseline (Figure 7H), consistent with previously observed cFos recruitment, however we did not observe changes in the number of calcium transients across time (Figure 7H). Curiously, in a separate saline-injected control group, we observed a slight

decrease in the number of calcium transients in BNST Guansembles over time when compared to baseline, suggesting the possibility that injection stress may mask the actions of guanfacine on transient number (Figure 7I). To investigate this idea further, we recorded BNST Guansemble calcium transients during different stressors, novel object exposure (Figure 7E) or restraint stress (Figure 9A). In both instances, we found a decrease in transient peaks per minute when compared to baseline activity suggesting that the inhibitory effects of prolonged stress/novelty may mask the excitatory effect of guanfacine on calcium transients (Figure 7J and 9B). We chose restraint stress in particular because it is known to stimulate noradrenaline release in the BNST(Cecchi et al., 2002; Schmidt et al., 2018). We recorded calcium activity in Guansembles during repeated days of restraint stress using our tethered fiber-compatible restraint device (RESTRAINT, *RE*cording *S*ignal *TRa*nsients *A*ccessible *IN* a *T*ube)(Joffe et al., 2022; Luchsinger et al., 2021) (Figure 9A). We found a significant decrease in activity on the first day of restraint that attenuated over repeated days (Figure 9B). We calculated the fold change from baseline across repeated days and found a significant difference from baseline on all days of repeated restraint when compared to the first day (Figure 9C). Therefore, stress exposure is inversely related to baseline activity in these defined ensembles.

Using RESTRAINT, we previously reported increased calcium activity in BNST neurons associated with active coping bouts, defined as instances during which the head and tail of the mouse is moving concurrently, during restraint stress(Luchsinger et al., 2021). While we find here that overall event frequency is decreased during restraint stress, Guansembles are recruited at the onset of active coping bouts (Figure 9D, 9E and 10), similar to our previous results with overall BNST GCaMP activity(Luchsinger et al., 2021). This Guansemble recruitment was diminished over time with repeated restraint stress (Figure 9D, 9E and 10).

Given these results suggesting an overall inhibitory action of stress on the baseline frequency of calcium transients in Guansembles, we investigated the overlap between guanfacine- and restraint stress-activated neurons in the BNST using FosTRAP combined with cFos immunohistochemistry (Figure 9F). Consistent with this idea, we found only a small portion of overlap between the two populations (Figure 9G, 9H). Further, we recorded the effect of repeated restraint stress on PKA activity in these cells (Figure 9I). We found that while acute restraint stress decreased PKA activity (Figure 9J, 9K), after repeated exposures, restraint stress produced PKA activation in these cells (Figure 9J, 9K). This is in agreement with a larger literature showing general PKA activation in association with chronic

stress(Agarwal et al., 2005; Hu et al., 2020). We did not see an effect of novel object exposure on PKA activity in Guansembles (Figure 8F, 8G).

BNST α_{2a}-ARs are proposed to play an active role in reinstatement of cocaine seeking behavior(Perez et al., 2020b), particularly in response to stress. Previous studies have noted that restraint stress does not reliably produce reinstatement of cocaine seeking/place preference in rodents(Shalev et al., 2000). Because of this, we assessed Guansemble responsiveness to unpredictable shock, a stressor that has been shown to reliably produce re-establishment of CPP behavior in rodents extinguished from a variety of drugs of misuse(Erb et al., 1996; Lu et al., 2002, 2001; Shaham and Stewart, 1995; Shalev et al., 2000) (Figure 9L). Consistent with this, we found that initial response to unpredictable shocks produces an increase in calcium activity (Figure 9M, 9N). On the second day of exposure, we found there was no significant effect of unsignaled shocks on Guansemble activity (Figure 9M, 9N). These results are similar to the attenuation of Guansemble response with repeated restraint stress confirming a role for Guansemble activity in the initial exposure to a stressor.

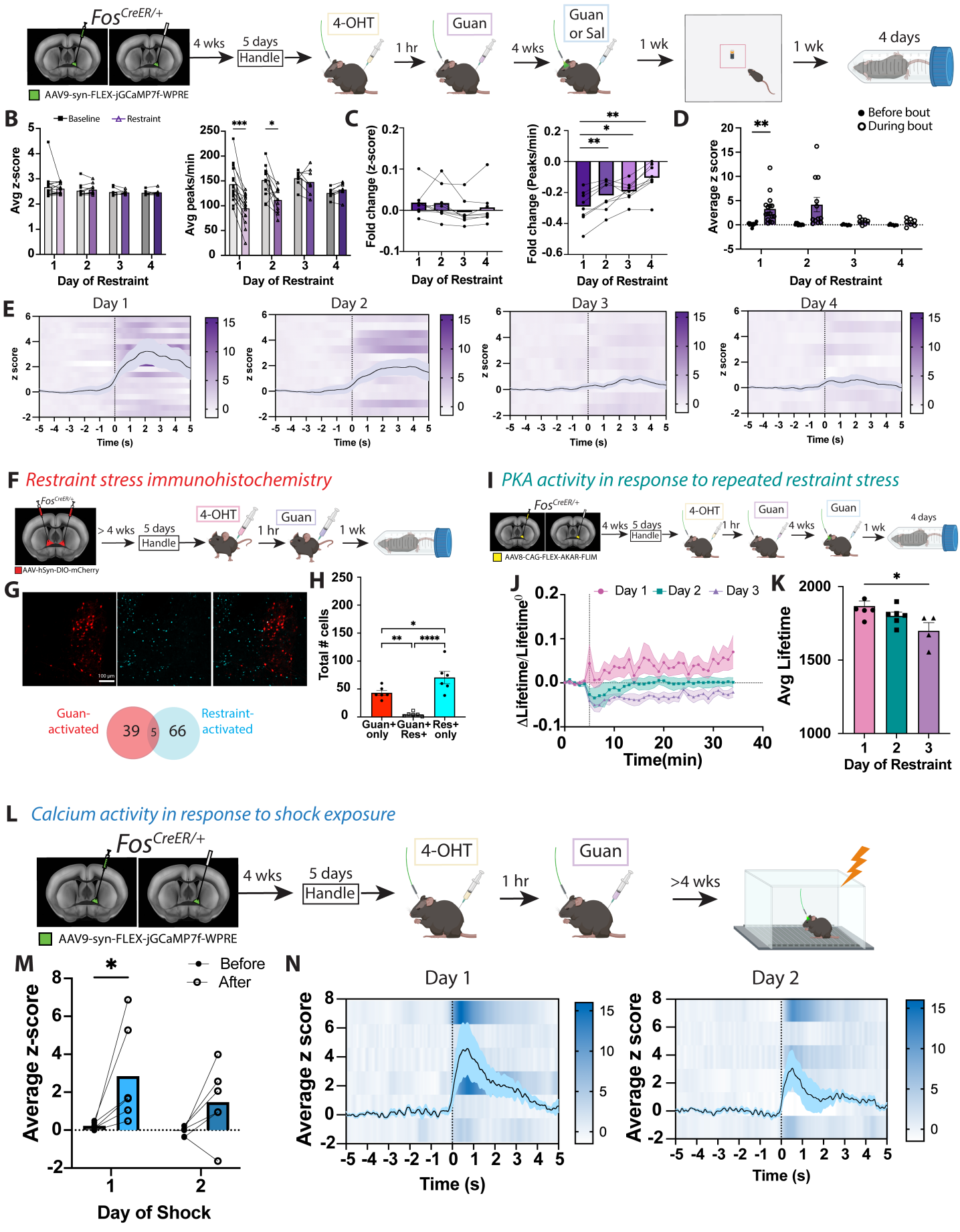
A Calcium activity in response to repeated restraint stress
Fos CreER/+
AAV9-syn-FLEX-jGCaMP7f-WPRE
4 wks
5 days
Handle
4-OHT
1 hr
Guan
4 wks
Guan or Sal
1 wk
1 wk
4 days
B
Baseline
Restraint
Avg z-score
Avg peaks/min
Day of Restraint
C
Fold change (z-score)
Fold change (Peaks/min)
Day of Restraint
D
Before bout
During bout
Average z score
Day of Restraint
E
Day 1
Day 2
Day 3
Day 4
z score
Time (s)
F Restraint stress immunohistochemistry
AAV-hSyn-DIO-mCherry
> 4 wks
5 days
Handle
4-OHT
1 hr
Guan
1 wk
G
100 µm
Guan-activated
39
5
66
Restraint-activated
H
Total # cells
Guan+ only
Guan+ Res+
Res+ only
I PKA activity in response to repeated restraint stress
AAV8-CAG-FLEX-AKAR-FLIM
4 wks
5 days
Handle
4-OHT
1 hr
Guan
4 wks
Guan
1 wk
4 days
J
Day 1
Day 2
Day 3
ΔLifetime/Lifetime0
Time(min)
K
Avg Lifetime
Day of Restraint
L Calcium activity in response to shock exposure
Fos CreER/+
AAV9-syn-FLEX-jGCaMP7f-WPRE
4 wks
5 days
Handle
4-OHT
1 hr
Guan
>4 wks
M
Before
After
Average z-score
Day of Shock
N
Day 1
Day 2
Average z score
Time (s)

Figure 9. Guansemble neuronal activity filtered by stress exposure.

(A) Experimental design and timeline for recording calcium activity in Guansembles using FosTRAP. **(B)** Average Z-score and peaks per minute recorded in Guansembles during repeated restraint stress (day 1: n=16, p=0.0004 day 2: n=12, p=0.0126, day 3: n=8, day 4: n=8). **(C)** Calculated fold change in Z-score and peaks per minute across repeated days of restraint stress (day 1: n=8, day 2: n=8, p=0.0034, day 3: n=8, p=0.0217, day 4: n=8, p=0.0005). **(D)** Combined average calcium activity before and during whole body bouts across four days of repeated restraint stress (day 1: n=16, p=0.0031, day 2: n=12, day 3: n=8, day 4: n=8). **(E)** Calcium activity time locked to the onset of whole body struggling bouts on first (n=16), second (n=12), third (n=8) and fourth day (n=8) of repeated restraint stress. **(F)** Experimental design to investigate the overlap between guanfacine- and stress-activated neurons in the BNST. **(G)** Representative image of guanfacine- and stress-activated neurons in the BNST. **(H)** Quantification of cells activated by guanfacine, restraint, or both (n=6) (p=0.0034, p=0.0324; and p<0.0001). **(I)** Experimental design and timeline for recording PKA activity in Guansembles during restraint stress using FosTRAP. **(J)** Individual curves showing change in fluorescence of PKA activity over three days of repeated restraint stress (day1-2: n=6, day 3: n=4). **(K)** Average fluorescence lifetime calculated over three days of restraint stress (day1-2: n=6, day 3: n=4 p=0.0209). (**L**) Experimental design and timeline for recording calcium activity in Guansembles during exposure to unpredictable foot shocks using FosTRAP. (**M**) Combined average changes in calcium activity before and after foot shock (n=6, p=0.00043). (**N**) Calcium activity timelocked to onset of foot shock on day 1 (n=6) and day 2 (n=6) of exposure. All error bars are mean ± SEM. Post-hoc p values derived from repeated measures one way ANOVA followed by Dunnett's multiple comparison test (C), mixed-effects analysis followed by Šídák's multiple comparisons test (B, D), ordinary one-way ANOVA followed by Tukey's multiple comparison test (H, K), or two way repeated measures ANOVA followed by Šídák's multiple comparisons test (M). *p<0.05, **p<0.01, ***p<0.001, ****p<0.0001.

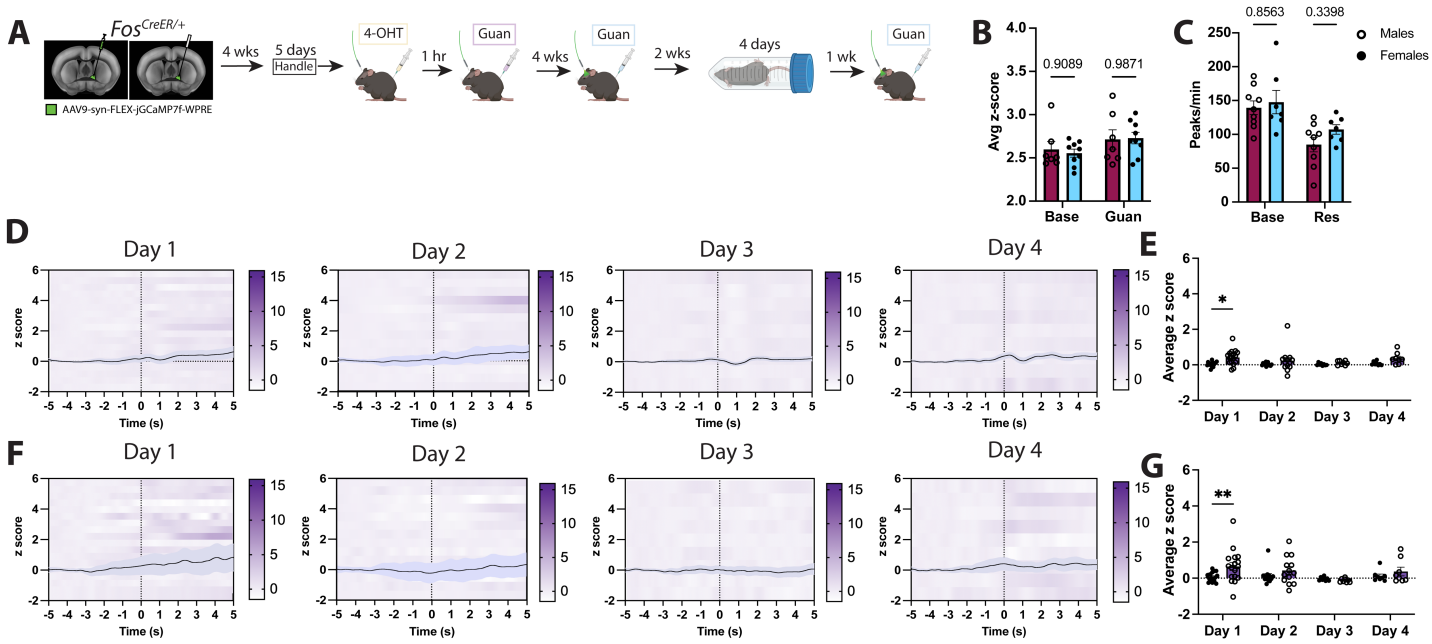

Figure 10. Time locked calcium activity in Guansembles of head and tail only bouts during repeated restraint stress

(**A)** Experimental timeline measuring calcium activity in BNST Guansembles using *in vivo* fiber photometry**. (B)** Average Z-scores in BNST Guansembles across males (n=7) and females (n=9) following guanfacine injection (1 mg/kg, n=16). **(C)** Average peaks/min in BNST Guansembles across males (n=9) and females (n=7) on the first day of restraint stress. **(D)** Calcium activity time locked to onset of head only bouts across four days of repeated restraint stress. **(E)** Quantification of calcium activity before and during head only bouts with repeated restraint stress. **(F)** Calcium activity time locked to onset of tail only bouts across four days of repeated restraint stress. **(G)** Quantification of calcium activity before and during tail only bouts with repeated restraint stress. All error bars are mean ± SEM. Post-hoc p values derived from mixed-effects analysis followed by Šídák's multiple comparisons test (C, E). *p<0.05, **p<0.01, ***p<0.001, ****p<0.0001.

Guanfacine differentially regulates ex vivo Guansemble activity.

We next took a single cell approach to further investigate the effects of guanfacine on Guansemble neuronal activity. We utilized *ex vivo* GCaMP imaging to visualize changes in fluorescence in Guansembles during guanfacine exposure (Figure 11A). To do this, we used the FosTRAP2 mouse line that can be bred to homozygosity and has increased efficiency in TRAPing (DeNardo et al., 2019). After confirming we were able to use this mouse line to capture

Guansembles in the BNST (Figure 6D-F), we repeated our GCaMP fiber photometry (Figure 12A-C) and found similar results to the initial FosTRAP line in response to guanfacine injection (Figure 12D) and repeated restraint stress (Figure 12E). We hypothesize that the variation in results across FosTRAP lines may be due to either greater recruitment of non-specific cells in the FosTRAP2 mouse line or that increased suppression of excitation in these experiments blunted excitability as seen in Figure S4. In another cohort of FosTRAP2 mice, we expressed FLEX-GCaMP7f in BNST Guansembles. We prepared BNST-containing brain slices for *ex vivo* calcium imaging and bath applied guanfacine (10μM) (Harris et al., 2018). As a control for fluorescence rundown during imaging, we recorded calcium spikes during an aCSF wash on. Using a combination of motion correction and signal deconvolution with CNMF-E (Constrained Nonnegative Matrix Factorization for microEndoscopic data)(Pnevmatikakis and Giovannucci, 2017; Zhou et al., 2018), we calculated spikes per minute and found an overall increase in calcium spikes during the drug wash on (Figure 11B, 11C), consistent with our *in vivo* data. When looking across all individual recorded cells, we found varied responses to guanfacine (Figure 11D), with a substantial cluster of cells that exhibited increased calcium activity with guanfacine, as well as cells in which activity was decreased or unaffected (Figure 11E). Our *ex vivo* calcium recordings confirm that Guansemble neurons are dynamically sensitive to guanfacine suggesting differential effects of activating α_{2a}-ARs on different cell types. Additionally, the excitatory actions of guanfacine we observed on Guansembles substantiates our *in vivo* results further confirming an excitatory effect of guanfacine on a portion of cells in the BNST.

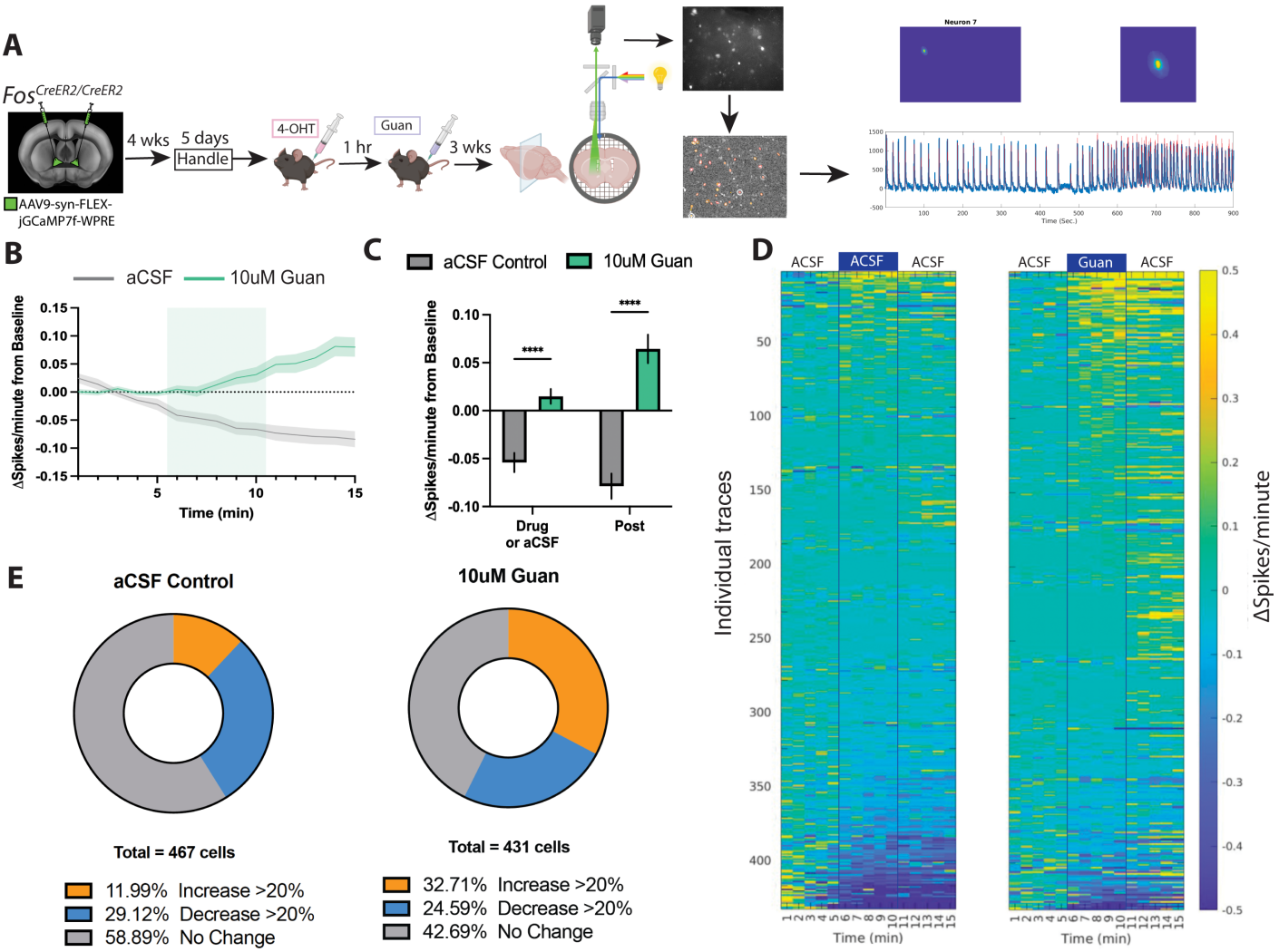

Figure 11. Guanfacine leads to an overall increase in *ex vivo* calcium activity in Guansembles.

(A) Experimental design and timeline for *ex vivo* imaging followed by CNMF-E analysis in FosTRAP2. **(B)** Time course of spikes per minute for aCSF and guanfacine wash on (aCSF: n=467 neurons, Guan: n=431 neurons; N=5 mice). **(C)** Calculated change in spikes per minute compared to baseline for aCSF and guanfacine wash on ($p<0.0001$). **(D)** Heat map showing change in spikes per minute of individual cell response to aCSF or 10µm guanfacine. Each horizontal line corresponds to the response of an individual cell across recording. **(E)** Pie charts showing representative number of cells that increased by 20%, decreased by 20% or did not change their calcium activity during wash on of aCSF or guanfacine. All error bars and shading (B) are mean ± SEM. Post-hoc p-values were derived from a two-way ANOVA followed by Šídák's multiple comparison test (C). *$p<0.05$, **$p<0.01$, ***$p<0.001$, ****$p<0.0001$.

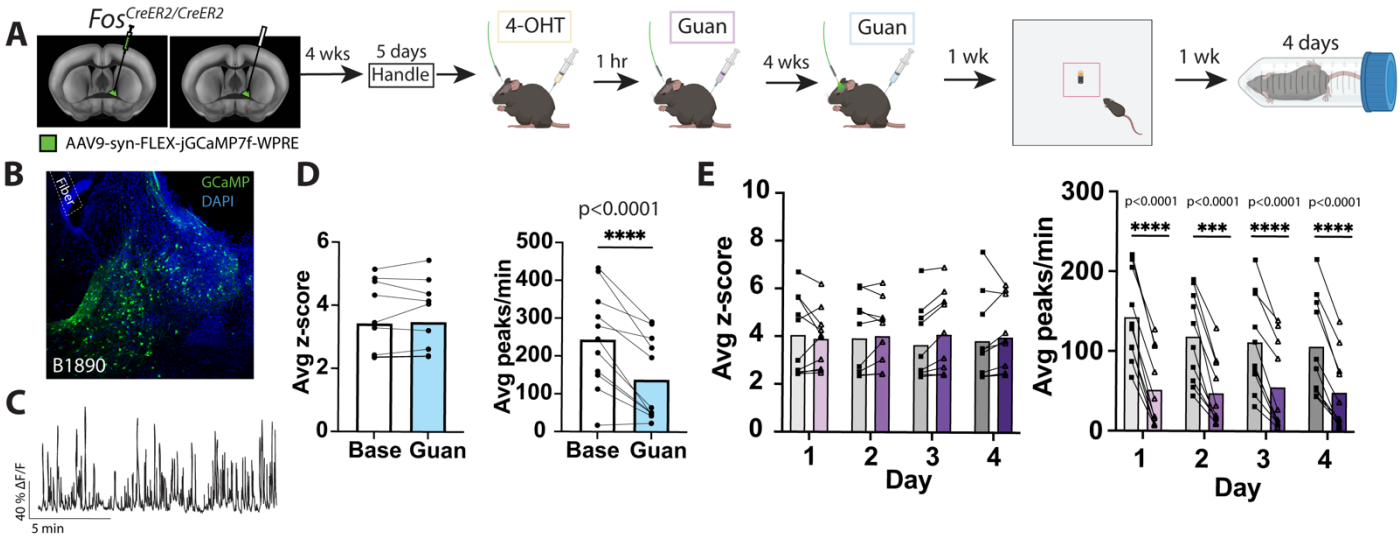

Figure 12. Calcium activity recorded in FosTRAP2 during Guanfacine injection and repeated restraint stress

(A) Experimental timeline measuring calcium activity in BNST Guansembles using *in vivo* fiber photometry in FosTRAP2 mice. **(B)** Representative image of viral and implant targeting in BNST Guansembles in FosTRAP2. **(C)** Example trace of calcium transients following guanfacine injection. **(D)** Change in calcium transient activity with guanfacine injection measured as average z-score (n=11, p= 0.9676) and average peaks per minute (n=11, p<0.0001). **(E)** Calcium activity recorded in Guansembles in FosTRAP2 mice across four days of restraint stress (n=10). All error bars are mean ± SEM. Post-hoc p values derived from two-tailed paired t-test (D), and mixed-effects analysis followed by Šídák's multiple comparisons test (E). *p<0.05, **p<0.01, ***p<0.001, ****p<0.0001.

Identification of monosynaptic inputs onto Guansembles in the BNST

To gain insight into the organization of neural inputs to BNST Guansemble neurons, we utilized a strategy that combined the FosTRAP approach with rabies virus-mediated monosynaptic tracing and brain-wide imaging of labeled neurons (Figure 13A). SHIELD-based optical clearing and light sheet microscopy followed by analysis with SmartAnalytics (LifeCanvas Technologies) were used to align 3D whole brain data sets with the Allen Brain Atlas and register locations of rabies-infected cells. We applied this imaging-registration pipeline to guanfacine- and saline-TRAPed brains and obtained high-resolution images of neurons that provide direct inputs to BNST Guansembles (Figure 13B-13E). The highest densities of labeled neurons were located in regions that provide strong input to BNST Guansembles, including the caudoputamen, hippocampus, and hypothalamus and also including postpiriform transitional area, substantia innominata, midline dorsal thalamus, and piriform and insula cortices (Figure 13F).

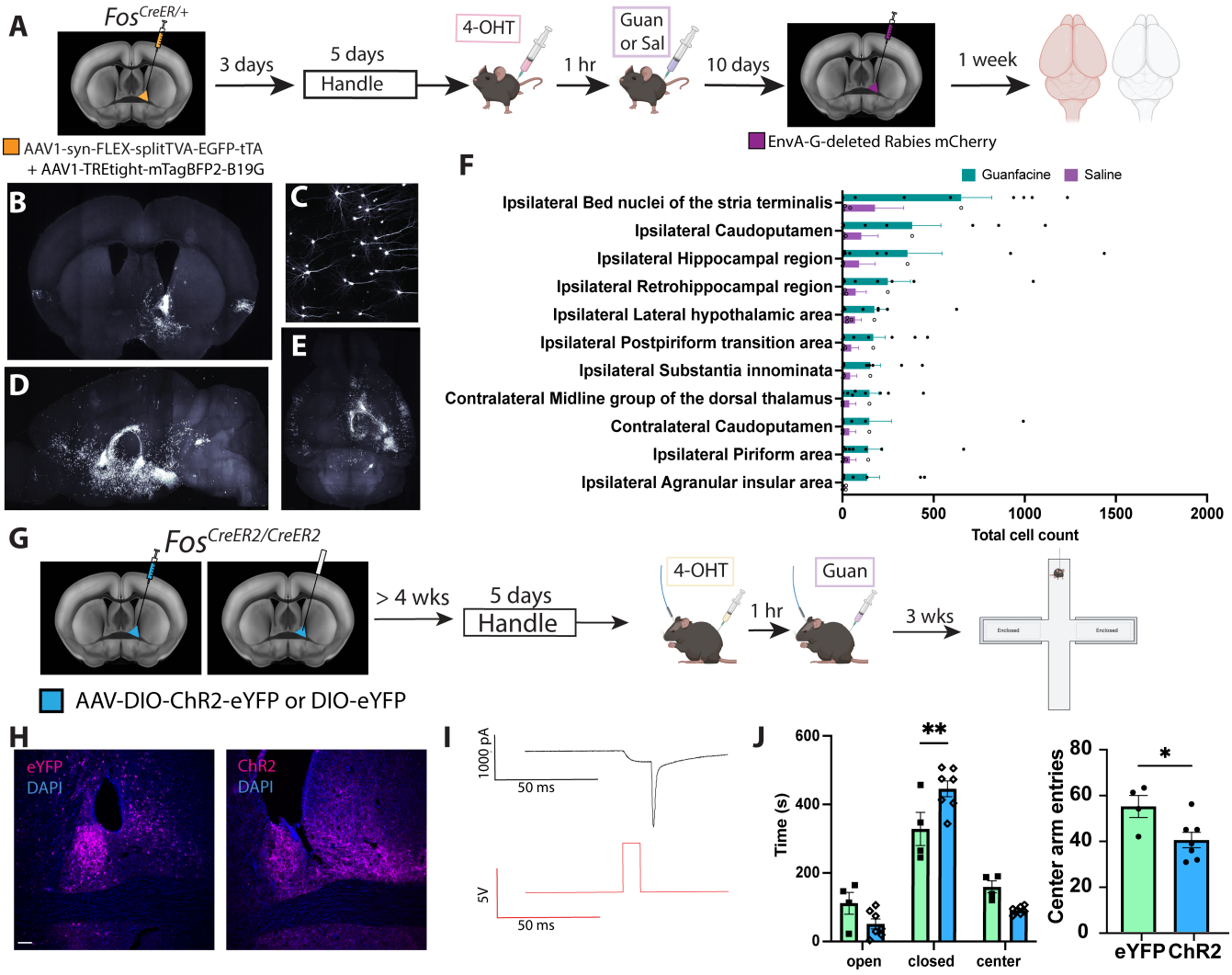

Figure 13. Anatomical and functional characterization of BNST Guansembles

(A) Experimental design of rabies injection and SHIELD clearing to investigate the afferent inputs onto Guansembles in the BNST using FosTRAP. **(B)** Light sheet image showing BNST injection site verification. **(C)** Individual neurons image showing fine detail of light sheet microscopy. **(D)** Sagittal view of light sheet image of whole cleared brain. **(E)** Transverse view of light sheet image of whole cleared brain. **(F)** Plot showing total cell count of top regions from cell registration of saline- and guanfacine- TRAPed brains (saline: n=4, guanfacine: n=8). **(G)** Experimental design and timeline of optogenetic activation of Guansembles in FosTRAP2. **(H)** Representative image of Channelrhodopsin (ChR2) or eYFP expression in FosTRAP2. **(I)** Optogenetic validation of ChR2 activity in Guansemble cell responding to blue light. **(J)** Effects of optogenetic stimulation of Guansembles on elevated plus maze (eYFP: n=4, ChR2: n=7, p=0.0044 and p=0.0314). All error bars are mean ± SEM. Post-hoc p-values are derived from two-way ANOVA followed by Šídák's multiple comparisons test or unpaired t-test (J). *p<0.05, **p<0.01, ***p<0.001, ****p<0.0001

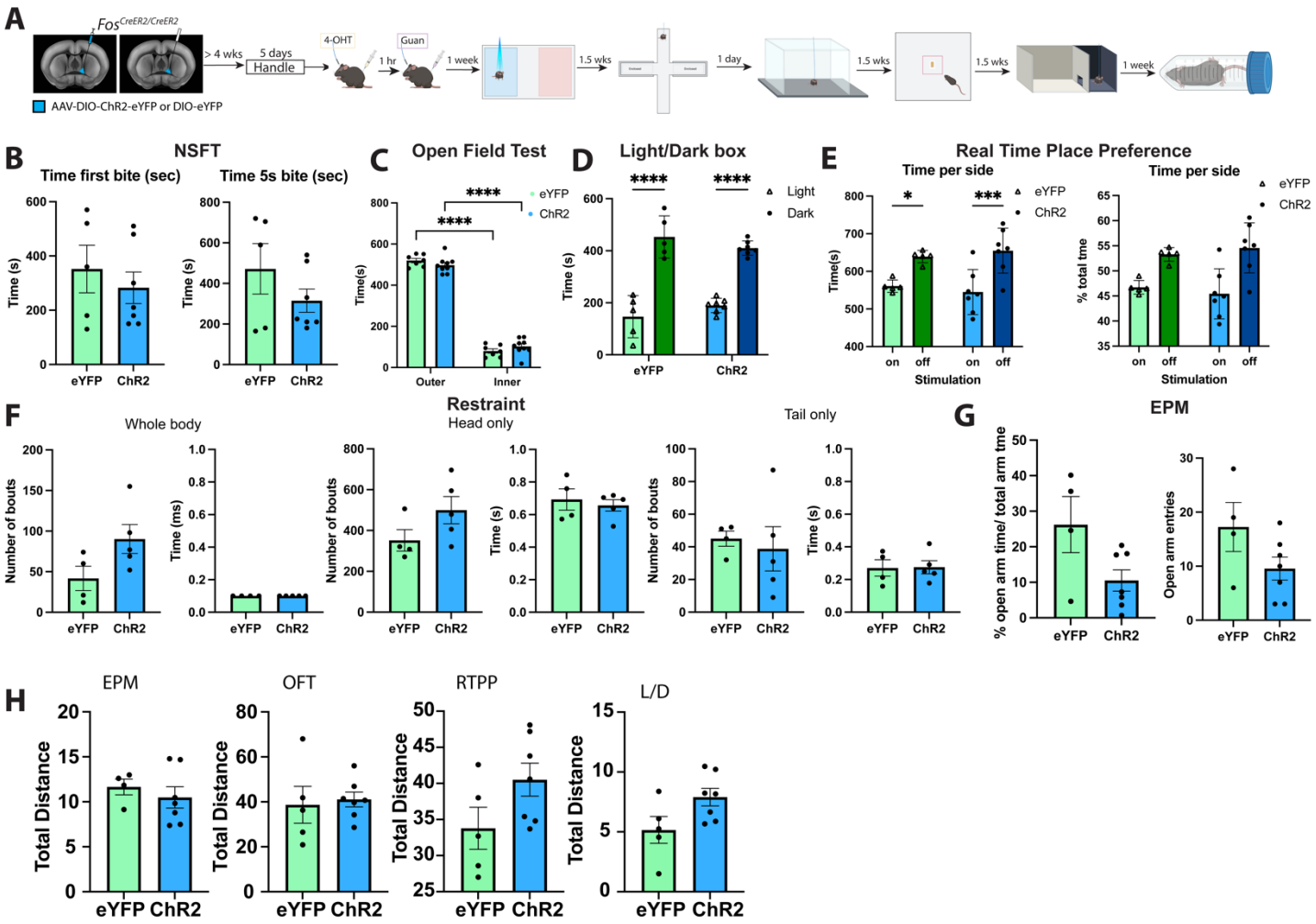

Figure 14. Additional results of behavioral assays during optogenetic stimulation of BNST Guansembles

(A) Experimental timeline of optogenetic activation of Guansembles in the BNST. **(B)** Effects of optogenetic activation of BNST Guansembles on novelty suppressed feeding task (NSFT). **(C)** Effects of optogenetic activation of BNST Guansembles on Open Field Test (OFT). **(D)** Effects of optogenetic activation of BNST Guansembles on light/dark assay. **(E)** Effects of activation of BNST Guansembles on real time place preference (RTPP). **(F)** Effects of optogenetic activation of BNST Guansembles on number and duration of whole body, head only, and tail only bouts during restraint stress. **(G)** Additional results of activation of BNST Guansembles on elevated plus maze. **(H)** Effects of activation of BNST Guansembles on locomotion on included behavioral paradigms. All error bars are mean ± SEM. Post-hoc p values derived from a two-way ANOVA followed by Šídák's multiple comparison test (C, D,). *p<0.05, **p<0.01, ***p<0.001, ****p<0.0001.

BNST Guansemble activation induces anxiogenic-like response

To explore the role that BNST Guansemble cells have in stress and anxiety-like behavior, we examined the effects of activation of these cells by expressing DIO-ChR2 in BNST Guansembles (Figure 13G-I). To fully investigate the role of Guansembles in anxiety-like behavior, we recorded from a battery of behavioral paradigms during optogenetic stimulation (20Hz, 10-13 mW) (Figure 14A). We found that optogenetic stimulation of Guansembles during elevated plus maze (EPM) resulted in an anxiogenic-like phenotype (Figure 13J and 14G). Activation of Guansembles in the BNST increased time spent in closed arms and decreased center arm entries. We did not observe an effect of Guansemble activation on the novelty suppressed feeding task (NSFT) (Figure 14B), open field test (OFT) (Figure 14C), or light/dark assay (Figure 14D). Additionally, we found that activation of Guansembles is not intrinsically reinforcing or aversive at the stimulus frequency and power utilized, as optogenetic activation did not result in a preference during real time place preference (RTPP) (Figure 14E). We also found that activation of Guansembles did not alter the number or length of active coping bouts during restraint stress (Figure 14F). We did not see an effect of Guansemble activation on locomotion (Figure S5H). Optogenetic stimulation altered EPM but not other behaviors, though it is also possible that the use of different frequencies or durations of stimulation would yield different outcomes.

2.4 Discussion

Our previous studies demonstrated a novel facilitatory role for α_{2a}-AR heteroceptors in stress-induced reinstatement of drug seeking behavior and implicated excitatory actions of BNST α_{2a}-ARs in these processes(Harris et al., 2018; Perez et al., 2020b). Here we define a population of neurons in the BNST recruited by α_{2a}-AR activation, demonstrating that these cells are neurochemically heterogeneous. We show that α_{2a}-AR activation inhibits PKA-dependent cAMP signaling and dynamically regulates activity of these cells and that *in vivo* stimulation of these cells produces task-specific behavioral phenotypes consistent with anxiety-like behavior. Further, we demonstrate that these cells function within a circuit involved in integration of stress signals and homeostatic functions. Finally, we show that the activity of these cells is filtered by specific stressors, decreasing basal activity during restraint stress while recruiting Guansemble activity during active stress coping responses and in response to unpredictable foot shocks.

Guansemble activity is dynamically regulated by guanfacine and stress.

Guanfacine produces excitatory and inhibitory effects through differential activation of noradrenergic autoreceptors and heteroceptors(Harris et al., 2018; Krawczyk et al., 2011; Perez et al., 2020b; Shields et al., 2009a). In the BNST, guanfacine can elicit increased cFos expression, a cell autonomous action that is dependent on α_{2a}-adrenergic heteroreceptor expression(Harris et al., 2018). We found that these cFos expressing cells are neurochemically heterogenous. The present studies define these BNST cells using a FosTRAP approach to capture and manipulate ensembles.

Alterations in PKA/cAMP activity through GPCR signaling have been repeatedly associated with anxiety disorders, addiction, and fear memory(Arnsten et al., 2005; Bernabeu et al., 1997; Dwivedi and Pandey, 2011). Guanfacine acts upon α_{2a}-ARs to decrease cAMP production and subsequent downstream decreases in PKA and HCN channel activity(Harris et al., 2018; Wang et al., 2007). Consistent with these data, here we provide direct evidence that PKA activity in Guansembles is decreased by guanfacine, consistent with direct α_{2a}-AR signaling.

We also investigated the effects of guanfacine on Guansemble activity using calcium imaging. Guanfacine elicited a significant overall increase in calcium activity *in vivo* and *ex vivo*. Conversely, we found that novel object exposure and saline injection decrease Guansemble activity. Similarly, we found that prolonged stress decreases Guansemble activity and that this effect attenuates over time. This is consistent with data showing that behavioral and endocrine responses to a homotypic stressor habituate over time with repeated exposure(Armario et al., 2004). While restraint stress decreased basal Guansemble activity, Guansemble activity increased in association with active coping during the stressor, suggesting that significant signal filtering by stress occurs. A similar effect was seen with unpredictable shocks, further confirming a role of Guansemble activity across multiple types of stressors. As footshock is a reliable inducer of reinstatement of drug seeking behavior, these results lead to the prediction that activation of Guansembles may facilitate cocaine seeking behavior. The response of Guansembles to repeated restraint stress and footshock attenuated over time, further suggesting these cells are disengaged with repeated and prolonged stress exposures. We hypothesize the differential effect of distinct stressors on Guansembles is due both to the nature of the stressors as well as the cells that make up the ensemble. For example, while shock is a very brief stressor that produces transient modulatory signaling in amygdalar circuits, restraint stress produces much more prolonged engagement of

neuromodulators and other signaling events. Further, we found that guanfacine activates cells that express several distinct cell markers (Figure 1). Specific BNST cell populations have varied roles in affect, reinforced behavior, and stress(Ahrens et al., 2018; Giardino and Pomrenze, 2021; Kash et al., 2015; Kim et al., 2013; Vranjkovic et al., 2017). Additionally, it has been shown that guanfacine blunts excitatory drive into the BNST from inputs such as the parabrachial nucleus which may override excitation in cells that receive these inputs (Fetterly et al., 2019; Flavin et al., 2014b).

Recruitment of α- and β-ARs in response to noradrenaline release is altered in response to chronic stressors. The disengagement of Guansembles with chronic stress could be due to strengthening of other signaling pathways. For example, noradrenaline release is increased with exposure to stress and over time this release could be activating pre-synaptic α_2-ARs that oppose α_2-ARs heteoreceptors activated by Guanfacine. While our *ex vivo* imaging increases our ability to record specifically from Guansembles with the removal of circuitry involvement, we cannot exclude the effects of microcircuits or secondary effects through network activity recorded in our *in vivo* recordings. However, similar findings across *ex vivo* and *in vivo* supports our conclusions that guanfacine has excitatory effects on Guansembles.

Guansembles receive afferent input from regions important in stress control of homeostatic functions.

We uncovered specific afferents to BNST Guansemble neurons. BNST Guansembles receive input from the caudoputamen, hippocampus, substantia innominata, lateral hypothalamus, dorsal thalamus, insula and piriform cortices amongst other structures. Of note, several regions known to provide large inputs to the BNST, such as the ventral tegmental area (VTA), central amygdala (CeA), and prefrontal cortex (PFC)(Ch'ng et al., 2018; Lebow and Chen, 2016; Vranjkovic et al., 2017) were not identified as Guansemble afferents, suggesting Guansembles may receive specific restricted input relative to other BNST neurons. Substantia innominata to CeA connections have been shown to be important in surprise-induced enhancements of attention and learning, fitting with a role for Guansembles in the initial response to stress(Han et al., 1999; Holland, 2006; Holland and Gallagher, 1999). The hippocampus and caudoputamen have also been heavily studied as regulators of learning and memory. Guansembles receive input from the piriform cortex and post-piriform transition area, two regions heavily involved in the processing of external stimuli, specifically odors, and perceptual learning(Kadohisa and Wilson, 2006; Li et al., 2008; Wilson et al., 2006). The inputs from regions involved in learning and memory could underlie the ability of repeated stress to filter Guansemble activity through

mechanisms such as synaptic plasticity. Specifically, alterations in synaptic connections between the BNST and upstream brain regions involved in the initial encoding of the memory could underlie the disengagement of Guansembles with repeated exposure to stress. The caudoputamen has also been associated with the conjunction of both movement and reward(Báez-Mendoza and Schultz, 2013). Various cell types in the lateral hypothalamus circuitry play a role in feeding and reward(Harris et al., 2005; Stuber and Wise, 2016). These reward-driven regions upstream of Guansembles may drive guanfacine's effects on stress-induced reinstatement of drug seeking behavior. Finally, BNST Guansembles receive input from the midline group of the dorsal thalamus (MTN) which encompasses the paraventricular nucleus of the thalamus (PVT), a region recently associated with stress, arousal and addiction(Groenewegen and Berendse, 1994; Hamlin et al., 2009; James et al., 2011; Kirouac, 2015; Matzeu et al., 2015). Specifically, the PVT to BNST has been associated with starvation-induced arousal, binge alcohol drinking and anxiety(Hua et al., 2018; Levine et al., 2021). The insula cortex projection into the BNST is engaged in struggling behavior and plays an active role in stress avoidance and negative affect (Centanni et al., 2019b; Luchsinger et al., 2021). Together our tracing studies shed light on regions that could underlie the effects of guanfacine on stress-induced reinstatement, the ability of Guansemble activation to induce task-specific anxiety-like behavior, and the filtering of Guansemble activity through acute but not chronic stress, summarized in Figure 15. Future studies will need to investigate each of these pathways and the role they play in anxiety-like behavior and stress. One limitation of our studies is a low n for the saline-injection ensemble tracing and optogenetic behavioral experiments that may require further investigation. Additionally, the downstream afferents of Guansembles in the BNST should be explored due to the BNST's influence over the HPA axis through the paraventricular hypothalamic nucleus (PVH).

Conclusions

The interplay of stress and noradrenergic signaling in the BNST plays a key role in directing control of homeostatic processes(Ch'ng et al., 2018; Flavin and Winder, 2013; Koob, 2008, 1999; Lebow and Chen, 2016; McElligott and Winder, 2009; Silberman and Winder, 2013; Vranjkovic et al., 2017). Our results show that guanfacine differentially affects signaling mechanisms in cells that express postsynaptic α_{2A}-adrenergic heteroreceptors. Additionally, we found that these α_{2a}-ARs filter a specific cell population in the BNST that is susceptible to restraint stress and foot shock and provide evidence for how these cells modulate stress-induced reinstatement of drug seeking behavior.

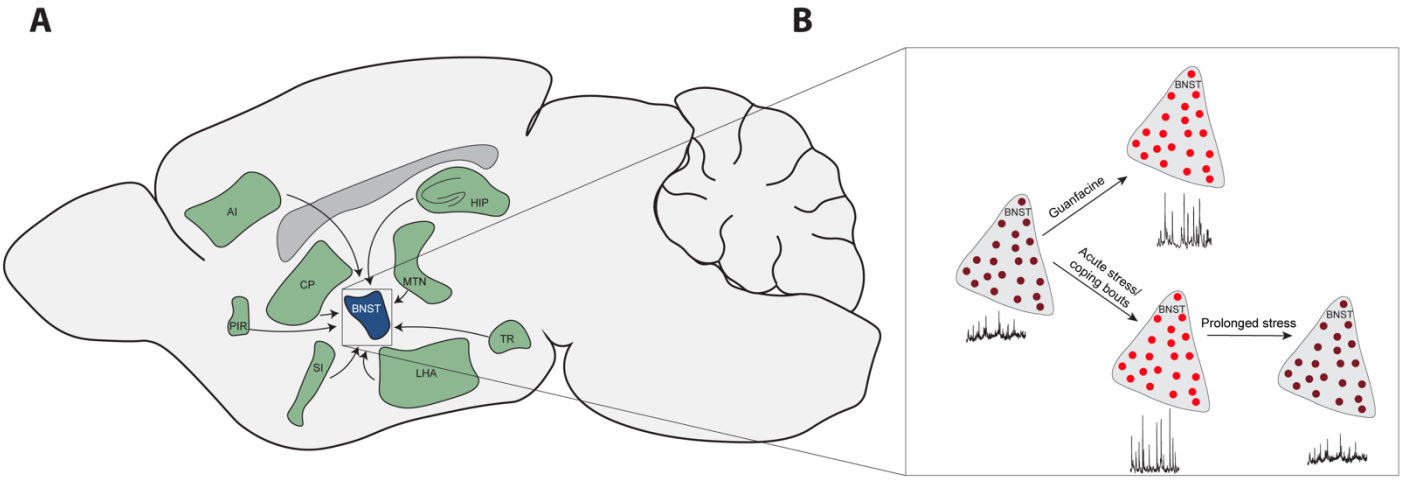

Figure 15. Model of BNST Guansembles

(A) *Afferent projects onto BNST Guansembles defined by rabies tracing, tissue clearing and light sheet microscopy.* ***(B)*** *Guansemble activation by guanfacine and regulation by guanfacine and acute and prolonged stress. TR= Post piriform transition area; PIR= Piriform area; CP= Caudoputamen; AI= Agranular insula area; SI= Substantia innominata; LHA= Lateral hypothalamic area; MTN=midline group of the dorsal thalamus; HIP= Hippocampus.*

CHAPTER 3

Discussion and Future Directions

3.1 Summary and discussion

The previous studies found the alpha2a adrenergic receptor partial agonist, guanfacine, activated an ensemble of cells expressing various cell markers in the BNST. Through the use of FosTRAP, we were able to isolate and characterize this ensemble of cells. Guanfacine activated guansembles as recorded through increased *in vivo* and *ex vivo* calcium activity and inhibited *in vivo* PKA activity. Stress in the forms of saline injection, novel object exposure and restraint stress overall inhibited Guansemble calcium activity. Interestingly, over repeated days of exposure to restraint, the effect of stress on Guansemble calcium activity diminishes and even inverts in terms of PKA activity. We found guansembles are distinct from restraint-stress activated cells suggesting a potential microcircuitry between the two ensembles. BNST Guansembles are connected to upstream brain regions such as the hypothalamus, caudoputamen and hippocampus, brain regions involved in memory, stress, and addiction. Furthermore, optogenetic activation of Guansembles in the BNST led to anxiogenic-like behavior.

Investigations of specific cell populations based on expression of certain cell markers or circuitry are easily achievable due to various transgenic mouse models and neuronal techniques. However, studies of neurons delineated by neuronal activation are not as easily accessible. Neuronal ensembles are defined as a group of neurons that are linked through activation of a specific stimuli (Bossert et al., 2011; Buzsáki and Moser, 2013; Cruz et al., 2015). Our studies describe a novel use of ensemble techniques for the study of a pharmacologically activated group of cells. Previous studies have supported the investigation of ensembles activated by pharmacology including cocaine-activated neurons in the nucleus accumbens and medial prefrontal cortex (Bossert et al., 2011; Kane et al., 2021; Koya et al., 2009). These studies investigated the effect of inactivation of cocaine-activated neurons on learned associations between contexts and drug-induced psychomotor sensitization. This method relies on a Fos-mediated labeling followed by daunorubicin inactivation allowing for inhibition of cells over a 3 day period. Similarly, methods using Fos-mediated expression of DREADDs have been utilized to study ensembles (Garner et al., 2012). The FosTRAP method provides

significant advantages over these techniques due to ability to combine with any cre-dependent virus to allow for temporally- and spatially-restricted manipulation. Our studies have provided the framework for using this approach to capture and characterize guansembles with future studies to further investigate these cells described below.

3.2 Effects of knockdown/knockout of Adra2a on guanfacine activation of BNST

While we have designed a novel way to investigate the ensemble of cells in the BNST that express α2a-adrenergic heteroreceptors and are activated by guanfacine, we do not have the tools to investigate the effects of knocking out these specific receptors. Previous research by our lab has fully investigated the effect of global knockout of alpha2a adrenergic receptors using mouse lines that have complete knockout of *Adra2a* or a transgenic rescue that expresses the *Adra2a* gene in cells that express dopamine B-hydroxylase, resulting in expression of alpha2a-AR only in noradrenergic neurons. We found that alpha2a heteroreceptors were required for cFos induction by guanfacine. We discovered this activation by guanfacine was due to its effects on HCN channels as cFos induction did not occur following HCN knockdown using viral shRNA in the BNST. Furthermore, we have shown that these heteroreceptors are required for stress induced reinstatement of cocaine CPP using the same mouse lines. An unpublished α2a-adrenergic receptor floxed mouse line was designed by a collaborator at University of Texas Southwestern. We were excited to use this mouse line to investigate the effect of specific knockdown of α2a adrenergic receptors in the BNST. Unfortunately, viral injection of AAV-CMV-Cre did not result in significant knockdown of α2a-AR in the BNST measured using RNAscope or RT-qPCR. We investigated the effects of various incubation periods following viral injection, ranging from 3-12 weeks and were still unable to validate this mouse line. Because this receptor is unusual in being a single exon, the distance of the loxp sites likely yields less efficient recombination. Indeed, our collaborators were able to confirm knockdown of this mouse line when crossed to a strong cre-driven mouse line. A transgenic mouse line that results in specific knockdown in the BNST would allow for increased opportunities to investigate the role of these BNST heteroreceptors in guanfacine activation. Furthermore, crossing this alpha2a floxed line with the FosTRAP2 line would allow for direct investigation of alpha2a-AR receptor KD in cells activated by guanfacine. Following this KD, using immunohistochemistry following guanfacine injection would investigate the requirement of alpha2a-AR in the effects of cFos induction of the BNST by guanfacine. One of the major limitations to this experiment would be that alpha2a-AR receptors would be knocked out

in cells activated guanfacine across the entire mouse. This would result in KD of receptors in cells outside of the BNST and could have off target effects. While the tamoxifen injections, limit the activation window of KD thus decreasing these effects, several controls would have to be implemented in addition to strict experimental protocols to reduce off target effects.

3.3 Effects of knockdown/knockout of Adra2a on stress-induced reinstatement

Another use for this mouse line would be to investigate the effects of knockdown of *Adra2a* in the BNST on stress-induced reinstatement of cocaine conditioned place preference (sirCPP). Our lab has shown that knockdown of alpha2a heteroreceptors prevents sirCPP without altering acquisition of original CPP. Evaluating the effects of specific knockdown or knockout of heteroreceptors in the BNST on sirCPP would add support for our hypothesis that these receptors have a pro-reinstatement role. If a validated floxed alpha2a line was established, limiting KD of alpha2a-AR to the BNST would directly investigate this. If there was a way to differentiate KD between alpha2a-AR in noradrenergic and non-noradrenergic in the BNST, in a manner similar to our current mouse lines, this would allow for direct investigation of these receptor cell populations confined to the BNST. Similar to the experiments described above, crossing the FosTRAP2 line with this floxed line would result in KD in Guansembles allowing for direct investigation of the alpha2a-AR receptors in guansembles on cocaine CPP.

3.4 Exploration of role of Guansembles in drug seeking behavior

Xylazine, an analogue of clonidine and agonist of alpha2 adrenergic receptor, has been increasingly associated with overdoses over the last decade (Friedman et al., 2022; Johnson et al., 2021; Reyes et al., 2012; Ruiz-Colón et al., 2014; Thangada et al., 2021). Xylazine is a non-opioid veterinary tranquilizer that has not been approved for human use. The addition of xylazine to opioid substances was first confirmed in Puerto Rico in the early 2000's (Reyes et al., 2012; Rodríguez et al., 2008). People report the addition of xylazine to opioids extends the euphoric effects often associated with opioids. However, due to xylazine's depressive effects on the central nervous system, this combination increases the chances of overdose (Friedman et al., 2022; Reyes et al., 2012). The interaction with alpha2a-AR activation and opioid use needs further investigation. Future studies could investigate the activation of BNST cells with xylazine.

Furthermore, xylazine-activated BNST cells could be compared to Guansembles to investigate if the two agonists activate similar cells. Morphine withdrawal increases noradrenaline release in the BNST (Fuentealba et al., 2002). Modulating noradrenergic signaling attenuates the effects of opioid withdrawal (Delfs et al., 2000; Greenwell et al., 2009; Harris and Aston-Jones, 1993; Sparber and Meyer, 1978). The FosTRAP model of Guansembles could be used to specifically investigate the role of alpha2a-AR signaling in the BNST in opioid withdrawal.

Interactions between noradrenergic and opioid signaling have also been associated with alcohol use disorders (Funk et al., 2022). In addition to the effects of alpha2a-AR on opioid withdrawal, the interaction between noradrenergic and opioid signaling should be investigated. To do this, future studies could compare opioid-activated cells in the BNST and Guansembles. The effects of manipulations of Guansemble activity on the effects of opioid and alcohol use disorders could be investigated using the FosTRAP mouse model. Chronic intermittent ethanol (CIE) results in increased basal activity of CRF-positive neurons in the BNST similarly to stress exposure (Snyder et al., 2019). It's been shown that this effect requires noradrenergic signaling. Measuring CRF activity in the BNST following inactivation of Guansembles using chemogenetics or opotogenetics in the FosTRAP mouse line would shed light on the role of alpha2a-AR activity in the BNST on this effect of chronic intermittent ethanol.

3.5 Effects of activation/inhibition of BNST Guansembles on stress-induced reinstatement of drug seeking behavior

Our effects of optogenetic activation on several different behavioral assays was minimal. We found a task-specific anxiogenic-like phenotype with elevated plus maze. We hypothesize this lack of effect could be due to paradigm choice. We have provided ample evidence that these heteroceptors play a role in sirCPP. We have shown that mimicking activation of these receptors using Gi-DREADD (Designer Receptors Exclusively Activated by Designer Drugs) in the BNST leads to reinstatement of drug seeking behavior. Future studies should investigate the effects of optogenetic or chemogenetic activation of Guansembles on conditioned place preference. I hypothesize that activation of Guansembles would reinstate a previously extinguished place preference. Guanfacine TRAPPING following injection of DIO-ChR2 into the BNST of the FosTRAP2 mouse model used previously would allow for direct investigation of this. Mice would be put through cocaine conditioned place preference (cCPP) followed by extinction training. Optogenetic activation during exploration of the CPP box would reinstate cocaine seeking behavior measured as increased time in previously paired

cocaine side of paradigm box. Similarly, injection of DIO-iC++ or DIO-halorhodopsin, an inhibitory channelrhopsin, in BNST guansembles could investigate the role these cells have in stress-induced reinstatement of CPP. Previous evidence from our lab showed that a low dose of guanfacine, hypothesized to act through alpha2a adrenergic autoreceptors, prevents sirCPP using forced swim as a stressor. Using the same cCPP and extinction protocol using above, optogenetic inhibition during reintroduction of CPP paradigm box following exposure to forced swim prior would look at the role these cells have in preventing stress-induced reinstatement. As our previous evidence showed that BNST heteroreceptors are required for stress-induced reinstatement of CPP, I hypothesize that inhibiting these cells would prevent stress-induced reinstatement.

3.6 Determination of downstream regions of guansembles

In Chapter 2, we investigated the brain regions that provide monosynaptic input onto Guansembles. To gain a clearer picture of the circuitry Guansembles reside in, future studies should investigate the brain regions that lie downstream of Guansembles. The BNST is a heterogenous brain region that consists of intricate intra-microcircuitry. A synaptophysin virus that allows for specific labeling of somatic and dendritic processes with separate fluorophores would delineate between microcircuits in the BNST and downstream brain regions that Guansembles project to. Unfortunately, this virus is not yet validated, and we have yet to use it successfully. Combining this virus with SHIELD clearing and light sheet microscopy, described in Chapter 2, would provide an insight into the circuitry of Guansembles. Preliminary studies with Channelrhodopsin expression in Guansembles showed dense projections from Guansembles to the paraventricular nucleus of the hypothalamus (PVN/PVH). If this holds true, it would support our hypothesis of role of Guansembles in anxiogenesis through modification of hormones released by the PVH.

3.7 Using channelrhodopsin-assisted circuit mapping to investigate regions upstream of Guansembles from top hits of rabies-mediated tracing

Our rabies viral-mediated tracing led to the discovery of several brain regions that form monosynaptic inputs onto Guansembles in the BNST. Channelrhopsin-assisted circuit mapping (CRACM) can be used to further investigate the effects of each of these circuits. While the majority of the cells in the BNST are GABAergic, several of the upstream

regions provide glutamatergic or GABAergic input onto the BNST. Differentiating whether the top regions provide excitatory or inhibitory projections could aid in deciphering the bimodal effects of guanfacine on cells in the BNST. Injection of Channelrhopsin into the top regions and cre-dependent mCherry into the BNST of the Fos-TRAP mouse model followed by subsequent guanfacine TRAPing could be used to investigate this. Following these studies with BLAQ staining could provide quantitative details of the amount and distribution of inputs from each of the regions across the Guansemble.

Combining optogenetics with in vivo behavioral assays could determine the contribution of each of the inputs onto various behavioral phenotype. Specifically, we found an anxiogenic-like response following optogenetic activation of Guansembles in the BNST. Stimulating various inputs onto Guansembles during elevated plus maze would determine if any upstream circuitry that resulted in Guansemble activation underlies this anxiogenic-like phenotype.

3.8 Further delineating the signaling pathways underlying guanfacine activation of the BNST

Our studies investigated the effects of guanfacine on *in vivo* cAMP and calcium signaling and *ex vivo* calcium signaling. Previous evidence from our lab showed that the excitatory effects of Guanfacine were due to effects on hyperpolarization-activated cyclic nucleotide-gated (HCN) ion channels. HCN channels are activated by hyperpolarization voltage and conduct hyperpolarization-activated current, termed I_h through the flow of K+ and Na+ ions. I_h current is inhibited with downregulation of cAMP (Chang et al., 2019). Neurons in the BNST that express cFos after guanfacine injection show high levels of HCN activity measured as hyperpolarization sag in current clamp profiles using electrophysiology (Harris et al., 2018). This HCN channel activity in these cells is diminished with incubation with ZD7288, HCN channel inhibitor. Using RNAscope, it was found that a majority of *adra2a+* cells in the BNST colocalize with *Hcn2* transcripts, confirming a role for this HCN subunit in the effects of guanfacine on the BNST. shRNA knockdown of *Hcn1* and *Hcn2* in the BNST decreased cFos induction by guanfacine. These studies investigated the effect of overall HCN channel inhibition on guanfacine. Pairing HCN channel inhibition through a cre-dependent shRNA and the Fos-TRAP mouse line and subsequent guanfacine-TRAPing would allow for specific investigation of the effects of HCN channels in Guansembles. Following confirmation of knockdown of HCN channels, injection of shRNA and DIO-mCherry in the FosTRAP mouse line with guanfacine-TRAPing and cFos staining following i.p. injection of guanfacine could investigate

the role of HCN channels in the excitatory role of guanfacine in BNST Guansembles. We hypothesize that the excitatory effects of guanfacine on calcium release and the inhibitory effect on PKA signaling is due to closing of HCN channels. Repeating our *in vivo* recordings of cAMP and calcium using fiber photometry following HCN channel shRNA knockdown could directly test this hypothesis. We hypothesize there would still be a decrease in cAMP signaling using the PKA sensor, but the excitatory effect of calcium would be decreased. This would confirm that guanfacine is still acting upon Gi-GPCR and subsequent cAMP signaling to have excitatory effects through HCN channels.

3.9 RNA sequencing of Guansembles in the BNST

Our initial studies investigated several markers to identify the cells in the BNST that are activated by guanfacine. We found that cFos partially colocalized with various cell markers including PKCd, CRF and SOM. Previous studies showed colocalization with *Adra2a* mRNA transcripts with *Penk*, *Calb2*, *Prkcd*, *Crh*, and *Npy*. These studies led us to the hypothesis that guanfacine activated an ensemble of cells in the BNST that express various cell markers. To further characterize the guansembles, RNA sequencing could profile the various cell types in the BNST. Expression of DIO-mCherry in the Fos-TRAP mouse model following guanfacine-TRAPing would allow for fluorescence-activated cell sorting (FACS) prior to single cell RNA-sequencing. The various cell types of the BNST have been assessed using single cell RNA-sequencing (Ortiz-Juza et al., 2021). It was found that there are primarily eleven clusters that express distinct cell markers. Each of these clusters are defined by cell markers and underlie various distinct behaviors including regulation of stress and anxiety. Sequencing of the BNST Guansemble similar to this would provide data showing the cell types and anatomical distribution of cells activated by guanfacine. Our studies have shown guansembles express five of the main cluster defined cell markers, confirming that guanfacine has distinct actions upon cell groups in the BNST. Full single cell-sequencing of BNST guansembles would further characterize the role these cells play in pro-reinstatement and stress coping.

CHAPTER 4

Appendices

4.1 Appendix I. Examining PBN input onto CRF+ and CRF- neurons in the BNST

Previous evidence from our lab has shown that the parabrachial nucleus (PBN) provides a prominent glutamatergic input onto cells in the BNST (Fetterly et al., 2019; Flavin et al., 2014b; Jaramillo et al., 2020). Specifically, we have shown that the PBN synapses onto two distinct populations of cells that are either excited or inhibited following PBN optogenetic stimulation (Flavin et al., 2014b). These two cell populations, referred to as PBN-inhibited and PBN-activated, had differing kinetic properties following PBN stimulation, including presence of I_h current at hyperpolarizing steps and action potential rise time during current clamp profiles. We found that guanfacine inhibited excitatory transmission from the PBN onto cells in the BNST. Furthermore, guanfacine decreased excitatory post-synaptic potentials (EPSPs) of PBN-activated neurons in the BNST following PBN stimulation, while there was overall no effect on PBN-inhibited neurons.

Additional studies in our lab found that guanfacine produce basal inhibition of CRF cells and prevented restraint-stress induced cFos activation of CRF cells (Fetterly et al., 2019). Guanfacine resulted in decreased excitatory drive onto CRF cells in the BNST through decreased excitatory post-synaptic current (EPSC) amplitude. These results were similar to the effects of noradrenaline on CRFC cells in the BNST. To investigate the brain regions upstream of these effects, we looked into the effects of guanfacine on excitatory drive from the PBN and insula, two prominent glutamatergic inputs onto the BNST. We found that guanfacine and noradrenaline inhibited optogenetic activation of PBN onto BNST CRF cells.

Overall, these studies led us to the hypothesis that the two cell populations, PBN-activated and PBN-inhibited were delineated based on CRF expression. To investigate this, we expressed channelrhodopsin in the PBN and recorded from CRF+ and CRF- cells in the BNST using electrophysiology. We obtained coronal slices (as detailed above) using a Leica vibratome at 300 um and recorded neuronal activity of CRF+ and CRF- cells. We recorded current clamp profiles of each cell population to determine action potential kinetics and presence of I_h current. CRF+ and CRF- cells in the BNST had varied electrical profiles (Figure 16). A larger proportion of CRF- cells presented with I_h current and had action potential time courses similar to those of PBN-inhibited. Unfortunately, the profiles did not completely match up to the

PBN-activated and PBN-inhibited as CRF+ and CRF- as we expected. Comparison of various electrophysiological profiles did not result in any large differences across the two cell populations (Figure 17). However, we did find a difference in half-width between CRF+ and CRF-.

We next investigated the response of CRF+ and CRF- cells to PBN stimulation (Figure 18). We found a majority of both CRF+ and CRF- cells optogenetic excitatory post synaptic potential (oEPSP). CRF+ cells resulted in a greater number of action potentials, while one optogenetic inhibitory post synaptic potential (oIPSP) was produced in CRF- cells. Overall, CRF+ cells more closely resembled PBN-activated while CRF- cells resembled PBN-inhibited, the delineation varied.

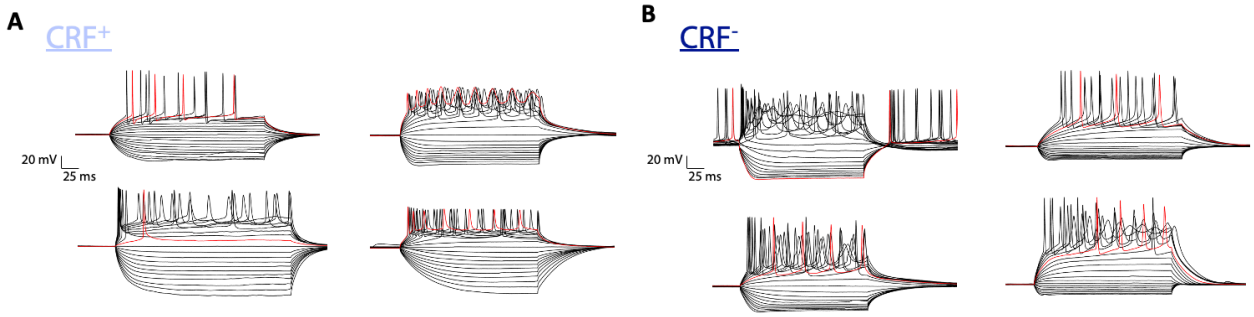

Figure 16. CRF+ and CRF- neurons have varied intrinsic electrical profiles.

Current clamp profiles of CRF+ (A) and CRF- (B) neurons in the BNST.

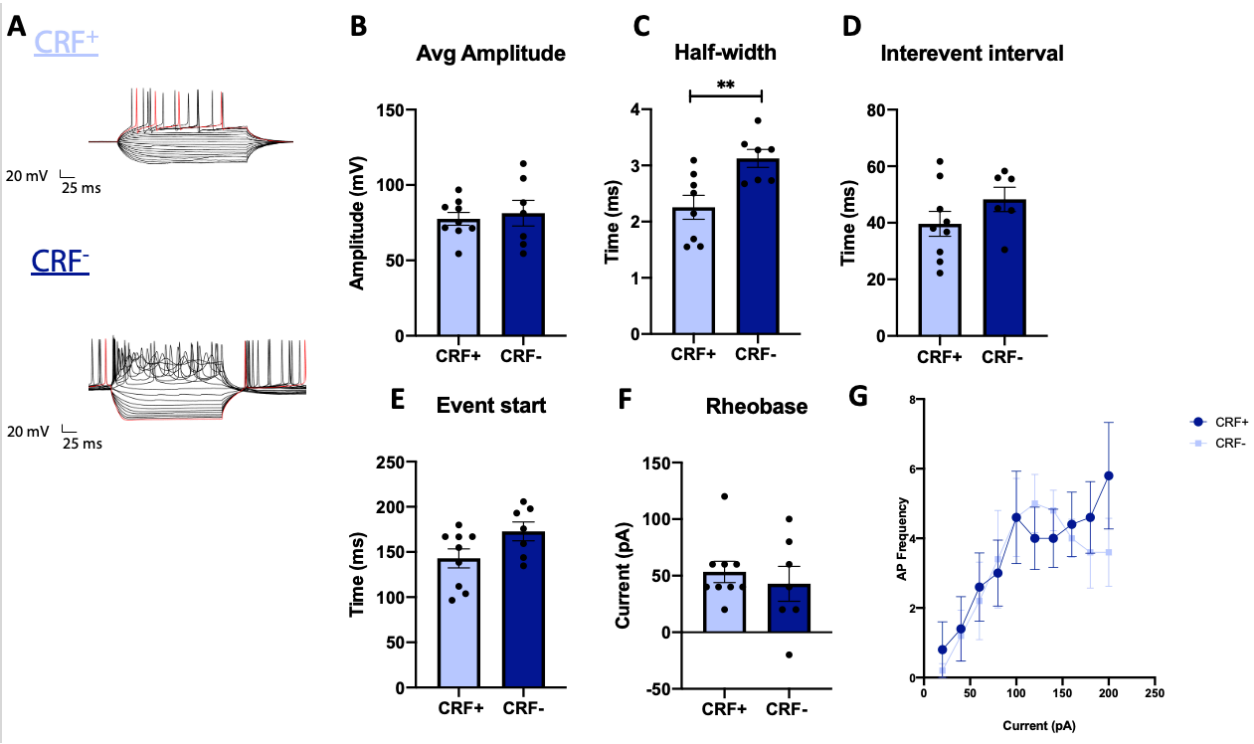

Figure 17: Electrophysiological profiles reveal potential differences across CRF+ and CRF- populations in the BNST.

(A) Current clamp profiles of CRF+ and CRF- cells. Average amplitude (B), half-width (B), interevent interval (D), event start (E) and rheobase (F) of action potential of CRF+ and CRF- during current clamp profile. (G) Action potential frequency across current steps of current clamp profiles of CRF+ and CRF- cells in the BNST.

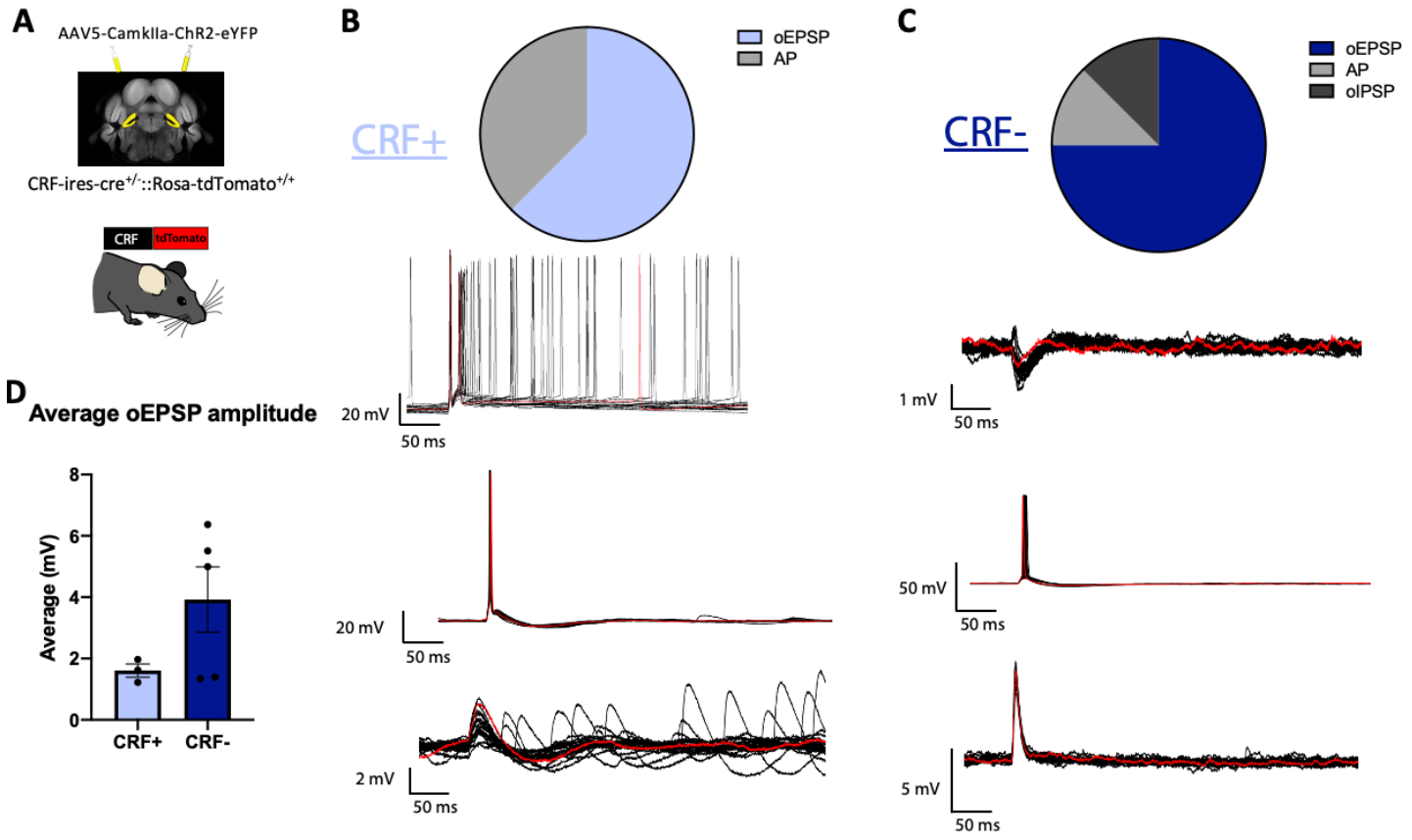

Figure 18: CRF+ and CRF- have varied responses following PBN stimulation.

(A) *Experimental design of using CRF-ROSA mice to investigate the effect of PBN optogenetic stimulation on CRF+ and CRF- cells in the BNST.* ***(B)*** *Percentage of CRF+ cells that result in optogenetic excitatory post-synaptic potential (oEPSP) or action potential (AP) following PBN stimulation. Current traces of CRF+ cells following PBN stimulation.* ***(C)*** *Percentage of CRF- cells that result in optogenetic excitatory post-synaptic potential (oEPSP), optogenetic inhibitory post-synaptic potential (oIPSP) or action potential (AP) following PBN stimulation. Current traces of CRF- cells following PBN stimulation.*

4.2 Appendix II. Guanfacine activates neurons in the BNST that are synapsed onto by the PBN

Previous studies in our lab showed that guanfacine activates a subset of neurons in the BNST through increases in cFos expression (Harris et al., 2018). We also found that guanfacine inhibits CRF+ cells in the BNST and upstream excitatory drive onto these cells by the PBN (Fetterly et al., 2019). This led to the hypothesis that the PBN synapses onto two cell populations in the BNST that are activated or inhibited by guanfacine and are CRF+ or CRF-, respectively. To investigate this, we used a CRF-ROSA mouse line that is created by crossing a CRF-Cre with a Rosa tdtomato mouse line

and results in fluorescent expression of tdtomato in CRF+ cells. We combined this with immunohistochemistry staining for CGRP, a marker of PBN synapses, and cFos to determine cells activated by guanfacine. We found that guanfacine activated a subset of cells in the BNST that are synapsed onto by the PBN (Figure 19). We found that guanfacine did not change the amount of CRF+ cells that are synapsed onto by the PBN. To investigate this further, we used a SOM-ROSA mouse line that is similar to the CRF-ROSA but using a SOM-Cre mouse line crossed to a Rosa-tdTomato that results in tdTomato fluorescence expression in Somatostatin expressing cells. We found that Guanfacine activates a subset of somatostatin cells that are synapsed onto by the PBN (Figure 20). These SOM+ cells made up a small portion of the total population of guanfacine-activated cells. This confirms that guanfacine activates a population of cells in the BNST that are downstream of the PBN that express various markers including somatostatin.

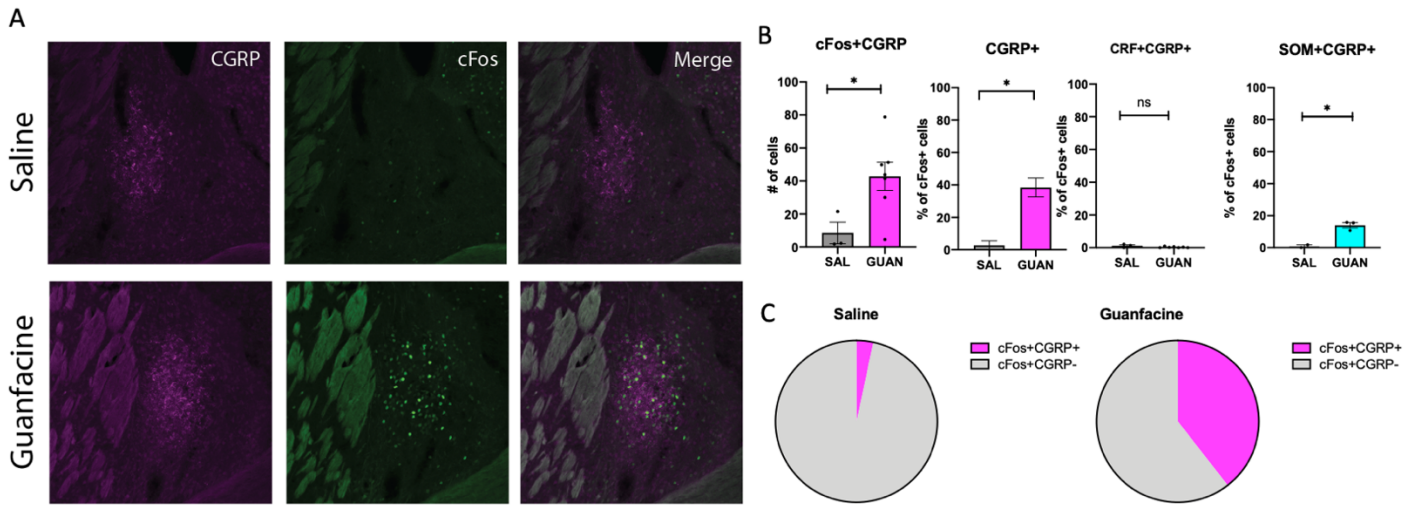

Figure 19: Guanfacine activates cells in the BNST synapsed onto by the PBN (BNST^{CGRP} or BNST^{PBN}). *(A) Representative image of CGRP expression surrounding guanfacine-activated neurons in the BNST. (B) Quantitative results of cFos+ surrounded by CGRP expression, total CGRP+ neurons, colocalization of cFos+ with SOM+ or CRF+ and CGRP following saline or guanfacine injection.*

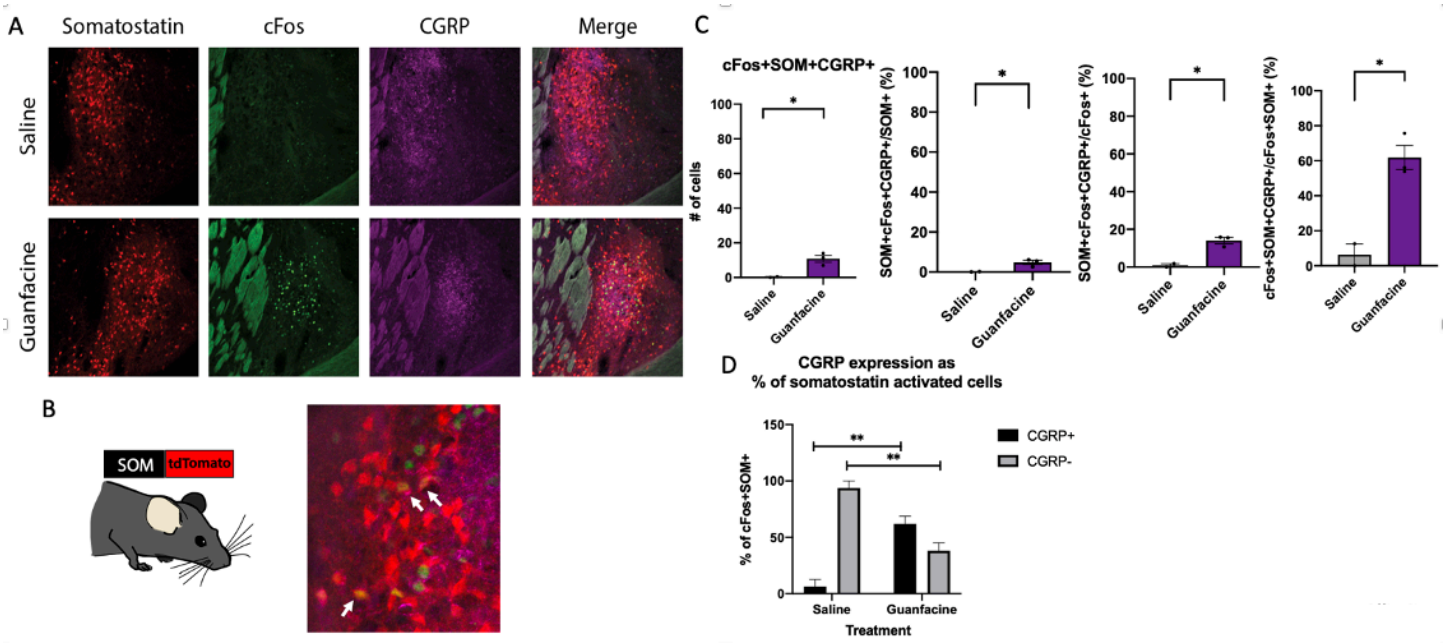

Figure 20: Guanfacine activates a small subset of somatostatin neurons in the BNST synapsed onto by the PBN (BNST$^{SOM\ or}$ SOM$^{PBN \rightarrow BNST}$).

(A) Representative images of SOM-ROSA to investigate CGRP and SOM expression with guanfacine-activated neurons in the BNST. (B) Zoomed in image showing colocalization of cFos, SOM and CGRP. (C) Quantitative results investigated cFos, SOM and CGRP colocalization. (D) CGRP expression of Somatostatin activated cells by guanfacine following guanfacine or saline injection.

4.3 Appendix III. Comparison of FosCreER and FosCreER2 mouse lines

After our initial experiments using the FosCreER or FosTRAP line, a new mouse line was released termed FosTRAP2 or FosCreER2 (DeNardo et al., 2019; Guenthner et al., 2013). The original FosTRAP line was genetically designed that the FosCreER allele when expressed resulted in the endogenous Fos gene becoming null due to placement of a stop codon in the CreER gene. Therefore, the line can only be used as heterozygous as knockout of the Fos gene results in embryonic lethality. In the FosTRAP2 line, the FosCreER sequence was moved behind the endogenous Fos gene and therefore expression of the CreER gene does not affect endogenous expression of the Fos gene. This new line also resulted in enhanced TRAPing of Fos-activated cells (DeNardo et al., 2019).

To compare the ability of FosTRAP2 to capture guansembles, we repeated our previous experiments comparing guanfacine activated cells to cells activated by saline or a second exposure to guanfacine. To do this we used

heterozygous FosTRAP and homozygous FosTRAP2 mice and followed our previous guanfacine-TRAP model. One week later, the mice were given saline or guanfacine followed by perfusion and immunohistochemistry staining for cFos (Figure 21A). We found that there was an increase in the number of guanfacine TRAPed cells in the FosTRAP2 mouse line compared to the original FosTRAP line (Figure 21B). However, we did not see an increase in the number of reactivated cells designated by mCherry+cFos+ expression (Figure 21C). While the FosTRAP2 line resulted in an increase in the number of cells TRAPed, it doesn't seem to be due to an increase in the ability capture Guansembles.

This led us to hypothesize that the second allele of the FosCreER2 gene was driving this enhanced TRAPing. To further investigate this, we repeated these experiments in heterozygous and homozygous FosTRAP2 mice (Figure 22). Similar to the difference between FosTRAP and FosTRAP2 lines, we found an increase in the number of TRAPed cells with homozygosity (Figure 22C). Again, we did not find an increase in the number of TRAPed cells that were reactivated with a second exposure to guanfacine (Figure 22B). These results suggest that the new FosTRAP line results in greater numbers of TRAPed cells but not necessarily greater specificity.

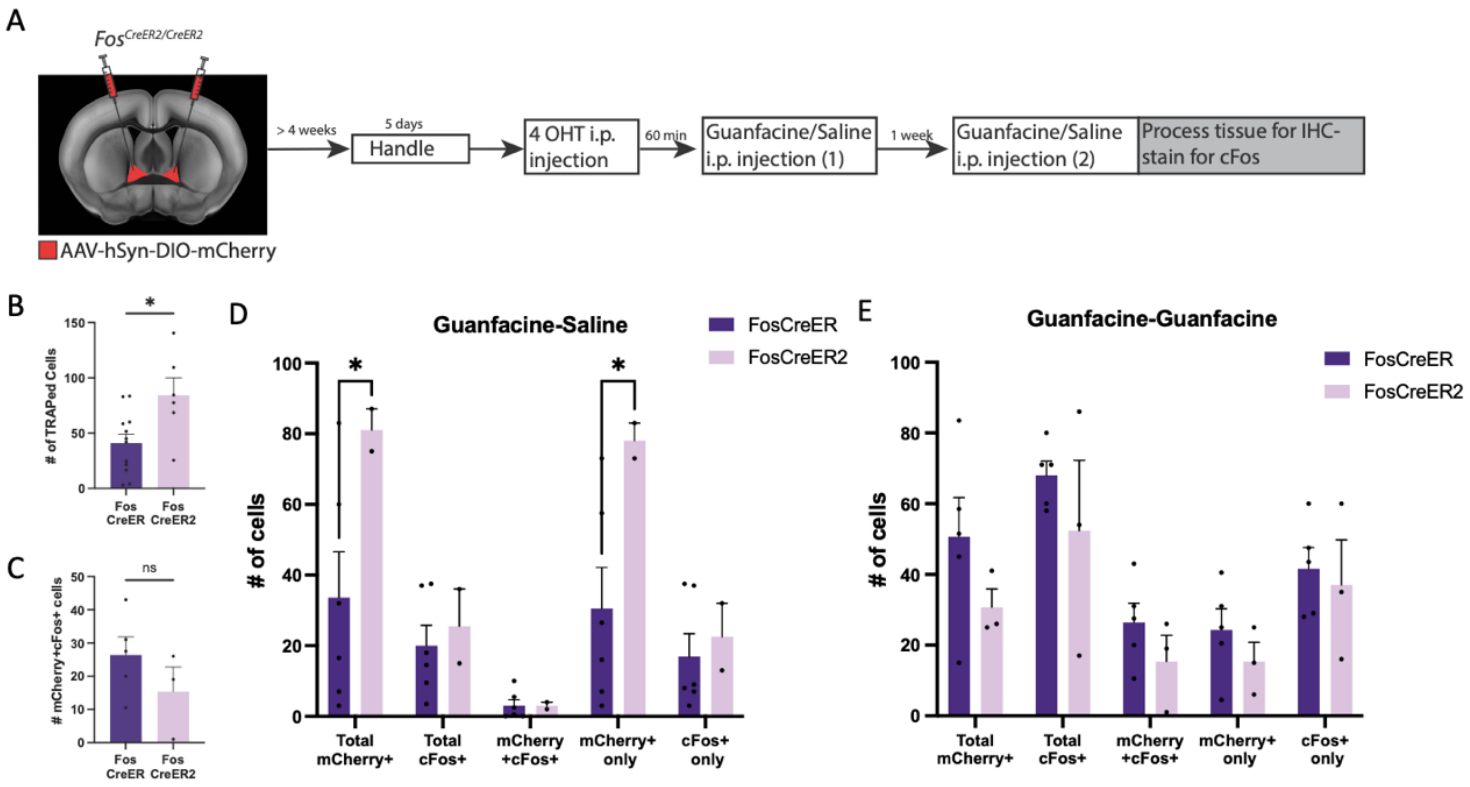

Figure 21: FosCreER2 +/+ express greater levels of guanfacine-activated neurons but similar levels of reactivated neurons with a second injection of guanfacine.

(A) Experimental design using heterozygous FosTRAP and homozygous FosTRAP2 mice to investigate guanfacine-activated neurons. (B) Comparison of guanfacine-TRAPed neurons in heterozygous FosTRAP and homozygous FosTRAP2 mice. (C) Comparison of neurons activated with repeated exposures to guanfacine in heterozygous FosTRAP and homozygous FosTRAP2 mice. (D) Number of cells per marker of heterozygous FosTRAP and homozygous FosTRAP2 mice giving injection of saline following guanfacine-TRAPing. (E) Number of cells per marker of FosTRAP heterozygous and homozygous FosTRAP2 mice following two injections of guanfacine.

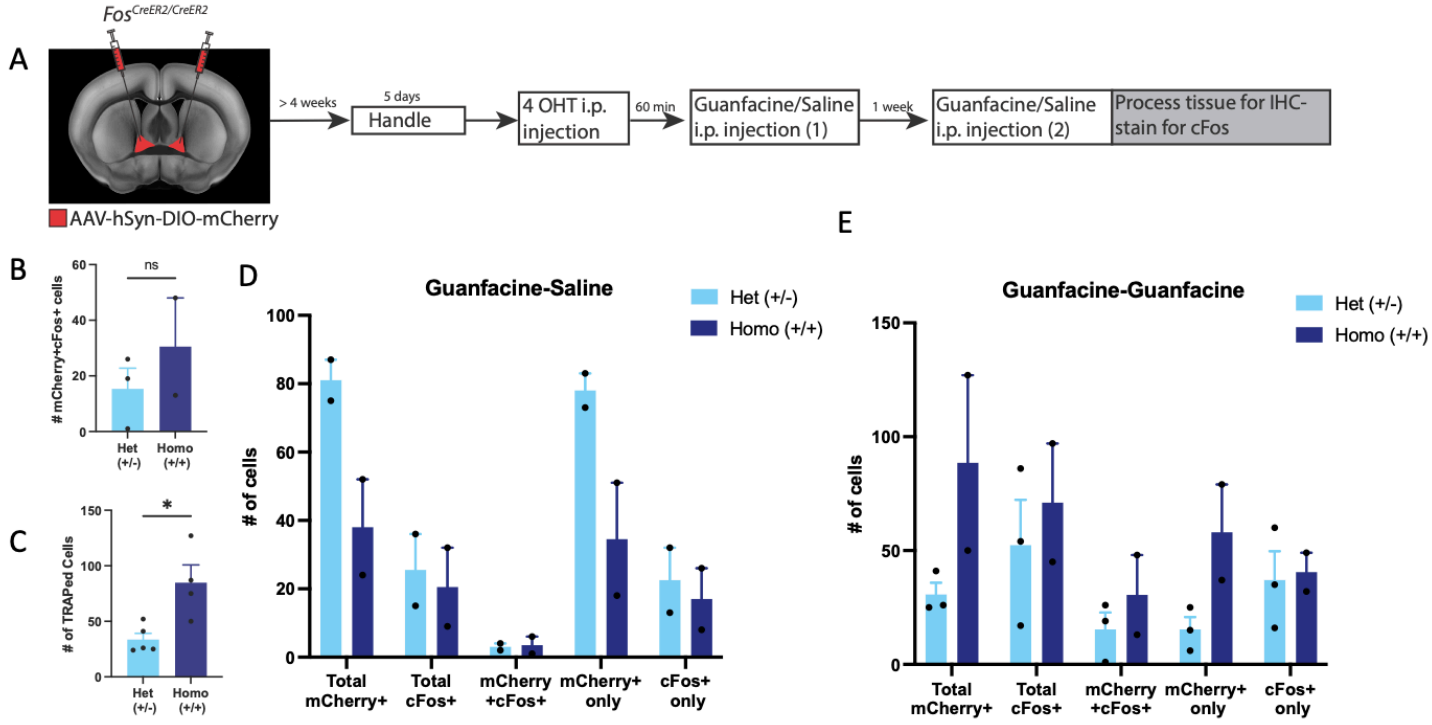

Figure 22: Homozygous FosCreER2 have greater expression of guanfacine-activated neurons.

(A) Experimental design using heterozygous and homozygous FosTRAP2 mice to investigate guanfacine-activated neurons. (B) Comparison of neurons activated with repeated exposures to guanfacine in heterozygous and homozygous FosTRAP2 mice. (C) Comparison of guanfacine-TRAPed neurons in heterozygous and homozygous FosTRAP2 mice. (D) Number of cells per marker of heterozygous and homozygous FosTRAP2 mice giving injection of saline following guanfacine-TRAPing. (E) Number of cells per marker of heterozygous and homozygous FosTRAP2 mice following two injections of guanfacine.

4.4 Appendix IV. Delination of guanfacine-activated cells into guanfacine-sensitive and guanfacine-resistant

Across mice we noticed a bimodal distribution in baseline calcium activity of Guansembles (Figure 23A). We found an inverse relationship between the baseline frequency (average peaks per minute) and the change in frequency following guanfacine injection, suggesting a further delineation of the effects of guanfacine across animals (Figure 23B). To further assess this, we separated the initial values of z-scores following guanfacine injection into two populations of mice based on median split analysis (Figure 23C). If a mouse had baseline activity, measured by peaks per minute, above the average of the entire population, it was designated as guanfacine-sensitive, and if activity was below, it was designated as guanfacine-resistant. We found the mice with low baseline activity (guanfacine-resistant), had an increase in average Z-score following guanfacine injection, while the mice with high baseline activity (guanfacine-sensitive) had a decrease in average peaks per minute (Figure 23C). These results further suggest two differential populations of animals effected by guanfacine, suggesting the potential for state-dependent differences or potentially two populations of cell types activated by guanfacine. Furthermore, when we looked into the effects of restraint on these populations, we found a greater affect with the guanfacine-sensitive than the guanfacine-resistant (Figure 23D).

We next performed median split analysis on FosTRAP2 mice. We found a significant difference between the average z-scores of guanfacine-resistant and guanfacine-sensitive mice based on their basal activity (Figure 23E). We found a greater effect of guanfacine on the average peaks per minute in the guanfacine-sensiitive than the guanfacine-resistant, simlar to our results in the FosTRAP. Invesigating the effects of restraint on the two populations, we found the guanfacine-sensitive mice had a stronger effect towards restraint compared to guanfacine-resistant (Figure 23F-23G). Additionally, the effect of restraint stress stayed highly significant across al four days of restraint while it was most highly significant on day one for guanfacine-resistant mice (Figure 23F-23G).

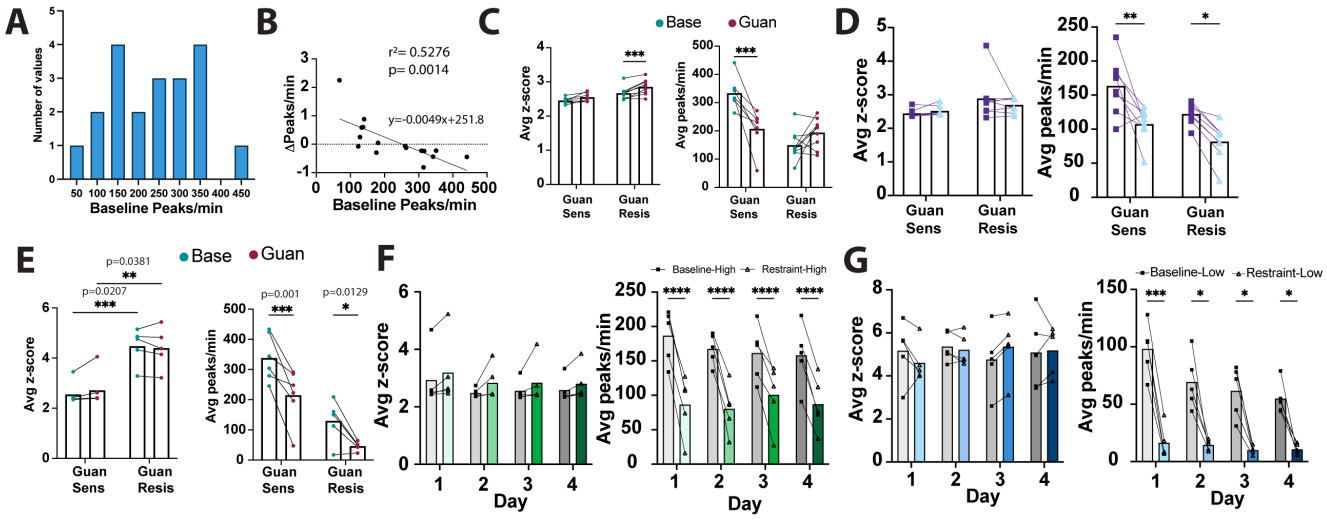

Figure 23: Delineation of Guansembles designated as guanfacine-sensitive and guanfacine-resistant and the effects of guanfacine and stress on each.

(A) Histogram of number of mice plotted against baselien peaks per minute. (B) Correlation graph showing relationship of baseline peaks per minute vs. change in peaks/minute following guanfacine injection (r^2=-0.5276, p=0.0014). ***(C)*** *Average Z-score and peaks per minute in FosTRAP following median split analysis based on baseline peaks per minute prior to guanfacine injection (guan-sensitive: n=7, p-0.0008, guan-resistant: n=9, p=0.0005). (D) Average Z-score and peaks per minute in FosTRAP following median split analysis based on baseline peaks per minute before and during restraint stress. (E) Average Z-score and peaks per minute in FosTRAP2 following median split analysis based on baseline peaks per minute prior to guanfacine injection. (F) Average Z-score and peaks per minute in FosTRAP2 in guanfacine-sensitive mice following median split analysis based on baseline peaks per minute before and during restraint stress. (G) Average Z-score and peaks per minute in FosTRAP2 in guanfacine-resistant mice following median split analysis based on baseline peaks per minute before and during restraint stress.*

4.5 Appendix V. Restraint bout movement analysis of Guansembles in the BNST

To investigate the effect of repeated restraint exposure on coping bouts, we performed analysis of bouts recorded using DeepLabCut (for description see chapter 2). We calculated changes in number of bouts, total time of bout, and average duration of bouts across four days of repeated restraint stress (Figure 24). Interestingly, we did not find a significant difference in these parameters across each day.

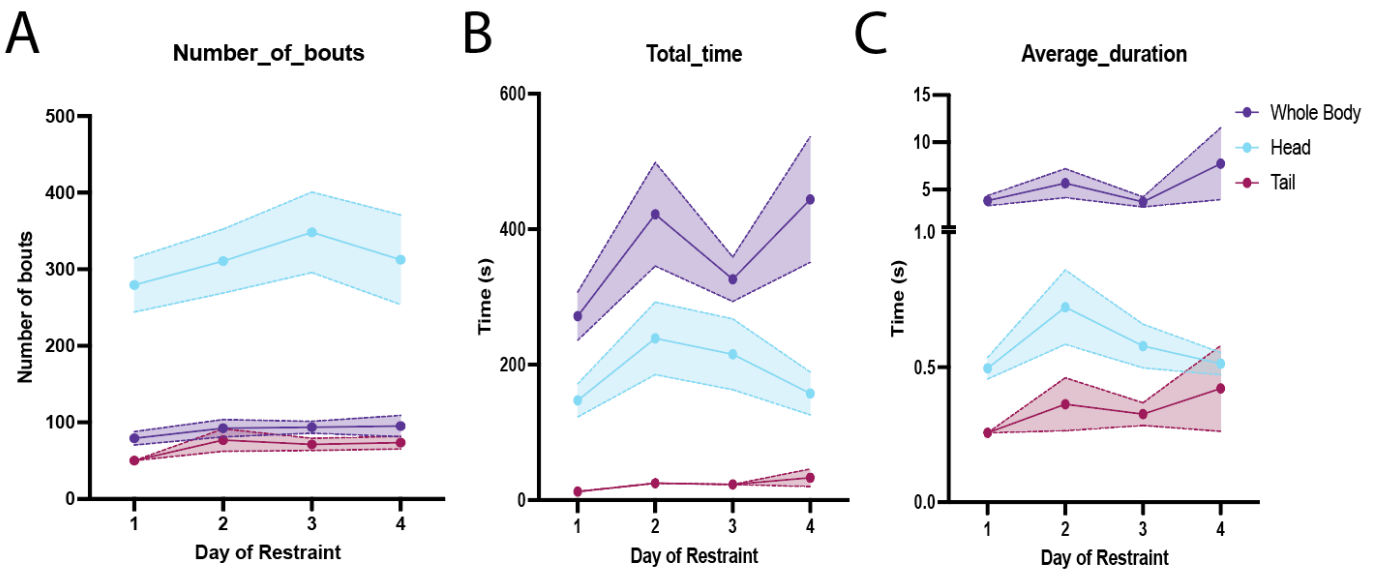

Figure 24. Movement analysis during restraint stress exposure of FosCreER.

(A) Calculated number of whole body, head, and tail coping bouts across four days of repeated restraint. (B) Calculated total duration of whole body, head, and tail coping bouts across four days of repeated restraint. (C) Calculate daverage duration of whole body, head, and tail coping bouts across four days of repeated restraint.

During our analysis of number of coping bouts and signal during guanfacine injection we noticed a correlation trend. We plotted correlation plots of calcium signals and number of coping bouts (Figure 25A). We found that number of bouts and calcium signal during guanfacine injection was negatively correlated. Further, this correlation decreased over time of repeated restraint stress. Similarly, we found a positive correlation between overall calcium activity in Guasnembles in response to guanfacine and signal during invidiaul coping bouts (Figure 25B). This correlation decreased over repeated days of restraint stress.

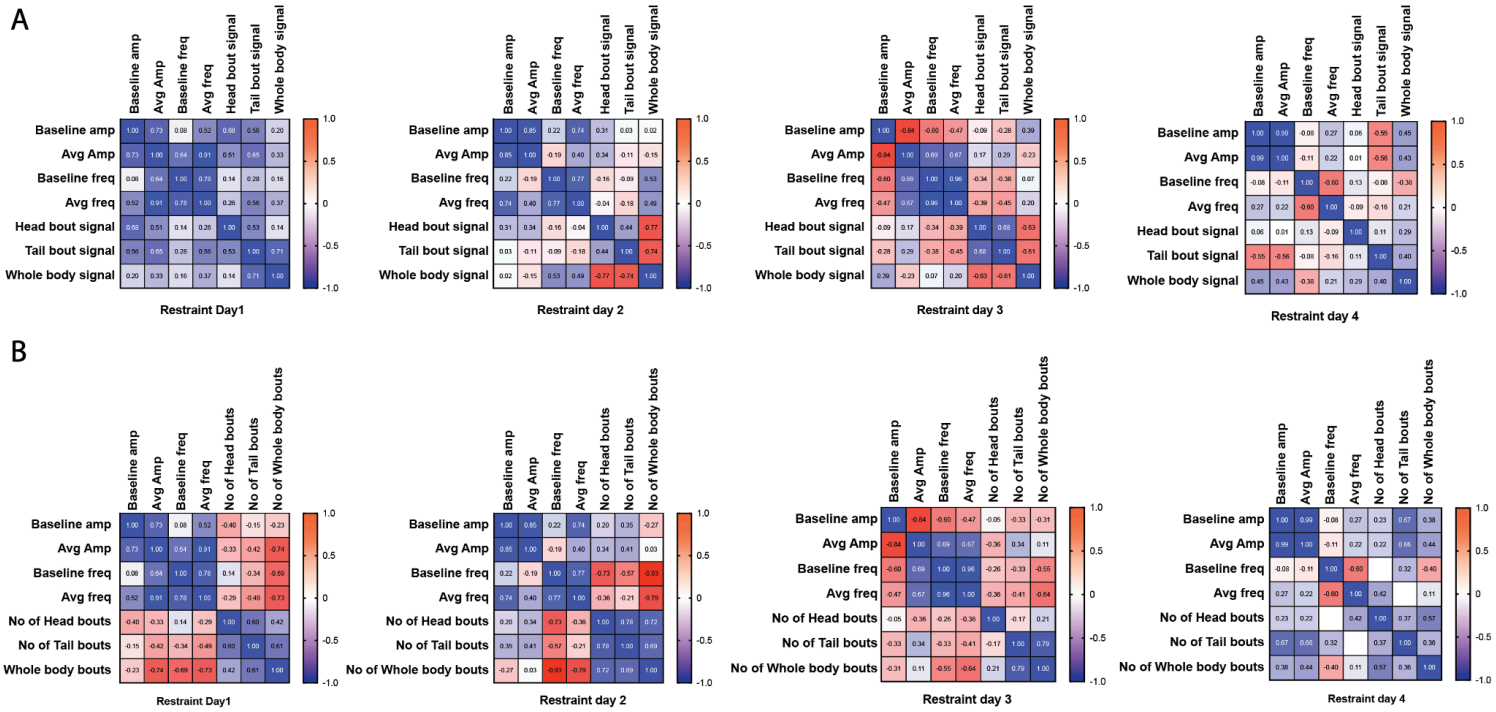

***Figure 25: Correlation of calcium signal and movement during restraint exposure in FosCreER*.**

(A) Correlation plots of calcium activity during restraint and number of head only, tail only, or whole body restraint bouts during four days of repeated restraint. **(**B) Correlation plots of calcium activity during guanfacine injection correlated with signal during head only, tail only, or whole body restraint bouts during four days of repeated restraint.

References

Agarwal, A., Halvorson, L.M., Legradi, G., 2005. Pituitary adenylate cyclase-activating polypeptide (PACAP) mimics neuroendocrine and behavioral manifestations of stress: Evidence for PKA-mediated expression of the corticotropin-releasing hormone (CRH) gene. Mol. Brain Res. 138, 45–57. https://doi.org/10.1016/j.molbrainres.2005.03.016

Ahrens, S., Wu, M.V., Furlan, A., Hwang, G.-R., Paik, R., Li, H., Penzo, M.A., Tollkuhn, J., Li, B., 2018. A Central Extended Amygdala Circuit That Modulates Anxiety. J. Neurosci. 38, 5567–5583. https://doi.org/10.1523/JNEUROSCI.0705-18.2018

Alamo, C., López-Muñoz, F., Sánchez-García, J., 2016. Mechanism of action of guanfacine: a postsynaptic differential approach to the treatment of attention deficit hyperactivity disorder (adhd). Actas Esp. Psiquiatr. 44, 107–112.

Albrechet-Souza, L., Viola, T.W., Grassi-Oliveira, R., Miczek, K.A., de Almeida, R.M.M., 2017. Corticotropin Releasing Factor in the Bed Nucleus of the Stria Terminalis in Socially Defeated and Non-stressed Mice with a History of Chronic Alcohol Intake. Front. Pharmacol. 8, 762. https://doi.org/10.3389/fphar.2017.00762

Alheid, G.F., 2006. Extended Amygdala and Basal Forebrain. Ann. N. Y. Acad. Sci. 985, 185–205. https://doi.org/10.1111/j.1749-6632.2003.tb07082.x

Alheid, G.F., Heimer, L., 1988. New perspectives in basal forebrain organization of special relevance for neuropsychiatric disorders: The striatopallidal, amygdaloid, and corticopetal components of substantia innominata. Neuroscience 27, 1–39. https://doi.org/10.1016/0306-4522(88)90217-5

Anderson, J., Wang, C., Zaidi, A., Rice, T., Coffey, B.J., 2020. Guanfacine as a Treatment for Posttraumatic Stress Disorder in an Adolescent Female. J. Child Adolesc. Psychopharmacol. 30, 398–401. https://doi.org/10.1089/cap.2020.29186.bjc

Armario, A., Vallès, A., Dal-Zotto, S., Márquez, C., Belda, X., 2004. A Single Exposure to Severe Stressors Causes Long-term Desensitisation of the Physiological Response to the Homotypic Stressor. Stress 7, 157–172. https://doi.org/10.1080/10253890400010721

Arnsten, A., Cai, J., Goldman-Rakic, P., 1988. The alpha-2 adrenergic agonist guanfacine improves memory in aged monkeys without sedative or hypotensive side effects: evidence for alpha-2 receptor subtypes. J. Neurosci. 8, 4287–4298. https://doi.org/10.1523/JNEUROSCI.08-11-04287.1988

Arnsten, A.F.T., Jin, L.E., 2012. Guanfacine for the treatment of cognitive disorders: a century of discoveries at Yale. Yale J. Biol. Med. 85, 45–58.

Arnsten, A.F.T., Ramos, B.P., Birnbaum, S.G., Taylor, J.R., 2005. Protein kinase A as a therapeutic target for memory disorders: rationale and challenges. Trends Mol. Med. 11, 121–128. https://doi.org/10.1016/j.molmed.2005.01.006

Aston-Jones, G., Delfs, J.M., Druhan, J., Zhu, Y., 1999. The Bed Nucleus of the Stria Terminalis: A Target Site for Noradrenergic Actions in Opiate Withdrawal. Ann. N. Y. Acad. Sci. 877, 486–498. https://doi.org/10.1111/j.1749-6632.1999.tb09284.x

Báez-Mendoza, R., Schultz, W., 2013. The role of the striatum in social behavior. Front. Neurosci. 7. https://doi.org/10.3389/fnins.2013.00233

Banihashemi, L., Rinaman, L., 2006. Noradrenergic Inputs to the Bed Nucleus of the Stria Terminalis and Paraventricular Nucleus of the Hypothalamus Underlie Hypothalamic-Pituitary-Adrenal Axis But Not Hypophagic or Conditioned

Avoidance Responses to Systemic Yohimbine. J. Neurosci. 26, 11442–11453. https://doi.org/10.1523/JNEUROSCI.3561-06.2006

Barrett, A.E., Turner, R.J., 2006. Family structure and substance use problems in adolescence and early adulthood: examining explanations for the relationship. Addiction 101, 109–120. https://doi.org/10.1111/j.1360-0443.2005.01296.x

Becker, W., 2021. The bh TCSPC handbook, 9th ed.

Becker, W., 2005. Advanced time-correlated single photon counting techniques. Springer, Berlin; New York.

Beerling, W., Koolhaas, J.M., Ahnaou, A., Bouwknecht, J.A., de Boer, S.F., Meerlo, P., Drinkenburg, W.H.I.M., 2011. Physiological and hormonal responses to novelty exposure in rats are mainly related to ongoing behavioral activity. Physiol. Behav. 103, 412–420. https://doi.org/10.1016/j.physbeh.2011.03.014

Berggren, U., 2000. Subsensitive alpha-2-adrenoceptor function in male alcohol-dependent individuals during 6 months of abstinence. Drug Alcohol Depend. 57, 255–260. https://doi.org/10.1016/S0376-8716(99)00051-4

Berk, M.L., Finkelstein, J.A., 1982. Efferent connections of the lateral hypothalamic area of the rat: An autoradiographic investigation. Brain Res. Bull. 8, 511–526. https://doi.org/10.1016/0361-9230(82)90009-0

Bernabeu, R., Bevilaqua, L., Ardenghi, P., Bromberg, E., Schmitz, P., Bianchin, M., Izquierdo, I., Medina, J.H., 1997. Involvement of hippocampal cAMP/cAMP-dependent protein kinase signaling pathways in a late memory consolidation phase of aversively motivated learning in rats. Proc. Natl. Acad. Sci. 94, 7041–7046. https://doi.org/10.1073/pnas.94.13.7041

Biederman, Joseph, Melmed, R.D., Patel, A., McBurnett, K., Donahue, J., Lyne, A., 2008. Long-Term, Open-Label Extension Study of Guanfacine Extended Release in Children and Adolescents with ADHD. CNS Spectr. 13, 1047–1055. https://doi.org/10.1017/S1092852900017107

Biederman, J., Melmed, R.D., Patel, A., McBurnett, K., Konow, J., Lyne, A., Scherer, N., for the SPD503 Study Group, 2008. A Randomized, Double-Blind, Placebo-Controlled Study of Guanfacine Extended Release in Children and Adolescents With Attention-Deficit/Hyperactivity Disorder. PEDIATRICS 121, e73–e84. https://doi.org/10.1542/peds.2006-3695

Blaschko, H., Bloom, F.E., Coupland, R.E., Euler, U.S., Furchgott, R.F., Haefely, W., Himms-Hagen, J., Holzbauer, M., Kopin, I.J., Kosterlitz, H.W., Lees, G.M., Marley, E., Muscholl, E., Sandler, M., Sharman, D.F., Smith, D.A., Stephenson, J.D., Stjärne, L., Thoenen, H., Trendelenburg, U., Welsh, J.H., Winkler, H., Blaschko, H., 1972. Catecholamines. Springer Berlin Heidelberg, Berlin, Heidelberg.

Block, C.H., Hoffman, G.E., 1987. Neuropeptide and monoamine components of the parabrachial pontine complex. Peptides 8, 267–283. https://doi.org/10.1016/0196-9781(87)90102-1

Blundell, J., Adamec, R., 2007. The NMDA receptor antagonist CPP blocks the effects of predator stress on pCREB in brain regions involved in fearful and anxious behavior. Brain Res. 1136, 59–76. https://doi.org/10.1016/j.brainres.2006.09.078

Boellner, S.W., Pennick, M., Fiske, K., Lyne, A., Shojaei, A., 2007. Pharmacokinetics of a Guanfacine Extended-Release Formulation in Children and Adolescents with Attention-Deficit–Hyperactivity Disorder. Pharmacotherapy 27, 1253–1262. https://doi.org/10.1592/phco.27.9.1253

Bossert, J.M., Stern, A.L., Theberge, F.R.M., Cifani, C., Koya, E., Hope, B.T., Shaham, Y., 2011. Ventral medial prefrontal cortex neuronal ensembles mediate context-induced relapse to heroin. Nat. Neurosci. 14, 420–422. https://doi.org/10.1038/nn.2758

Bowers, L.K., Swisher, C.B., Behbehani, M.M., 2003. Membrane and synaptic effects of corticotropin-releasing factor on periaqueductal gray neurons of the rat. Brain Res. 981, 52–57. https://doi.org/10.1016/S0006-8993(03)02886-5

Brady, K.T., Sinha, R., 2005. Co-Occurring Mental and Substance Use Disorders: The Neurobiological Effects of Chronic Stress. Am. J. Psychiatry 162, 1483–1493. https://doi.org/10.1176/appi.ajp.162.8.1483

Bria, A., Bernaschi, M., Guarrasi, M., Iannello, G., 2019. Exploiting Multi-Level Parallelism for Stitching Very Large Microscopy Images. Front. Neuroinformatics 13, 41. https://doi.org/10.3389/fninf.2019.00041

Briand, L.A., Vassoler, F.M., Pierce, R.C., Valentino, R.J., Blendy, J.A., 2010. Ventral Tegmental Afferents in Stress-Induced Reinstatement: The Role of cAMP Response Element-Binding Protein. J. Neurosci. 30, 16149–16159. https://doi.org/10.1523/JNEUROSCI.2827-10.2010

Bridgewater, N.J., 2006. Tenex (guanfacine HCl tablets), product information.

Britton, D.R., Britton, K.T., 1981. A sensitive open field measure of anxiolytic drug activity. Pharmacol. Biochem. Behav. 15, 577–582. https://doi.org/10.1016/0091-3057(81)90212-4

Brown, Z.J., Nobrega, J.N., Erb, S., 2011. Central injections of noradrenaline induce reinstatement of cocaine seeking and increase c-fos mRNA expression in the extended amygdala. Behav. Brain Res. 217, 472–476. https://doi.org/10.1016/j.bbr.2010.09.025

Buffalari, D.M., Baldwin, C.K., See, R.E., 2012. Treatment of cocaine withdrawal anxiety with guanfacine: relationships to cocaine intake and reinstatement of cocaine seeking in rats. Psychopharmacology (Berl.) 223, 179–190. https://doi.org/10.1007/s00213-012-2705-1

Buzsáki, G., Moser, E.I., 2013. Memory, navigation and theta rhythm in the hippocampal-entorhinal system. Nat. Neurosci. 16, 130–138. https://doi.org/10.1038/nn.3304

Cai, H., 2014. Central amygdala PKC-δ+ neurons mediate the influence of multiple anorexigenic signals. Nat. Neurosci. 17, 11.

Caillé, S., Guillem, K., Cador, M., Manzoni, O., Georges, F., 2009. Voluntary nicotine consumption triggers in vivo potentiation of cortical excitatory drives to midbrain dopaminergic neurons. J. Neurosci. Off. J. Soc. Neurosci. 29, 10410–10415. https://doi.org/10.1523/JNEUROSCI.2950-09.2009

Campbell, R.R., Domingo, R.D., Williams, A.R., Wroten, M.G., McGregor, H.A., Waltermire, R.S., Greentree, D.I., Goulding, S.P., Thompson, A.B., Lee, K.M., Quadir, S.G., Jimenez Chavez, C.L., Coelho, M.A., Gould, A.T., von Jonquieres, G., Klugmann, M., Worley, P.F., Kippin, T.E., Szumlinski, K.K., 2019. Increased Alcohol-Drinking Induced by Manipulations of mGlu5 Phosphorylation within the Bed Nucleus of the Stria Terminalis. J. Neurosci. 39, 2745–2761. https://doi.org/10.1523/JNEUROSCI.1909-18.2018

Campos, C.A., Bowen, A.J., Schwartz, M.W., Palmiter, R.D., 2016. Parabrachial CGRP Neurons Control Meal Termination. Cell Metab. 23, 811–820. https://doi.org/10.1016/j.cmet.2016.04.006

Canteras, N.S., Swanson, L.W., 1992. Projections of the ventral subiculum to the amygdala, septum, and hypothalamus: A PHAL anterograde tract-tracing study in the rat. J. Comp. Neurol. 324, 180–194. https://doi.org/10.1002/cne.903240204

Carboni, E., Silvagni, A., Rolando, M.T.P., Di Chiara, G., 2000. Stimulation of *In Vivo* Dopamine Transmission in the Bed Nucleus of Stria Terminalis by Reinforcing Drugs. J. Neurosci. 20, RC102–RC102. https://doi.org/10.1523/JNEUROSCI.20-20-j0002.2000

Carter, M.E., Soden, M.E., Zweifel, L.S., Palmiter, R.D., 2013. Genetic identification of a neural circuit that suppresses appetite. Nature 503, 111–114. https://doi.org/10.1038/nature12596

Cecchi, M., Khoshbouei, H., Morilak, D.A., 2002. Modulatory effects of norepinephrine, acting on alpha1 receptors in the central nucleus of the amygdala, on behavioral and neuroendocrine responses to acute immobilization stress. Neuropharmacology 43, 1139–1147. https://doi.org/10.1016/S0028-3908(02)00292-7

Centanni, S.W., Bedse, G., Patel, S., Winder, D.G., 2019a. Driving the Downward Spiral: Alcohol-Induced Dysregulation of Extended Amygdala Circuits and Negative Affect. Alcohol. Clin. Exp. Res. 43, 2000–2013. https://doi.org/10.1111/acer.14178

Centanni, S.W., Morris, B.D., Luchsinger, J.R., Bedse, G., Fetterly, T.L., Patel, S., Winder, D.G., 2019b. Endocannabinoid control of the insular-bed nucleus of the stria terminalis circuit regulates negative affective behavior associated with alcohol abstinence. Neuropsychopharmacology 44, 526–537. https://doi.org/10.1038/s41386-018-0257-8

Chang, X., Wang, J., Jiang, H., Shi, L., Xie, J., 2019. Hyperpolarization-Activated Cyclic Nucleotide-Gated Channels: An Emerging Role in Neurodegenerative Diseases. Front. Mol. Neurosci. 12, 141. https://doi.org/10.3389/fnmol.2019.00141

Chen, Y., Saulnier, J.L., Yellen, G., Sabatini, B.L., 2014. A PKA activity sensor for quantitative analysis of endogenous GPCR signaling via 2-photon FRET-FLIM imaging. Front. Pharmacol. 5. https://doi.org/10.3389/fphar.2014.00056

Childress, A.C., 2012. Guanfacine Extended Release as Adjunctive Therapy to Psychostimulants in Children and Adolescents With Attention-Deficit/Hyperactivity Disorder. Adv. Ther. 29, 385–400. https://doi.org/10.1007/s12325-012-0020-1

Ch'ng, S., Fu, J., Brown, R.M., McDougall, S.J., Lawrence, A.J., 2018. The intersection of stress and reward: BNST modulation of aversive and appetitive states. Prog. Neuropsychopharmacol. Biol. Psychiatry 87, 108–125. https://doi.org/10.1016/j.pnpbp.2018.01.005

Clark, D., 2003. Physical and sexual abuse, depression and alcohol use disorders in adolescents: onsets and outcomes. Drug Alcohol Depend. 69, 51–60. https://doi.org/10.1016/S0376-8716(02)00254-5

Clark, D.B., Lesnick, L., Hegedus, A.M., 1997. Traumas and Other Adverse Life Events in Adolescents With Alcohol Abuse and Dependence. J. Am. Acad. Child Adolesc. Psychiatry 36, 1744–1751. https://doi.org/10.1097/00004583-199712000-00023

Commons, K.G., Connolley, K.R., Valentino, R.J., 2003. A Neurochemically Distinct Dorsal Raphe-Limbic Circuit with a Potential Role in Affective Disorders. Neuropsychopharmacology 28, 206–215. https://doi.org/10.1038/sj.npp.1300045

Connor, D.F., Findling, R.L., Kollins, S.H., Sallee, F., López, F.A., Lyne, A., Tremblay, G., 2010. Effects of Guanfacine Extended Release on Oppositional Symptoms in Children Aged 6–12 Years with Attention-Deficit Hyperactivity Disorder and Oppositional Symptoms: A Randomized, Double-Blind, Placebo-Controlled Trial. CNS Drugs 1. https://doi.org/10.2165/11537790-000000000-00000

Crankshaw, D.L., Briggs, J.E., Olszewski, P.K., Shi, Q., Grace, M.K., Billington, C.J., Levine, A.S., 2003. Effects of intracerebroventricular ethanol on ingestive behavior and induction of c-Fos immunoreactivity in selected brain regions. Physiol. Behav. 79, 113–120. https://doi.org/10.1016/S0031-9384(03)00111-2

Cruz, F.C., Javier Rubio, F., Hope, B.T., 2015. Using c-fos to study neuronal ensembles in corticostriatal circuitry of addiction. Brain Res. 1628, 157–173. https://doi.org/10.1016/j.brainres.2014.11.005

Cruz, M.P., n.d. Guanfacine Extended-Release Tablets (Intuniv), a Nonstimulant Selective Alpha2A-Adrenergic Receptor Agonist For Attention-Deficit/Hyperactivity Disorder 4.

Cui, G., Jun, S.B., Jin, X., Pham, M.D., Vogel, S.S., Lovinger, D.M., Costa, R.M., 2013. Concurrent activation of striatal direct and indirect pathways during action initiation. Nature 494, 238–242. https://doi.org/10.1038/nature11846

Cullinan, W.E., Herman, J.P., Watson, S.J., 1993. Ventral subicular interaction with the hypothalamic paraventricular nucleus: Evidence for a relay in the bed nucleus of the stria terminalis. J. Comp. Neurol. 332, 1–20. https://doi.org/10.1002/cne.903320102

Davis, L.L., Ward, C., Rasmusson, A., Newell, J.M., Frazier, E., Southwick, S.M., 2008. A placebo-controlled trial of guanfacine for the treatment of posttraumatic stress disorder in veterans. Psychopharmacol. Bull. 41, 8–18.

Davis, M., Whalen, P.J., 2001. The amygdala: vigilance and emotion. Mol. Psychiatry 6, 13–34. https://doi.org/10.1038/sj.mp.4000812

Dean, K.M., Roudot, P., Welf, E.S., Danuser, G., Fiolka, R., 2015. Deconvolution-free Subcellular Imaging with Axially Swept Light Sheet Microscopy. Biophys. J. 108, 2807–2815. https://doi.org/10.1016/j.bpj.2015.05.013

Delfs, J.M., Zhu, Y., Druhan, J.P., Aston-Jones, G., 2000. Noradrenaline in the ventral forebrain is critical for opiate withdrawal-induced aversion. Nature 403, 430–434. https://doi.org/10.1038/35000212

Dembo, R., Dertke, M., Borders, S., Washburn, M., Schmeidler, J., 1988. The Relationship Between Physical and Sexual Abuse and Tobacco, Alcohol, and Illicit Drug Use Among Youths in a Juvenile Detention Center. Int. J. Addict. 23, 351–378. https://doi.org/10.3109/10826088809039203

DeNardo, L.A., Liu, C.D., Allen, W.E., Adams, E.L., Friedmann, D., Fu, L., Guenthner, C.J., Tessier-Lavigne, M., Luo, L., 2019. Temporal evolution of cortical ensembles promoting remote memory retrieval. Nat. Neurosci. 22, 460–469. https://doi.org/10.1038/s41593-018-0318-7

Dong, H.-W., Petrovich, G.D., Swanson, L.W., 2001a. Topography of projections from amygdala to bed nuclei of the stria terminalisq. Brain Res. Rev. 55.

Dong, H.-W., Petrovich, G.D., Watts, A.G., Swanson, L.W., 2001b. Basic organization of projections from the oval and fusiform nuclei of the bed nuclei of the stria terminalis in adult rat brain. J. Comp. Neurol. 436, 430–455. https://doi.org/10.1002/cne.1079

Dong, H.-W., Swanson, L.W., 2006. Projections from bed nuclei of the stria terminalis, anteromedial area: Cerebral hemisphere integration of neuroendocrine, autonomic, and behavioral aspects of energy balance. J. Comp. Neurol. 494, 142–178. https://doi.org/10.1002/cne.20788

Dong, H.-W., Swanson, L.W., 2004. Organization of axonal projections from the anterolateral area of the bed nuclei of the stria terminalis. J. Comp. Neurol. 468, 277–298. https://doi.org/10.1002/cne.10949

Douglas, K.R., Chan, G., Gelernter, J., Arias, A.J., Anton, R.F., Weiss, R.D., Brady, K., Poling, J., Farrer, L., Kranzler, H.R., 2010. Adverse childhood events as risk factors for substance dependence: Partial mediation by mood and anxiety disorders. Addict. Behav. 35, 7–13. https://doi.org/10.1016/j.addbeh.2009.07.004

Dumont, E.C., 2004. Noradrenaline Triggers GABAA Inhibition of Bed Nucleus of the Stria Terminalis Neurons Projecting to the Ventral Tegmental Area. J. Neurosci. 24, 8198–8204. https://doi.org/10.1523/JNEUROSCI.0425-04.2004

Dumont, E.C., Mark, G.P., Mader, S., Williams, J.T., 2005. Self-administration enhances excitatory synaptic transmission in the bed nucleus of the stria terminalis. Nat. Neurosci. 8, 413–414. https://doi.org/10.1038/nn1414

Dwivedi, Y., Pandey, G.N., 2011. Elucidating biological risk factors in suicide: Role of protein kinase A. Prog. Neuropsychopharmacol. Biol. Psychiatry 35, 831–841. https://doi.org/10.1016/j.pnpbp.2010.08.025

Egli, R.E., Kash, T.L., Choo, K., Savchenko, V., Matthews, R.T., Blakely, R.D., Winder, D.G., 2005. Norepinephrine Modulates Glutamatergic Transmission in the Bed Nucleus of the Stria Terminalis. Neuropsychopharmacology 30, 657–668. https://doi.org/10.1038/sj.npp.1300639

Eiler, W.J.A., Seyoum, R., Foster, K.L., Mailey, C., June, H.L., 2003. D1 dopamine receptor regulates alcohol-motivated behaviors in the bed nucleus of the stria terminalis in alcohol-preferring (P) rats. Synapse 48, 45–56. https://doi.org/10.1002/syn.10181

Erb, S., Hitchcott, P.K., Rajabi, H., Mueller, D., Shaham, Y., Stewart, J., 2000. Alpha-2 adrenergic receptor agonists block stress-induced reinstatement of cocaine seeking. Neuropsychopharmacol. Off. Publ. Am. Coll. Neuropsychopharmacol. 23, 138–150. https://doi.org/10.1016/S0893-133X(99)00158-X

Erb, S., Shaham, Y., Stewart, J., 1996. Stress reinstates cocaine-seeking behavior after prolonged extinction and a drug-free period. Psychopharmacology (Berl.) 128, 408–412. https://doi.org/10.1007/s002130050150

Erb, S., Stewart, J., 1999. A Role for the Bed Nucleus of the Stria Terminalis, But Not the Amygdala, in the Effects of Corticotropin-Releasing Factor on Stress-Induced Reinstatement of Cocaine Seeking. J. Neurosci. 19, RC35–RC35. https://doi.org/10.1523/JNEUROSCI.19-20-j0006.1999

Fadok, J.P., Krabbe, S., Markovic, M., Courtin, J., Xu, C., Massi, L., Botta, P., Bylund, K., Müller, C., Kovacevic, A., Tovote, P., Lüthi, A., 2017. A competitive inhibitory circuit for selection of active and passive fear responses. Nature 542, 96–100. https://doi.org/10.1038/nature21047

Fetterly, T.L., Basu, A., Nabit, B.P., Awad, E., Williford, K.M., Centanni, S.W., Matthews, R.T., Silberman, Y., Winder, D.G., 2019. α_{2A} -Adrenergic Receptor Activation Decreases Parabrachial Nucleus Excitatory Drive onto BNST CRF Neurons and Reduces Their Activity *In Vivo*. J. Neurosci. 39, 472–484. https://doi.org/10.1523/JNEUROSCI.1035-18.2018

Flavin, S.A., Matthews, R.T., Wang, Q., Muly, E.C., Winder, D.G., 2014a. 2A-Adrenergic Receptors Filter Parabrachial Inputs to the Bed Nucleus of the Stria Terminalis. J. Neurosci. 34, 9319–9331. https://doi.org/10.1523/JNEUROSCI.0822-14.2014

Flavin, S.A., Matthews, R.T., Wang, Q., Muly, E.C., Winder, D.G., 2014b. 2A-Adrenergic Receptors Filter Parabrachial Inputs to the Bed Nucleus of the Stria Terminalis. J. Neurosci. 34, 9319–9331. https://doi.org/10.1523/JNEUROSCI.0822-14.2014

Flavin, S.A., Winder, D.G., 2013. Noradrenergic control of the bed nucleus of the stria terminalis in stress and reward. Neuropharmacology 70, 324–330. https://doi.org/10.1016/j.neuropharm.2013.02.013

Folkes, O.M., Báldi, R., Kondev, V., Marcus, D.J., Hartley, N.D., Turner, B.D., Ayers, J.K., Baechle, J.J., Misra, M.P., Altemus, M., Grueter, C.A., Grueter, B.A., Patel, S., 2020. An endocannabinoid-regulated basolateral amygdala–nucleus accumbens circuit modulates sociability. J. Clin. Invest. 130, 1728–1742. https://doi.org/10.1172/JCI131752

Forray, M.I., Gysling, K., 2004. Role of noradrenergic projections to the bed nucleus of the stria terminalis in the regulation of the hypothalamic–pituitary–adrenal axis. Brain Res. Rev. 47, 145–160. https://doi.org/10.1016/j.brainresrev.2004.07.011

Fox, A.S., Oler, J.A., Tromp, D.P.M., Fudge, J.L., Kalin, N.H., 2015. Extending the amygdala in theories of threat processing. Trends Neurosci. 38, 319–329. https://doi.org/10.1016/j.tins.2015.03.002

Fox, H., Sinha, R., 2014. The Role of Guanfacine as a Therapeutic Agent to Address Stress-Related Pathophysiology in Cocaine-Dependent Individuals, in: Advances in Pharmacology. Elsevier, pp. 217–265. https://doi.org/10.1016/B978-0-12-420118-7.00006-8

Fox, H.C., Morgan, P.T., Sinha, R., 2014. Sex Differences in Guanfacine Effects on Drug Craving and Stress Arousal in Cocaine-Dependent Individuals. Neuropsychopharmacology 39, 1527–1537. https://doi.org/10.1038/npp.2014.1

Fox, H.C., Seo, D., Tuit, K., Hansen, J., Kimmerling, A., Morgan, P.T., Sinha, R., 2012. Guanfacine effects on stress, drug craving and prefrontal activation in cocaine dependent individuals: preliminary findings. J. Psychopharmacol. (Oxf.) 26, 958–972. https://doi.org/10.1177/0269881111430746

Freedman, L.J., Cassell, M.D., 1994. Distribution of dopaminergic fibers in the central division of the extended amygdala of the rat. Brain Res. 633, 243–252. https://doi.org/10.1016/0006-8993(94)91545-8

Friedman, J., Montero, F., Bourgois, P., Wahbi, R., Dye, D., Goodman-Meza, D., Shover, C., 2022. Xylazine spreads across the US: A growing component of the increasingly synthetic and polysubstance overdose crisis. Drug Alcohol Depend. 233, 109380. https://doi.org/10.1016/j.drugalcdep.2022.109380

Fuentealba, J.A., Forray, M.I., Gysling, K., 2002. Chronic Morphine Treatment and Withdrawal Increase Extracellular Levels of Norepinephrine in the Rat Bed Nucleus of the Stria Terminalis. J. Neurochem. 75, 741–748. https://doi.org/10.1046/j.1471-4159.2000.0750741.x

Funk, D., Mak, D., Coen, K., Lê, A.D., 2022. Role of alpha-2 adrenergic and kappa opioid receptors in the effects of alcohol gavage-induced dependence on alcohol seeking. Behav. Brain Res. 434, 114032. https://doi.org/10.1016/j.bbr.2022.114032

García-Carmona, J.-A., Milanés, M.-V., Laorden, M.-L., 2013. Brain stress system response after morphine-conditioned place preference. Int. J. Neuropsychopharmacol. 16, 1999–2011. https://doi.org/10.1017/S1461145713000588

Garner, A.R., Rowland, D.C., Hwang, S.Y., Baumgaertel, K., Roth, B.L., Kentros, C., Mayford, M., 2012. Generation of a Synthetic Memory Trace. Science 335, 1513–1516. https://doi.org/10.1126/science.1214985

Geisler, S., Zahm, D.S., 2005. Afferents of the ventral tegmental area in the rat-anatomical substratum for integrative functions. J. Comp. Neurol. 490, 270–294. https://doi.org/10.1002/cne.20668

Georges, F., Aston-Jones, G., 2002. Activation of Ventral Tegmental Area Cells by the Bed Nucleus of the Stria Terminalis: A Novel Excitatory Amino Acid Input to Midbrain Dopamine Neurons. J. Neurosci. 22, 5173–5187. https://doi.org/10.1523/JNEUROSCI.22-12-05173.2002

Giardino, W.J., Eban-Rothschild, A., Christoffel, D.J., Li, S.-B., Malenka, R.C., de Lecea, L., 2018. Parallel circuits from the bed nuclei of stria terminalis to the lateral hypothalamus drive opposing emotional states. Nat. Neurosci. 21, 1084–1095. https://doi.org/10.1038/s41593-018-0198-x

Giardino, W.J., Pomrenze, M.B., 2021. Extended Amygdala Neuropeptide Circuitry of Emotional Arousal: Waking Up on the Wrong Side of the Bed Nuclei of Stria Terminalis. Front. Behav. Neurosci. 15, 613025. https://doi.org/10.3389/fnbeh.2021.613025

Gibbons, C.H., 2019. Basics of autonomic nervous system function, in: Handbook of Clinical Neurology. Elsevier, pp. 407–418. https://doi.org/10.1016/B978-0-444-64032-1.00027-8

Girasole, A.E., Lum, M.Y., Nathaniel, D., Bair-Marshall, C.J., Guenthner, C.J., Luo, L., Kreitzer, A.C., Nelson, A.B., 2018. A Subpopulation of Striatal Neurons Mediates Levodopa-Induced Dyskinesia. Neuron 97, 787-795.e6. https://doi.org/10.1016/j.neuron.2018.01.017

Glangetas, C., Girard, D., Groc, L., Marsicano, G., Chaouloff, F., Georges, F., 2013. Stress Switches Cannabinoid Type-1 (CB1) Receptor-Dependent Plasticity from LTD to LTP in the Bed Nucleus of the Stria Terminalis. J. Neurosci. 33, 19657–19663. https://doi.org/10.1523/JNEUROSCI.3175-13.2013

Glavin, G.B., 1985. Stress and brain noradrenaline: A review. Neurosci. Biobehav. Rev. 9, 233–243. https://doi.org/10.1016/0149-7634(85)90048-X

Gomes, F.V., Alves, F.H.F., Guimarães, F.S., Correa, F.M.A., Resstel, L.B.M., Crestani, C.C., 2013. Cannabidiol administration into the bed nucleus of the stria terminalis alters cardiovascular responses induced by acute restraint stress through 5-HT1A receptor. Eur. Neuropsychopharmacol. 23, 1096–1104. https://doi.org/10.1016/j.euroneuro.2012.09.007

Gomes, F.V., Reis, D.G., Alves, F.H., Corrêa, F.M., Guimarães, F.S., Resstel, L.B., 2012. Cannabidiol injected into the bed nucleus of the stria terminalis reduces the expression of contextual fear conditioning via 5-HT $_{1A}$ receptors. J. Psychopharmacol. (Oxf.) 26, 104–113. https://doi.org/10.1177/0269881110389095

Gomes, F.V., Resstel, L.B.M., Guimarães, F.S., 2011. The anxiolytic-like effects of cannabidiol injected into the bed nucleus of the stria terminalis are mediated by 5-HT1A receptors. Psychopharmacology (Berl.) 213, 465–473. https://doi.org/10.1007/s00213-010-2036-z

Gomes-de-Souza, L., Bianchi, P.C., Costa-Ferreira, W., Tomeo, R.A., Cruz, F.C., Crestani, C.C., 2021. CB1 and CB2 receptors in the bed nucleus of the stria terminalis differently modulate anxiety-like behaviors in rats. Prog. Neuropsychopharmacol. Biol. Psychiatry 110284. https://doi.org/10.1016/j.pnpbp.2021.110284

Gong, S., Doughty, M., Harbaugh, C.R., Cummins, A., Hatten, M.E., Heintz, N., Gerfen, C.R., 2007. Targeting Cre Recombinase to Specific Neuron Populations with Bacterial Artificial Chromosome Constructs. J. Neurosci. 27, 9817–9823. https://doi.org/10.1523/JNEUROSCI.2707-07.2007

Gould, G.G., Burke, T.F., Osorio, M.D., Smolik, C.M., Zhang, W.Q., Onaivi, E.S., Gu, T.-T., DeSilva, M.N., Hensler, J.G., 2014. Enhanced novelty-induced corticosterone spike and upregulated serotonin 5-HT1A and cannabinoid CB1 receptors in adolescent BTBR mice. Psychoneuroendocrinology 39, 158–169. https://doi.org/10.1016/j.psyneuen.2013.09.003

Gowing, L., Farrell, M., Ali, R., White, J.M., 2004. Alpha2 adrenergic agonists for the management of opioid withdrawal, in: The Cochrane Collaboration (Ed.), Cochrane Database of Systematic Reviews. John Wiley & Sons, Ltd, Chichester, UK, p. CD002024.pub2. https://doi.org/10.1002/14651858.CD002024.pub2

Grant, B.F., Goldstein, R.B., Saha, T.D., Chou, S.P., Jung, J., Zhang, H., Pickering, R.P., Ruan, W.J., Smith, S.M., Huang, B., Hasin, D.S., 2015. Epidemiology of *DSM-5* Alcohol Use Disorder: Results From the National Epidemiologic Survey on Alcohol and Related Conditions III. JAMA Psychiatry 72, 757. https://doi.org/10.1001/jamapsychiatry.2015.0584

Greenwell, T.N., Walker, B.M., Cottone, P., Zorrilla, E.P., Koob, G.F., 2009. The alpha1 adrenergic receptor antagonist prazosin reduces heroin self-administration in rats with extended access to heroin administration. Pharmacol. Biochem. Behav. 91, 295–302. https://doi.org/10.1016/j.pbb.2008.07.012

Groenewegen, H.J., Berendse, H.W., 1994. The specificity of the 'nonspecific' midline and intralaminar thalamic nuclei. Trends Neurosci. 17, 52–57. https://doi.org/10.1016/0166-2236(94)90074-4

Grueter, B.A., 2006. Extracellular-Signal Regulated Kinase 1-Dependent Metabotropic Glutamate Receptor 5-Induced Long-Term Depression in the Bed Nucleus of the Stria Terminalis Is Disrupted by Cocaine Administration. J. Neurosci. 26, 3210–3219. https://doi.org/10.1523/JNEUROSCI.0170-06.2006

Guenthner, C.J., Miyamichi, K., Yang, H.H., Heller, H.C., Luo, L., 2013. Permanent Genetic Access to Transiently Active Neurons via TRAP: Targeted Recombination in Active Populations. Neuron 78, 773–784. https://doi.org/10.1016/j.neuron.2013.03.025

Guo, J.-D., Rainnie, D.G., 2010. Presynaptic 5-HT1B receptor-mediated serotonergic inhibition of glutamate transmission in the bed nucleus of the stria terminalis. Neuroscience 165, 1390–1401. https://doi.org/10.1016/j.neuroscience.2009.11.071

Gyawali, U., Martin, D.A., Sulima, A., Rice, K.C., Calu, D.J., 2020. Role of BNST CRFR1 Receptors in Incubation of Fentanyl Seeking. Front. Behav. Neurosci. 14, 153. https://doi.org/10.3389/fnbeh.2020.00153

Hajós-Korcsok, É., Robinson, D.D., Yu, J.H., Fitch, C.S., Walker, E., Merchant, K.M., 2003. Rapid habituation of hippocampal serotonin and norepinephrine release and anxiety-related behaviors, but not plasma corticosterone levels, to repeated footshock stress in rats. Pharmacol. Biochem. Behav. 74, 609–616. https://doi.org/10.1016/S0091-3057(02)01047-X

Hamlin, A.S., Clemens, K.J., Choi, E.A., McNally, G.P., 2009. Paraventricular thalamus mediates context-induced reinstatement (renewal) of extinguished reward seeking. Eur. J. Neurosci. 29, 802–812. https://doi.org/10.1111/j.1460-9568.2009.06623.x

Hammack, S.E., Mania, I., Rainnie, D.G., 2007. Differential Expression of Intrinsic Membrane Currents in Defined Cell Types of the Anterolateral Bed Nucleus of the Stria Terminalis. J. Neurophysiol. 98, 638–656. https://doi.org/10.1152/jn.00382.2007

Hammack, S.E., Schmid, M.J., LoPresti, M.L., Der-Avakian, A., Pellymounter, M.A., Foster, A.C., Watkins, L.R., Maier, S.F., 2003. Corticotropin Releasing Hormone Type 2 Receptors in the Dorsal Raphe Nucleus Mediate the Behavioral Consequences of Uncontrollable Stress. J. Neurosci. 23, 1019–1025. https://doi.org/10.1523/JNEUROSCI.23-03-01019.2003

Han, J.S., 2005. Critical Role of Calcitonin Gene-Related Peptide 1 Receptors in the Amygdala in Synaptic Plasticity and Pain Behavior. J. Neurosci. 25, 10717–10728. https://doi.org/10.1523/JNEUROSCI.4112-05.2005

Han, J.-S., Holland, P.C., Gallagher, M., 1999. Disconnection of the amygdala central nucleus and substantia innominata/nucleus basalis disrupts increments in conditioned stimulus processing in rats. Behav. Neurosci. 113, 143–151. https://doi.org/10.1037/0735-7044.113.1.143

Han, S., Soleiman, M.T., Soden, M.E., Zweifel, L.S., Palmiter, R.D., 2015. Elucidating an Affective Pain Circuit that Creates a Threat Memory. Cell 162, 363–374. https://doi.org/10.1016/j.cell.2015.05.057

Harmon, R.J., Riggs, P.D., 1996. Clonidine for Posttraumatic Stress Disorder in Preschool Children. J. Am. Acad. Child Adolesc. Psychiatry 35, 1247–1249. https://doi.org/10.1097/00004583-199609000-00022

Harris, G.C., Aston-Jones, G., 1993. β-adrenergic antagonists attenuate withdrawal anxiety in cocaine-and morphine-dependent rats. Psychopharmacology (Berl.) 113, 131–136. https://doi.org/10.1007/BF02244345

Harris, G.C., Wimmer, M., Aston-Jones, G., 2005. A role for lateral hypothalamic orexin neurons in reward seeking. Nature 437, 556–559. https://doi.org/10.1038/nature04071

Harris, N.A., Isaac, A.T., Günther, A., Merkel, K., Melchior, J., Xu, M., Eguakun, E., Perez, R., Nabit, B.P., Flavin, S., Gilsbach, R., Shonesy, B., Hein, L., Abel, T., Baumann, A., Matthews, R., Centanni, S.W., Winder, D.G., 2018. Dorsal BNST α2A-adrenergic receptors produce HCN-dependent excitatory actions that initiate anxiogenic behaviors. J. Neurosci. 0963–18. https://doi.org/10.1523/JNEUROSCI.0963-18.2018

Harrison, P.A., Fulkerson, J.A., Beebe, T.J., 1997. Multiple substance use among adolescent physical and sexual abuse victims. Child Abuse Negl. 21, 529–539. https://doi.org/10.1016/S0145-2134(97)00013-6

Hedde, P.N., Gratton, E., 2018. Selective plane illumination microscopy with a light sheet of uniform thickness formed by an electrically tunable lens. Microsc. Res. Tech. 81, 924–928. https://doi.org/10.1002/jemt.22707

Hein, L., Altman, J.D., Kobilka, B.K., 1999. Two functionally distinct a2-adrenergic receptors regulate sympathetic neurotransmission 402, 4.

Hennessy, M.B., 1991. Sensitization of the plasma corticosterone response to novel environments. Physiol. Behav. 50, 1175–1179. https://doi.org/10.1016/0031-9384(91)90579-D

Hervas, A., Huss, M., Johnson, M., McNicholas, F., van Stralen, J., Sreckovic, S., Lyne, A., Bloomfield, R., Sikirica, V., Robertson, B., 2014. Efficacy and safety of extended-release guanfacine hydrochloride in children and adolescents with attention-deficit/hyperactivity disorder: A randomized, controlled, Phase III trial. Eur. Neuropsychopharmacol. 24, 1861–1872. https://doi.org/10.1016/j.euroneuro.2014.09.014

Holland, P.C., 2006. Different Roles for Amygdala Central Nucleus and Substantia Innominata in the Surprise-Induced Enhancement of Learning. J. Neurosci. 26, 3791–3797. https://doi.org/10.1523/JNEUROSCI.0390-06.2006

Holland, P.C., Gallagher, M., 1999. Amygdala circuitry in attentional and representational processes. Trends Cogn. Sci. 3, 65–73. https://doi.org/10.1016/S1364-6613(98)01271-6

Holleran, K.M., Wilson, H.H., Fetterly, T.L., Bluett, R.J., Centanni, S.W., Gilfarb, R.A., Rocco, L.E.R., Patel, S., Winder, D.G., 2016. Ketamine and MAG Lipase Inhibitor-Dependent Reversal of Evolving Depressive-Like Behavior During Forced Abstinence From Alcohol Drinking. Neuropsychopharmacology 41, 2062–2071. https://doi.org/10.1038/npp.2016.3

Horrigan, J.P., 1996. GUANFACINE FOR PTSD NIGHTMARES. J. Am. Acad. Child Adolesc. Psychiatry 35, 975–976. https://doi.org/10.1097/00004583-199608000-00006

Hu, P., Liu, J., Maita, I., Kwok, C., Gu, E., Gergues, M.M., Kelada, F., Phan, M., Zhou, J.-N., Swaab, D.F., Pang, Z.P., Lucassen, P.J., Roepke, T.A., Samuels, B.A., 2020. Chronic Stress Induces Maladaptive Behaviors by Activating Corticotropin-Releasing Hormone Signaling in the Mouse Oval Bed Nucleus of the Stria Terminalis. J. Neurosci. 40, 2519–2537. https://doi.org/10.1523/JNEUROSCI.2410-19.2020

Hua, R., Wang, Xu, Chen, X., Wang, Xinxin, Huang, P., Li, P., Mei, W., Li, H., 2018. Calretinin Neurons in the Midline Thalamus Modulate Starvation-Induced Arousal. Curr. Biol. 28, 3948-3959.e4. https://doi.org/10.1016/j.cub.2018.11.020

Hurley, K.M., Herbert, H., Moga, M.M., Saper, C.B., 1991. Efferent projections of the infralimbic cortex of the rat. J. Comp. Neurol. 308, 249–276. https://doi.org/10.1002/cne.903080210

Huss, M., Chen, W., Ludolph, A.G., 2016. Guanfacine Extended Release: A New Pharmacological Treatment Option in Europe. Clin. Drug Investig. 36, 1–25. https://doi.org/10.1007/s40261-015-0336-0

Hyytiä, P., Koob, G.F., 1995. GABAA receptor antagonism in the extended amygdala decreases ethanol self-administration in rats. Eur. J. Pharmacol. 283, 151–159. https://doi.org/10.1016/0014-2999(95)00314-B

Jadzic, D., Bassareo, V., Carta, A.R., Carboni, E., 2021. Nicotine, cocaine, amphetamine, morphine, and ethanol increase norepinephrine output in the bed nucleus of stria terminalis of freely moving rats. Addict. Biol. 26. https://doi.org/10.1111/adb.12864

Jäkälä, P., 1999. Guanfacine, But Not Clonidine, Improves Planning and Working Memory Performance in Humans. Neuropsychopharmacology 20, 460–470. https://doi.org/10.1016/S0893-133X(98)00127-4

Jalabert, M., Aston-Jones, G., Herzog, E., Manzoni, O., Georges, F., 2009. Role of the bed nucleus of the stria terminalis in the control of ventral tegmental area dopamine neurons. Prog. Neuropsychopharmacol. Biol. Psychiatry 33, 1336–1346. https://doi.org/10.1016/j.pnpbp.2009.07.010

James, M.H., Charnley, J.L., Flynn, J.R., Smith, D.W., Dayas, C.V., 2011. Propensity to 'relapse' following exposure to cocaine cues is associated with the recruitment of specific thalamic and epithalamic nuclei. Neuroscience 199, 235–242. https://doi.org/10.1016/j.neuroscience.2011.09.047

Jaramillo, A.A., Williford, K.M., Marshall, C., Winder, D.G., Centanni, S.W., 2020. BNST transient activity associates with approach behavior in a stressful environment and is modulated by the parabrachial nucleus. Neurobiol. Stress 13, 100247. https://doi.org/10.1016/j.ynstr.2020.100247

Jarroit, B., Louis, W.J., Summers, R.J., n.d. [3H]-GUANFACINE: A RADIOLIGAND THAT SELECTIVELY LABELS HIGH AFFINITY O2-ADRENOCEPTOR SITES IN HOMOGENATES OF RAT BRAIN 8.

Jennings, J.H., Sparta, D.R., Stamatakis, A.M., Ung, R.L., Pleil, K.E., Kash, T.L., Stuber, G.D., 2013. Distinct extended amygdala circuits for divergent motivational states. Nature 496, 224–228. https://doi.org/10.1038/nature12041

Jerie, P., n.d. CLINICAL EXPERIENCE WITH GUANFACINE IN LONG-TERM TREATMENT OF HYPERTENSION 8.

Joffe, M.E., Maksymetz, J., Luschinger, J.R., Dogra, S., Ferranti, A.S., Luessen, D.J., Gallinger, I.M., Xiang, Z., Branthwaite, H., Melugin, P.R., Williford, K.M., Centanni, S.W., Shields, B.C., Lindsley, C.W., Calipari, E.S., Siciliano, C.A., Niswender, C.M., Tadross, M.R., Winder, D.G., Conn, P.J., 2022. Acute restraint stress redirects prefrontal cortex circuit function through mGlu5 receptor plasticity on somatostatin-expressing interneurons. Neuron S0896627321010448. https://doi.org/10.1016/j.neuron.2021.12.027

Joffe, M.E., Turner, B.D., Delpire, E., Grueter, B.A., 2018. Genetic loss of GluN2B in D1-expressing cell types enhances long-term cocaine reward and potentiation of thalamo-accumbens synapses. Neuropsychopharmacol. Off. Publ. Am. Coll. Neuropsychopharmacol. 43, 2383–2389. https://doi.org/10.1038/s41386-018-0131-8

Joffe, M.E., Vitter, S.R., Grueter, B.A., 2017. GluN1 deletions in D1- and A2A-expressing cell types reveal distinct modes of behavioral regulation. Neuropharmacology 112, 172–180. https://doi.org/10.1016/j.neuropharm.2016.03.026

Johnson, J., Pizzicato, L., Johnson, C., Viner, K., 2021. Increasing presence of xylazine in heroin and/or fentanyl deaths, Philadelphia, Pennsylvania, 2010–2019. Inj. Prev. 27, 395–398. https://doi.org/10.1136/injuryprev-2020-043968

Kadohisa, M., Wilson, D.A., 2006. Separate encoding of identity and similarity of complex familiar odors in piriform cortex. Proc. Natl. Acad. Sci. 103, 15206–15211. https://doi.org/10.1073/pnas.0604313103

Kandel, D.B., Johnson, J.G., Bird, H.R., Canino, G., Goodman, S.H., Lahey, B.B., Regier, D.A., Schwab-Stone, M., 1997. Psychiatric disorders associated with substance use among children and adolescents: findings from the Methods for the Epidemiology of Child and Adolescent Mental Disorders (MECA) Study. J. Abnorm. Child Psychol. 25, 121–132. https://doi.org/10.1023/A:1025779412167

Kane, L., Venniro, M., Quintana-Feliciano, R., Madangopal, R., Rubio, F.J., Bossert, J.M., Caprioli, D., Shaham, Y., Hope, B.T., Warren, B.L., 2021. Fos-expressing neuronal ensemble in rat ventromedial prefrontal cortex encodes cocaine seeking but not food seeking in rats. Addict. Biol. 26. https://doi.org/10.1111/adb.12943

Kash, T.L., Baucum, A.J., Conrad, K.L., Colbran, R.J., Winder, D.G., 2009. Alcohol Exposure Alters NMDAR Function in the Bed Nucleus of the Stria Terminalis. Neuropsychopharmacology 34, 2420–2429. https://doi.org/10.1038/npp.2009.69

Kash, T.L., Nobis, W.P., Matthews, R.T., Winder, D.G., 2008. Dopamine Enhances Fast Excitatory Synaptic Transmission in the Extended Amygdala by a CRF-R1-Dependent Process. J. Neurosci. 28, 13856–13865. https://doi.org/10.1523/JNEUROSCI.4715-08.2008

Kash, T.L., Pleil, K.E., Marcinkiewcz, C.A., Lowery-Gionta, E.G., Crowley, N., Mazzone, C., Sugam, J., Hardaway, J.A., McElligott, Z.A., 2015. Neuropeptide Regulation of Signaling and Behavior in the BNST. Mol. Cells 38, 1–13. https://doi.org/10.14348/molcells.2015.2261

Kash, T.L., Winder, D.G., 2006. Neuropeptide Y and corticotropin-releasing factor bi-directionally modulate inhibitory synaptic transmission in the bed nucleus of the stria terminalis. Neuropharmacology 51, 1013–1022. https://doi.org/10.1016/j.neuropharm.2006.06.011

Kessler, R.C., Nelson, C.B., McGonagle, K.A., Edlund, M.J., Frank, R.G., Leaf, P.J., 1996. The epidemiology of co-occurring addictive and mental disorders: Implications for prevention and service utilization. Am. J. Orthopsychiatry 66, 17–31. https://doi.org/10.1037/h0080151

Khoury, L., Tang, Y.L., Bradley, B., Cubells, J.F., Ressler, K.J., 2010. Substance use, childhood traumatic experience, and Posttraumatic Stress Disorder in an urban civilian population. Depress. Anxiety 27, 1077–1086. https://doi.org/10.1002/da.20751

Kiechel, J.R., 1980. Pharmacokinetics and metabolism of guanfacine in man: a review. Br. J. Clin. Pharmacol. 10, 25S-32S. https://doi.org/10.1111/j.1365-2125.1980.tb04901.x

Kim, B., Yoon, S., Nakajima, R., Lee, H.J., Lim, H.J., Lee, Y.-K., Choi, J.-S., Yoon, B.-J., Augustine, G.J., Baik, J.-H., 2018. Dopamine D2 receptor-mediated circuit from the central amygdala to the bed nucleus of the stria terminalis regulates impulsive behavior. Proc. Natl. Acad. Sci. 115, E10730–E10739. https://doi.org/10.1073/pnas.1811664115

Kim, S.-Y., Adhikari, A., Lee, S.Y., Marshel, J.H., Kim, C.K., Mallory, C.S., Lo, M., Pak, S., Mattis, J., Lim, B.K., Malenka, R.C., Warden, M.R., Neve, R., Tye, K.M., Deisseroth, K., 2013. Diverging neural pathways assemble a behavioural state from separable features in anxiety. Nature 496, 219–223. https://doi.org/10.1038/nature12018

King, C.A., Ghaziuddin, N., McGOVERN, L., Brand, E., Hill, E., Naylor, M., 1996. Predictors of Comorbid Alcohol and Substance Abuse in Depressed Adolescents. J. Am. Acad. Child Adolesc. Psychiatry 35, 743–751. https://doi.org/10.1097/00004583-199606000-00014

Kirouac, G.J., 2015. Placing the paraventricular nucleus of the thalamus within the brain circuits that control behavior. Neurosci. Biobehav. Rev. 56, 315–329. https://doi.org/10.1016/j.neubiorev.2015.08.005

Kobilka, B.K., Matsui, H., Kobilka, T.S., Yang-Feng, T.L., Francke, U., Caron, M.G., Lefkowitz, R.J., Regan, J.W., n.d. Cloning, Sequencing, and Expression of the Gene Coding for the Human Platelet c2-Adrenergic Receptor 8.

Koob, G.F., 2008. A Role for Brain Stress Systems in Addiction. Neuron 59, 11–34. https://doi.org/10.1016/j.neuron.2008.06.012

Koob, G.F., 1999. Corticotropin-releasing factor, norepinephrine, and stress. Biol. Psychiatry 46, 1167–1180. https://doi.org/10.1016/S0006-3223(99)00164-X

Koob, G.F., Volkow, N.D., 2010. Neurocircuitry of Addiction. Neuropsychopharmacology 35, 217–238. https://doi.org/10.1038/npp.2009.110

Kovner, R., Oler, J.A., Kalin, N.H., 2019. Cortico-Limbic Interactions Mediate Adaptive and Maladaptive Responses Relevant to Psychopathology. Am. J. Psychiatry 176, 987–999. https://doi.org/10.1176/appi.ajp.2019.19101064

Koya, E., Golden, S.A., Harvey, B.K., Guez-Barber, D.H., Berkow, A., Simmons, D.E., Bossert, J.M., Nair, S.G., Uejima, J.L., Marin, M.T., Mitchell, T.B., Farquhar, D., Ghosh, S.C., Mattson, B.J., Hope, B.T., 2009. Targeted disruption of cocaine-activated nucleus accumbens neurons prevents context-specific sensitization. Nat. Neurosci. 12, 1069–1073. https://doi.org/10.1038/nn.2364

Kozicz, T., Arimura, A., 2001. Axon terminals containing CGRP-immunoreactivity form synapses with CRF- and Met-enkephalin-immunopositive neurons in the laterodorsal division of the bed nucleus of the stria terminalis in the rat. Brain Res. 10.

Kozicz, T., Vigh, S., Arimura, A., 1997. Axon terminals containing PACAP- and VIP-immunoreactivity form synapses with CRF-immunoreactive neurons in the dorsolateral division of the bed nucleus of the stria terminalis in the rat. Brain Res. 767, 109–119. https://doi.org/10.1016/S0006-8993(97)00737-3

Krawczyk, M., Georges, F., Sharma, R., Mason, X., Berthet, A., Bézard, E., Dumont, É.C., 2011. Double-Dissociation of the Catecholaminergic Modulation of Synaptic Transmission in the Oval Bed Nucleus of the Stria Terminalis. J. Neurophysiol. 105, 145–153. https://doi.org/10.1152/jn.00710.2010

Krettek, J.E., Price, J.L., 1978. Amygdaloid projections to subcortical structures within the basal forebrain and brainstem in the rat and cat. J. Comp. Neurol. 178, 225–253. https://doi.org/10.1002/cne.901780204

Krupitsky, E., Zvartau, E., Blokhina, E., Verbitskaya, E., Tsoy, M., Wahlgren, V., Burakov, A., Masalov, D., Romanova, T.N., Palatkin, V., Tyurina, A., Yaroslavtseva, T., Sinha, R., Kosten, T.R., 2013. Naltrexone with or without guanfacine for preventing relapse to opiate addiction in St.-Petersburg, Russia. Drug Alcohol Depend. 132, 674–680. https://doi.org/10.1016/j.drugalcdep.2013.04.021

Kudo, T., Uchigashima, M., Miyazaki, T., Konno, K., Yamasaki, M., Yanagawa, Y., Minami, M., Watanabe, M., 2012. Three Types of Neurochemical Projection from the Bed Nucleus of the Stria Terminalis to the Ventral Tegmental Area in Adult Mice. J. Neurosci. 32, 18035–18046. https://doi.org/10.1523/JNEUROSCI.4057-12.2012

Kupferschmidt, D.A., Cody, P.A., Lovinger, D.M., Davis, M.I., 2015. Brain BLAQ: Post-hoc thick-section histochemistry for localizing optogenetic constructs in neurons and their distal terminals. Front. Neuroanat. 9. https://doi.org/10.3389/fnana.2015.00006

Lange, M.D., Daldrup, T., Remmers, F., Szkudlarek, H.J., Lesting, J., Guggenhuber, S., Ruehle, S., Jüngling, K., Seidenbecher, T., Lutz, B., Pape, H.C., 2017. Cannabinoid CB1 receptors in distinct circuits of the extended amygdala determine fear responsiveness to unpredictable threat. Mol. Psychiatry 22, 1422–1430. https://doi.org/10.1038/mp.2016.156

Lapiz, M.D.S., Morilak, D.A., 2006. Noradrenergic modulation of cognitive function in rat medial prefrontal cortex as measured by attentional set shifting capability. Neuroscience 137, 1039–1049. https://doi.org/10.1016/j.neuroscience.2005.09.031

Lavin, T.K., Jin, L., Lea, N.E., Wickersham, I.R., 2020. Monosynaptic Tracing Success Depends Critically on Helper Virus Concentrations. Front. Synaptic Neurosci. 12, 6. https://doi.org/10.3389/fnsyn.2020.00006

Lebow, M.A., Chen, A., 2016. Overshadowed by the amygdala: the bed nucleus of the stria terminalis emerges as key to psychiatric disorders. Mol. Psychiatry 21, 450–463. https://doi.org/10.1038/mp.2016.1

Lee, S.J., Chen, Y., Lodder, B., Sabatini, B.L., 2019. Monitoring Behaviorally Induced Biochemical Changes Using Fluorescence Lifetime Photometry. Front. Neurosci. 13, 766. https://doi.org/10.3389/fnins.2019.00766

Lemberger, T., Parlato, R., Dassesse, D., Westphal, M., Casanova, E., Turiault, M., Tronche, F., Schiffmann, S.N., Schütz, G., 2007. Expression of Cre recombinase in dopaminoceptive neurons. BMC Neurosci. 8, 4. https://doi.org/10.1186/1471-2202-8-4

Leriche, M., Méndez, M., Zimmer, L., Bérod, A., 2008. Acute ethanol induces Fos in GABAergic and non-GABAergic forebrain neurons: A double-labeling study in the medial prefrontal cortex and extended amygdala. Neuroscience 153, 259–267. https://doi.org/10.1016/j.neuroscience.2008.01.069

Levine, O.B., Skelly, M.J., Miller, J.D., Rivera-Irizarry, J.K., Rowson, S.A., DiBerto, J.F., Rinker, J.A., Thiele, T.E., Kash, T.L., Pleil, K.E., 2021. The paraventricular thalamus provides a polysynaptic brake on limbic CRF neurons to sex-dependently blunt binge alcohol drinking and avoidance behavior in mice. Nat. Commun. 12, 5080. https://doi.org/10.1038/s41467-021-25368-y

Li, H., Penzo, M.A., Taniguchi, H., Kopec, C.D., Huang, Z.J., Li, B., 2013. Experience-dependent modification of a central amygdala fear circuit. Nat. Neurosci. 16, 332–339. https://doi.org/10.1038/nn.3322

Li, H.Y., Sawchenko, P.E., 1998. Hypothalamic effector neurons and extended circuitries activated in “neurogenic” stress: a comparison of footshock effects exerted acutely, chronically, and in animals with controlled glucocorticoid levels. J. Comp. Neurol. 393, 244–266.

Li, J.-N., Sheets, P.L., 2020. Spared nerve injury differentially alters parabrachial monosynaptic excitatory inputs to molecularly specific neurons in distinct subregions of the central amygdala: PAIN 161, 166–176. https://doi.org/10.1097/j.pain.0000000000001691

Li, W., Howard, J.D., Parrish, T.B., Gottfried, J.A., 2008. Aversive Learning Enhances Perceptual and Cortical Discrimination of Indiscriminable Odor Cues. Science 319, 1842–1845. https://doi.org/10.1126/science.1152837

Li, X., Li, N., Sun, X., Yang, W., Dai, Y., Xu, J., Zhang, W., Wang, C., Wang, S., Chen, X., 2013. Development and validation of a simple, sensitive and accurate LC-MS/MS method for the determination of guanfacine, a selective α_{2A}-adrenergicreceptor agonist, in plasma and its application to a pharmacokinetic study: Determination of guanfacine in beagle dog plasma. Biomed. Chromatogr. 27, 1708–1713. https://doi.org/10.1002/bmc.2983

Lomasney, J.W., LORENZt, W., ALLENt, L.F., KINGtt, K., Regan, J.W., Yang-Feng, T.L., Ii, M.G.Caron., LEFKOWITZtt, R.J., n.d. Expansion of the a2-adrenergic receptor family: Cloning and characterization of a human a2-adrenergic receptor subtype, the gene for which is located on chromosome 2 5.

Lowry, C.A., Hale, M.W., Evans, A.K., Heerkens, J., Staub, D.R., Gasser, P.J., Shekhar, A., 2008. Serotonergic Systems, Anxiety, and Affective Disorder. Ann. N. Y. Acad. Sci. 1148, 86–94. https://doi.org/10.1196/annals.1410.004

Lu, L., Liu, D., Ceng, X., 2001. Corticotropin-releasing factor receptor type 1 mediates stress-induced relapse to cocaine-conditioned place preference in rats. Eur. J. Pharmacol. 415, 203–208. https://doi.org/10.1016/S0014-2999(01)00840-8

Lu, L., Zhang, B., Liu, Z., Zhang, Z., 2002. Reactivation of cocaine conditioned place preference induced by stress is reversed by cholecystokinin-B receptors antagonist in rats. Brain Res. 954, 132–140. https://doi.org/10.1016/S0006-8993(02)03359-0

Lucassen, P.J., Pruessner, J., Sousa, N., Almeida, O.F.X., Van Dam, A.M., Rajkowska, G., Swaab, D.F., Czéh, B., 2014. Neuropathology of stress. Acta Neuropathol. (Berl.) 127, 109–135. https://doi.org/10.1007/s00401-013-1223-5

Luchsinger, J.R., Fetterly, T.L., Williford, K.M., Salimando, G.J., Doyle, M.A., Maldonado, J., Simerly, R.B., Winder, D.G., Centanni, S.W., 2021. Delineation of an insula-BNST circuit engaged by struggling behavior that regulates avoidance in mice. Nat. Commun. 12, 3561. https://doi.org/10.1038/s41467-021-23674-z

L, A.D., Harding, S., Juzytsch, W., Funk, D., Shaham, Y., 2005. Role of alpha-2 adrenoceptors in stress-induced reinstatement of alcohol seeking and alcohol self-administration in rats. Psychopharmacology (Berl.) 179, 366–373. https://doi.org/10.1007/s00213-004-2036-y

Ma, X.-M., Aguilera, G., 1999. Transcriptional responses of the vasopressin and corticotropin-releasing hormone genes to acute and repeated intraperitoneal hypertonic saline injection in rats. Mol. Brain Res. 68, 129–140. https://doi.org/10.1016/S0169-328X(99)00080-7

Mahler, S.V., Aston-Jones, G.S., 2012. Fos Activation of Selective Afferents to Ventral Tegmental Area during Cue-Induced Reinstatement of Cocaine Seeking in Rats. J. Neurosci. 32, 13309–13325. https://doi.org/10.1523/JNEUROSCI.2277-12.2012

Mantsch, J.R., Weyer, A., Vranjkovic, O., Beyer, C.E., Baker, D.A., Caretta, H., 2010. Involvement of Noradrenergic Neurotransmission in the Stress- but not Cocaine-Induced Reinstatement of Extinguished Cocaine-Induced Conditioned Place Preference in Mice: Role for β-2 Adrenergic Receptors. Neuropsychopharmacology 35, 2165–2178. https://doi.org/10.1038/npp.2010.86

Martí, O., Armario, A., 1998. Anterior pituitary response to stress : time-related changes and adaptation. Int. J. Dev. Neurosci. 16, 241–260. https://doi.org/10.1016/S0736-5748(98)00030-6

Martianova, E., Aronson, S., Proulx, C.D., 2019. Multi-Fiber Photometry to Record Neural Activity in Freely-Moving Animals. J. Vis. Exp. 60278. https://doi.org/10.3791/60278

Massi, L., Elezgarai, I., Puente, N., Reguero, L., Grandes, P., Manzoni, O.J., Georges, F., 2008. Cannabinoid Receptors in the Bed Nucleus of the Stria Terminalis Control Cortical Excitation of Midbrain Dopamine Cells In Vivo. J. Neurosci. 28, 10496–10508. https://doi.org/10.1523/JNEUROSCI.2291-08.2008

Matzeu, A., Weiss, F., Martin-Fardon, R., 2015. Transient inactivation of the posterior paraventricular nucleus of the thalamus blocks cocaine-seeking behavior. Neurosci. Lett. 608, 34–39. https://doi.org/10.1016/j.neulet.2015.10.016

McDonald, A.J., 1998. Cortical pathways to the mammalian amygdala. Prog. Neurobiol. 55, 257–332. https://doi.org/10.1016/S0301-0082(98)00003-3

McElligott, Z.A., Winder, D.G., 2009. Modulation of glutamatergic synaptic transmission in the bed nucleus of the stria terminalis. Prog. Neuropsychopharmacol. Biol. Psychiatry 33, 1329–1335. https://doi.org/10.1016/j.pnpbp.2009.05.022

McElligott, Z.A., Winder, D.G., 2008. α_1-Adrenergic Receptor-Induced Heterosynaptic Long-Term Depression in the Bed Nucleus of the Stria Terminalis Is Disrupted in Mouse Models of Affective Disorders. Neuropsychopharmacology 33, 2313–2323. https://doi.org/10.1038/sj.npp.1301635

McReynolds, J.R., Peña, D.F., Blacktop, J.M., Mantsch, J.R., 2014a. Neurobiological mechanisms underlying relapse to cocaine use: contributions of CRF and noradrenergic systems and regulation by glucocorticoids. Stress 17, 22–38. https://doi.org/10.3109/10253890.2013.872617

McReynolds, J.R., Vranjkovic, O., Thao, M., Baker, D.A., Makky, K., Lim, Y., Mantsch, J.R., 2014b. Beta-2 adrenergic receptors mediate stress-evoked reinstatement of cocaine-induced conditioned place preference and increases in CRF mRNA in the bed nucleus of the stria terminalis in mice. Psychopharmacology (Berl.) 231, 3953–3963. https://doi.org/10.1007/s00213-014-3535-0

Meloni, E.G., 2006. Behavioral and Anatomical Interactions between Dopamine and Corticotropin-Releasing Factor in the Rat. J. Neurosci. 26, 3855–3863. https://doi.org/10.1523/JNEUROSCI.4957-05.2006

Milivojevic, V., Angarita, G.A., Hermes, G., Sinha, R., Fox, H.C., 2020. Effects of Prazosin on Provoked Alcohol Craving and Autonomic and Neuroendocrine Response to Stress in Alcohol Use Disorder. Alcohol. Clin. Exp. Res. 44, 1488–1496. https://doi.org/10.1111/acer.14378

Millan, M.J., Lejeune, F., Gobert, A., 2000. Reciprocal autoreceptor and heteroreceptor control of serotonergic, dopaminergic and noradrenergic transmission in the frontal cortex: relevance to the actions of antidepressant agents. J. Psychopharmacol. (Oxf.) 14, 114–138. https://doi.org/10.1177/026988110001400202

Mingione, C.J., Heffner, J.L., Blom, T.J., Anthenelli, R.M., 2012. Childhood adversity, serotonin transporter (5-HTTLPR) genotype, and risk for cigarette smoking and nicotine dependence in alcohol dependent adults. Drug Alcohol Depend. 123, 201–206. https://doi.org/10.1016/j.drugalcdep.2011.11.013

Missig, G., Mei, L., Vizzard, M.A., Braas, K.M., Waschek, J.A., Ressler, K.J., Hammack, S.E., May, V., 2017. Parabrachial Pituitary Adenylate Cyclase-Activating Polypeptide Activation of Amygdala Endosomal Extracellular Signal–Regulated Kinase Signaling Regulates the Emotional Component of Pain. Biol. Psychiatry 81, 671–682. https://doi.org/10.1016/j.biopsych.2016.08.025

Missig, G., Roman, C.W., Vizzard, M.A., Braas, K.M., Hammack, S.E., May, V., 2014. Parabrachial nucleus (PBn) pituitary adenylate cyclase activating polypeptide (PACAP) signaling in the amygdala: Implication for the sensory and behavioral effects of pain. Neuropharmacology 86, 38–48. https://doi.org/10.1016/j.neuropharm.2014.06.022

Moore, R.Y., Bloom, F.E., 1979. Central Catecholamine Neuron Systems: Anatomy and Physiology of the Norepinephrine and Epinephrine Systems. Annu. Rev. Neurosci. 2, 113–168. https://doi.org/10.1146/annurev.ne.02.030179.000553

Moore, S.J., Deshpande, K., Stinnett, G.S., Seasholtz, A.F., Murphy, G.G., 2013. Conversion of short-term to long-term memory in the novel object recognition paradigm. Neurobiol. Learn. Mem. 105, 174–185. https://doi.org/10.1016/j.nlm.2013.06.014

Morrison, J.H., Foote, S.L., O'Connor, D., Bloom, F.E., 1982. Laminar, tangential and regional organization of the noradrenergic innervation of monkey cortex: dopamine-beta-hydroxylase immunohistochemistry. Brain Res. Bull. 9, 309–319. https://doi.org/10.1016/0361-9230(82)90144-7

Morrison, J.H., Grzanna, R., Molliver, M.E., Coyle, J.T., 1978. The distribution and orientation of noradrenergic fibers in neocortex of the rat: an immunofluorescence study. J. Comp. Neurol. 181, 17–39. https://doi.org/10.1002/cne.901810103

Mulkey, S.B., du Plessis, A.J., 2019. Autonomic nervous system development and its impact on neuropsychiatric outcome. Pediatr. Res. 85, 120–126. https://doi.org/10.1038/s41390-018-0155-0

Myers, B., Mark Dolgas, C., Kasckow, J., Cullinan, W.E., Herman, J.P., 2014. Central stress-integrative circuits: forebrain glutamatergic and GABAergic projections to the dorsomedial hypothalamus, medial preoptic area, and bed nucleus of the stria terminalis. Brain Struct. Funct. 219, 1287–1303. https://doi.org/10.1007/s00429-013-0566-y

Navarro, M., Cubero, I., Knapp, D.J., Breese, G.R., Thiele, T.E., 2008. Decreased Immunoreactivity of the Melanocortin Neuropeptide α-Melanocyte-Stimulating Hormone (α-MSH) After Chronic Ethanol Exposure in Sprague-Dawley Rats. Alcohol. Clin. Exp. Res. 32, 266–276. https://doi.org/10.1111/j.1530-0277.2007.00578.x

Neugebauer, V., 2020. Amygdala, neuropeptides, and chronic pain-related affective behaviors 13.

Newcorn, J.H., Stein, M.A., Childress, A.C., Youcha, S., White, C., Enright, G., Rubin, J., 2013. Randomized, Double-Blind Trial of Guanfacine Extended Release in Children With Attention-Deficit/Hyperactivity Disorder: Morning or

Evening Administration. J. Am. Acad. Child Adolesc. Psychiatry 52, 921–930. https://doi.org/10.1016/j.jaac.2013.06.006

Nobis, W.P., Kash, T.L., Silberman, Y., Winder, D.G., 2011. β-Adrenergic Receptors Enhance Excitatory Transmission in the Bed Nucleus of the Stria Terminalis Through a Corticotrophin-Releasing Factor Receptor–Dependent and Cocaine-Regulated Mechanism. Biol. Psychiatry 69, 1083–1090. https://doi.org/10.1016/j.biopsych.2010.12.030

O'Connor, D., 2014. Time-correlated single photon counting. Elsevier Science, Saint Louis.

Olsen, C.M., Winder, D.G., 2010. Operant Sensation Seeking in the Mouse. J. Vis. Exp. 2292. https://doi.org/10.3791/2292

Ortiz-Juza, M.M., Alghorazi, R.A., Rodriguez-Romaguera, J., 2021. Cell-type diversity in the bed nucleus of the stria terminalis to regulate motivated behaviors. Behav. Brain Res. 411, 113401. https://doi.org/10.1016/j.bbr.2021.113401

Pacha, W., Salzmann, R., Scholtysik, G., 1975. INHIBITORY EFFECTS OF CLONIDINE AND BS 100-141 ON RESPONSES TO SYMPATHETIC NERVE STIMULATION IN CATS AND RABBITS. Br. J. Pharmacol. 53, 513–516. https://doi.org/10.1111/j.1476-5381.1975.tb07388.x

Palmiter, R.D., 2018. The Parabrachial Nucleus: CGRP Neurons Function as a General Alarm. Trends Neurosci. 41, 280–293. https://doi.org/10.1016/j.tins.2018.03.007

Park, J., Kile, B.M., Mark Wightman, R., 2009. *In vivo* voltammetric monitoring of norepinephrine release in the rat ventral bed nucleus of the stria terminalis and anteroventral thalamic nucleus. Eur. J. Neurosci. 30, 2121–2133. https://doi.org/10.1111/j.1460-9568.2009.07005.x

Park, Y.-G., Sohn, C.H., Chen, R., McCue, M., Yun, D.H., Drummond, G.T., Ku, T., Evans, N.B., Oak, H.C., Trieu, W., Choi, H., Jin, X., Lilascharoen, V., Wang, J., Truttmann, M.C., Qi, H.W., Ploegh, H.L., Golub, T.R., Chen, S.-C., Frosch, M.P., Kulik, H.J., Lim, B.K., Chung, K., 2019. Protection of tissue physicochemical properties using polyfunctional crosslinkers. Nat. Biotechnol. 37, 73–83. https://doi.org/10.1038/nbt.4281

Perez, R.E., Basu, A., Nabit, B.P., Harris, N.A., Folkes, O.M., Patel, S., Gilsbach, R., Hein, L., Winder, D.G., 2020a. α2A-adrenergic heteroreceptors are required for stress-induced reinstatement of cocaine conditioned place preference. Neuropsychopharmacology 45, 1473–1481. https://doi.org/10.1038/s41386-020-0641-z

Perez, R.E., Basu, A., Nabit, B.P., Harris, N.A., Folkes, O.M., Patel, S., Gilsbach, R., Hein, L., Winder, D.G., 2020b. α2A-adrenergic heteroreceptors are required for stress-induced reinstatement of cocaine conditioned place preference. Neuropsychopharmacology. https://doi.org/10.1038/s41386-020-0641-z

Pergolizzi, J.V., Annabi, H., Gharibo, C., LeQuang, J.A., 2019. The Role of Lofexidine in Management of Opioid Withdrawal. Pain Ther. 8, 67–78. https://doi.org/10.1007/s40122-018-0108-7

Perkins, H.W., 1999. Stress-motivated drinking in collegiate and postcollegiate young adulthood: life course and gender patterns. J. Stud. Alcohol 60, 219–227. https://doi.org/10.15288/jsa.1999.60.219

Peyron, C., Tighe, D.K., van den Pol, A.N., de Lecea, L., Heller, H.C., Sutcliffe, J.G., Kilduff, T.S., 1998. Neurons Containing Hypocretin (Orexin) Project to Multiple Neuronal Systems. J. Neurosci. 18, 9996–10015. https://doi.org/10.1523/JNEUROSCI.18-23-09996.1998

Phelix, C.F., Liposits, Z., Paull, W.K., 1992. Monoamine innervation of bed nucleus of stria terminalis: An electron microscopic investigation. Brain Res. Bull. 28, 949–965. https://doi.org/10.1016/0361-9230(92)90218-M

Pina, M.M., Young, E.A., Ryabinin, A.E., Cunningham, C.L., 2015. The bed nucleus of the stria terminalis regulates ethanol-seeking behavior in mice. Neuropharmacology 99, 627–638. https://doi.org/10.1016/j.neuropharm.2015.08.033

Pleil, K.E., Rinker, J.A., Lowery-Gionta, E.G., Mazzone, C.M., McCall, N.M., Kendra, A.M., Olson, D.P., Lowell, B.B., Grant, K.A., Thiele, T.E., Kash, T.L., 2015. NPY signaling inhibits extended amygdala CRF neurons to suppress binge alcohol drinking. Nat. Neurosci. 18, 545–552. https://doi.org/10.1038/nn.3972

Pnevmatikakis, E.A., Giovannucci, A., 2017. NoRMCorre: An online algorithm for piecewise rigid motion correction of calcium imaging data. J. Neurosci. Methods 291, 83–94. https://doi.org/10.1016/j.jneumeth.2017.07.031

Puente, N., Elezgarai, I., Lafourcade, M., Reguero, L., Marsicano, G., Georges, F., Manzoni, O.J., Grandes, P., 2010. Localization and Function of the Cannabinoid CB1 Receptor in the Anterolateral Bed Nucleus of the Stria Terminalis. PLoS ONE 5, e8869. https://doi.org/10.1371/journal.pone.0008869

Radley, J.J., Gosselink, K.L., Sawchenko, P.E., 2009. A Discrete GABAergic Relay Mediates Medial Prefrontal Cortical Inhibition of the Neuroendocrine Stress Response. J. Neurosci. 29, 7330–7340. https://doi.org/10.1523/JNEUROSCI.5924-08.2009

Ramos, B.P., Stark, D., Verduzco, L., van Dyck, C.H., Arnsten, A.F.T., 2006. 2A-adrenoceptor stimulation improves prefrontal cortical regulation of behavior through inhibition of cAMP signaling in aging animals. Learn. Mem. 13, 770–776. https://doi.org/10.1101/lm.298006

Regan, J.W., Kobilka, T.S., YANG-FENGt, T.L., Caron, M.G., Lefkowitz, R.J., Kobilka, B.K., n.d. Cloning and expression of a human kidney cDNA for an a2-adrenergic receptor subtype 5.

Reichard, R.A., Subramanian, S., Desta, M.T., Sura, T., Becker, M.L., Ghobadi, C.W., Parsley, K.P., Zahm, D.S., 2017. Abundant collateralization of temporal lobe projections to the accumbens, bed nucleus of stria terminalis, central amygdala and lateral septum. Brain Struct. Funct. 222, 1971–1988. https://doi.org/10.1007/s00429-016-1321-y

Reisiger, A.-R., Kaufling, J., Manzoni, O., Cador, M., Georges, F., Caille, S., 2014. Nicotine Self-Administration Induces CB1-Dependent LTP in the Bed Nucleus of the Stria Terminalis. J. Neurosci. 34, 4285–4292. https://doi.org/10.1523/JNEUROSCI.3149-13.2014

Reyes, J.C., Negrón, J.L., Colón, H.M., Padilla, A.M., Millán, M.Y., Matos, T.D., Robles, R.R., 2012. The Emerging of Xylazine as a New Drug of Abuse and its Health Consequences among Drug Users in Puerto Rico. J. Urban Health 89, 519–526. https://doi.org/10.1007/s11524-011-9662-6

Rho, H.-J., Kim, J.-H., Lee, S.-H., 2018. Function of Selective Neuromodulatory Projections in the Mammalian Cerebral Cortex: Comparison Between Cholinergic and Noradrenergic Systems. Front. Neural Circuits 12, 47. https://doi.org/10.3389/fncir.2018.00047

Ricardo, J.A., Tongju Koh, E., 1978. Anatomical evidence of direct projections from the nucleus of the solitary tract to the hypothalamus, amygdala, and other forebrain structures in the rat. Brain Res. 153, 1–26. https://doi.org/10.1016/0006-8993(78)91125-3

Rinker, J.A., Marshall, S.A., Mazzone, C.M., Lowery-Gionta, E.G., Gulati, V., Pleil, K.E., Kash, T.L., Navarro, M., Thiele, T.E., 2017. Extended Amygdala to Ventral Tegmental Area Corticotropin-Releasing Factor Circuit Controls Binge Ethanol Intake. Biol. Psychiatry 81, 930–940. https://doi.org/10.1016/j.biopsych.2016.02.029

Rodríguez, N., Vargas Vidot, J., Panelli, J., Colón, H., Ritchie, B., Yamamura, Y., 2008. GC–MS confirmation of xylazine (Rompun), a veterinary sedative, in exchanged needles. Drug Alcohol Depend. 96, 290–293. https://doi.org/10.1016/j.drugalcdep.2008.03.005

Ruiz-Colón, K., Chavez-Arias, C., Díaz-Alcalá, J.E., Martínez, M.A., 2014. Xylazine intoxication in humans and its importance as an emerging adulterant in abused drugs: A comprehensive review of the literature. Forensic Sci. Int. 240, 1–8. https://doi.org/10.1016/j.forsciint.2014.03.015

Saalfield, J., Spear, L., 2019. Fos activation patterns related to acute ethanol and conditioned taste aversion in adolescent and adult rats. Alcohol 78, 57–68. https://doi.org/10.1016/j.alcohol.2019.02.004

Saameli, K., Jerie, P., Scholtysik, G., 1982. Guanfacine and other centrally acting drugs in antihypertensive therapy; pharmacological and clinical aspects. Clin. Exp. Hypertens. A. 4, 209–219. https://doi.org/10.3109/10641968209061586

Safar, M.E., Loria, Y., Weiss, Y.A., Boutier, J.R., 1982. Antihypertensive Effects and Plasma Levels of Guanfacine in Man. J. Clin. Pharmacol. 22, 385–390. https://doi.org/10.1002/j.1552-4604.1982.tb02690.x

Sakharkar, A.J., Zhang, H., Tang, L., Baxstrom, K., Shi, G., Moonat, S., Pandey, S.C., 2014. Effects of histone deacetylase inhibitors on amygdaloid histone acetylation and neuropeptide Y expression: a role in anxiety-like and alcohol-drinking behaviours. Int. J. Neuropsychopharmacol. 17, 1207–1220. https://doi.org/10.1017/S1461145714000054

Salimando, G.J., Hyun, M., Boyt, K.M., Winder, D.G., 2020. BNST GluN2D-Containing NMDA Receptors Influence Anxiety- and Depressive-like Behaviors and ModulateCell-Specific Excitatory/Inhibitory Synaptic Balance. J. Neurosci. 40, 3949–3968. https://doi.org/10.1523/JNEUROSCI.0270-20.2020

Sallee, F.R., Lyne, A., Wigal, T., McGough, J.J., 2009a. Long-Term Safety and Efficacy of Guanfacine Extended Release in Children and Adolescents with Attention-Deficit/Hyperactivity Disorder. J. Child Adolesc. Psychopharmacol. 19, 215–226. https://doi.org/10.1089/cap.2008.0080

Sallee, F.R., Mcgough, J., Wigal, T., Donahue, J., Lyne, A., Biederman, J., 2009b. Guanfacine Extended Release in Children and Adolescents With Attention-Deficit/Hyperactivity Disorder: A Placebo-Controlled Trial. J. Am. Acad. Child Adolesc. Psychiatry 48, 155–165. https://doi.org/10.1097/CHI.0b013e318191769e

Sallinen, J., Haapalinna, A., MacDonald, E., Viitamaa, T., Lähdesmäki, J., Rybnikova, E., Pelto-Huikko, M., Kobilka, B.K., Scheinin, M., 1999. Genetic alteration of the α2-adrenoceptor subtype c in mice affects the development of behavioral despair and stress-induced increases in plasma corticosterone levels. Mol. Psychiatry 4, 443–452. https://doi.org/10.1038/sj.mp.4000543

Salmaso, N., Rodaros, D., Stewart, J., Erb, S., 2001. A role for the CRF-containing pathway from central nucleus of the amygdala to bed nucleus of the stria terminalis in the stress-induced reinstatement of cocaine seeking in rats. Psychopharmacology (Berl.) 158, 360–365. https://doi.org/10.1007/s002130000642

Sartor, G.C., Aston-Jones, G., 2012. Regulation of the ventral tegmental area by the bed nucleus of the stria terminalis is required for expression of cocaine preference. Eur. J. Neurosci. 36, 3549–3558. https://doi.org/10.1111/j.1460-9568.2012.08277.x

Schmidt, E., Janszen, A., Wouterlood, F., Tilders, F., 1995. Interleukin-1-induced long-lasting changes in hypothalamic corticotropin-releasing hormone (CRH)--neurons and hyperresponsiveness of the hypothalamus-pituitary-adrenal axis. J. Neurosci. 15, 7417–7426. https://doi.org/10.1523/JNEUROSCI.15-11-07417.1995

Schmidt, E.D., Binnekade, R., Janszen, A.W., Tilders, F.J., 1996. Short stressor induced long-lasting increases of vasopressin stores in hypothalamic corticotropin-releasing hormone (CRH) neurons in adult rats. J. Neuroendocrinol. 8, 703–712.

Schmidt, E.D., Schoffelmeer, A.N.M., De Vries, T.J., Wardeh, G., Dogterom, G., Bol, J.G.J.M., Binnekade, R., Tilders, F.J.H., 2001. A single administration of interleukin-1 or amphetamine induces long-lasting increases in evoked noradrenaline release in the hypothalamus and sensitization of ACTH and corticosterone responses in rats: Noradrenergic transmission and long-term HPA sensitization. Eur. J. Neurosci. 13, 1923–1930. https://doi.org/10.1046/j.0953-816x.2001.01569.x

Schmidt, K.T., Makhijani, V.H., Boyt, K.M., Pati, D., Pina, M.M., Bravo, I.M., Locke, J.L., Jones, S.R., Besheer, J., McElligott, Z.A., 2018. Stress-induced alterations of norepinephrine release in the bed nucleus of the stria terminalis of mice (preprint). Neuroscience. https://doi.org/10.1101/335653

Scholtysik, G., 1986. Animal pharmacology of guanfacine. Am. J. Cardiol. 57, E13–E17. https://doi.org/10.1016/0002-9149(86)90717-4

Schreiber, A.L., McGinn, M.A., Edwards, S., Gilpin, N.W., 2019. Predator odor stress blunts alcohol conditioned aversion. Neuropharmacology 144, 82–90. https://doi.org/10.1016/j.neuropharm.2018.10.019

Shackman, A.J., Fox, A.S., 2016. Contributions of the Central Extended Amygdala to Fear and Anxiety. J. Neurosci. 36, 8050–8063. https://doi.org/10.1523/JNEUROSCI.0982-16.2016

Shaham, Y., Erb, S., Stewart, J., 2000. Stress-induced relapse to heroin and cocaine seeking in rats: a review. Brain Res. Rev. 33, 13–33. https://doi.org/10.1016/S0165-0173(00)00024-2

Shaham, Y., Shalev, U., Lu, L., de Wit, H., Stewart, J., 2003. The reinstatement model of drug relapse: history, methodology and major findings. Psychopharmacology (Berl.) 168, 3–20. https://doi.org/10.1007/s00213-002-1224-x

Shaham, Y., Stewart, J., 1995. Stress reinstates heroin-seeking in drug-free animals: An effect mimicking heroin, not withdrawal. Psychopharmacology (Berl.) 119, 334–341. https://doi.org/10.1007/BF02246300

Shalev, U., Highfield, D., Yap, J., Shaham, Y., 2000. Stress and relapse to drug seeking in rats: studies on the generality of the effect. Psychopharmacology (Berl.) 150, 337–346. https://doi.org/10.1007/s002130000441

Shanks, N., Griffiths, J., Zalcman, S., Zacharko, R.M., Anisman, H., 1990. Mouse strain differences in plasma corticosterone following uncontrollable footshock. Pharmacol. Biochem. Behav. 36, 515–519. https://doi.org/10.1016/0091-3057(90)90249-H

Sharko, A.C., Kaigler, K.F., Fadel, J.R., Wilson, M.A., 2016. Ethanol-induced anxiolysis and neuronal activation in the amygdala and bed nucleus of the stria terminalis. Alcohol 50, 19–25. https://doi.org/10.1016/j.alcohol.2015.11.001

Sher, K.J., Gershuny, B.S., Peterson, L., Raskin, G., 1997. The role of childhood stressors in the intergenerational transmission of alcohol use disorders. J. Stud. Alcohol 58, 414–427. https://doi.org/10.15288/jsa.1997.58.414

Shields, A.D., Wang, Q., Winder, D.G., 2009a. α2A-adrenergic receptors heterosynaptically regulate glutamatergic transmission in the bed nucleus of the stria terminalis. Neuroscience 163, 339–351. https://doi.org/10.1016/j.neuroscience.2009.06.022

Shields, A.D., Wang, Q., Winder, D.G., 2009b. α2A-adrenergic receptors heterosynaptically regulate glutamatergic transmission in the bed nucleus of the stria terminalis. Neuroscience 163, 339–351. https://doi.org/10.1016/j.neuroscience.2009.06.022

Shoji, H., Miyakawa, T., 2020. Differential effects of stress exposure via two types of restraint apparatuses on behavior and plasma corticosterone level in inbred male BALB/cAJcl mice. Neuropsychopharmacol. Rep. 40, 73–84. https://doi.org/10.1002/npr2.12093

Silberman, Y., Matthews, R.T., Winder, D.G., 2013. A Corticotropin Releasing Factor Pathway for Ethanol Regulation of the Ventral Tegmental Area in the Bed Nucleus of the Stria Terminalis. J. Neurosci. 33, 950–960. https://doi.org/10.1523/JNEUROSCI.2949-12.2013

Silberman, Y., Winder, D.G., 2013. Emerging Role for Corticotropin Releasing Factor Signaling in the Bed Nucleus of the Stria Terminalis at the Intersection of Stress and Reward. Front. Psychiatry 4. https://doi.org/10.3389/fpsyt.2013.00042

Simpson, T.L., Malte, C.A., Dietel, B., Tell, D., Pocock, I., Lyons, R., Varon, D., Raskind, M., Saxon, A.J., 2015. A Pilot Trial of Prazosin, an Alpha-1 Adrenergic Antagonist, for Comorbid Alcohol Dependence and Posttraumatic Stress Disorder. Alcohol. Clin. Exp. Res. 39, 808–817. https://doi.org/10.1111/acer.12703

Simpson, T.L., Saxon, A.J., Stappenbeck, C., Malte, C.A., Lyons, R., Tell, D., Millard, S.P., Raskind, M., 2018. Double-Blind Randomized Clinical Trial of Prazosin for Alcohol Use Disorder. Am. J. Psychiatry 175, 1216–1224. https://doi.org/10.1176/appi.ajp.2018.17080913

Singh, M.E., McGregor, I.S., Mallet, P.E., 2006. Perinatal Exposure to Δ9-Tetrahydrocannabinol Alters Heroin-Induced Place Conditioning and Fos-Immunoreactivity. Neuropsychopharmacology 31, 58–69. https://doi.org/10.1038/sj.npp.1300770

Singh, M.E., McGregor, I.S., Mallet, P.E., 2005. Repeated exposure to Δ9-tetrahydrocannabinol alters heroin-induced locomotor sensitisation and Fos-immunoreactivity. Neuropharmacology 49, 1189–1200. https://doi.org/10.1016/j.neuropharm.2005.07.008

Sinha, R., 2008. Chronic stress, drug use, and vulnerability to addiction. Ann. N. Y. Acad. Sci. 1141, 105–130. https://doi.org/10.1196/annals.1441.030

Sinha, R., 2007. The role of stress in addiction relapse. Curr. Psychiatry Rep. 9, 388–395. https://doi.org/10.1007/s11920-007-0050-6

Sinha, R., 2001. How does stress increase risk of drug abuse and relapse? Psychopharmacology (Berl.) 158, 343–359. https://doi.org/10.1007/s002130100917

Sink, K.S., Davis, M., Walker, D.L., 2013. CGRP antagonist infused into the bed nucleus of the stria terminalis impairs the acquisition and expression of context but not discretely cued fear. Learn. Mem. 20, 730–739. https://doi.org/10.1101/lm.032482.113

Snyder, A.E., Salimando, G.J., Winder, D.G., Silberman, Y., 2019. Chronic Intermittent Ethanol and Acute Stress Similarly Modulate BNST CRF Neuron Activity via Noradrenergic Signaling. Alcohol. Clin. Exp. Res. 43, 1695–1701. https://doi.org/10.1111/acer.14118

Sorkin, E.M., Heel, R.C., 1986. Guanfacine. A review of its pharmacodynamic and pharmacokinetic properties, and therapeutic efficacy in the treatment of hypertension. Drugs 31, 301–336. https://doi.org/10.2165/00003495-198631040-00003

Sparber, S.B., Meyer, D.R., 1978. Clonidine antagonizes naloxone-induced suppression of conditioned behavior and body weight loss in morphine-dependent rats. Pharmacol. Biochem. Behav. 9, 319–325. https://doi.org/10.1016/0091-3057(78)90292-7

Strange, B.C., 2008. Once-daily treatment of ADHD with guanfacine: patient implications. Neuropsychiatr. Dis. Treat. 4, 499–506. https://doi.org/10.2147/ndt.s1711

Stuber, G.D., Wise, R.A., 2016. Lateral hypothalamic circuits for feeding and reward. Nat. Neurosci. 19, 198–205. https://doi.org/10.1038/nn.4220

Szabadi, E., 2013. Functional neuroanatomy of the central noradrenergic system. J. Psychopharmacol. (Oxf.) 27, 659–693. https://doi.org/10.1177/0269881113490326

Takagishi, M., Chiba, T., 1991. Efferent projections of the infralimbic (area 25) region of the medial prefrontal cortex in the rat: an anterograde tracer PHA-L study. Brain Res. 566, 26–39. https://doi.org/10.1016/0006-8993(91)91677-S

Thangada, S., Clinton, H.A., Ali, S., Nunez, J., Gill, J.R., Lawlor, R.F., Logan, S.B., 2021. *Notes from the Field* : Xylazine, a Veterinary Tranquilizer, Identified as an Emerging Novel Substance in Drug Overdose Deaths — Connecticut, 2019–2020. MMWR Morb. Mortal. Wkly. Rep. 70, 1303–1304. https://doi.org/10.15585/mmwr.mm7037a5

Tronel, S., 2004. Noradrenergic Action in Prefrontal Cortex in the Late Stage of Memory Consolidation. Learn. Mem. 11, 453–458. https://doi.org/10.1101/lm.74504

Trzaskowska, E., Kostowski, W., 1983. Further studies on the role of noradrenergic mechanisms in ethanol withdrawal syndrome in rats. Pol. J. Pharmacol. Pharm. 35, 351–358.

Usher, M., 1999. The Role of Locus Coeruleus in the Regulation of Cognitive Performance. Science 283, 549–554. https://doi.org/10.1126/science.283.5401.549

van Dijken, H.H., de Goeij, D.C.E., Sutanto, W., Mos, J., de Kloet, R., Tilders, F.J.H., 1993. Short Inescapable Stress Produces Long-Lasting Changes in the Brain-Pituitary-Adrenal Axis of Adult Male Rats. Neuroendocrinology 58, 57–64. https://doi.org/10.1159/000126512

Van Dijken, H.H., Van Der Heyden, J.A.M., Mos, J., Tilders, F.J.H., 1992. Inescapable footshocks induce progressive and long-lasting behavioural changes in male rats. Physiol. Behav. 51, 787–794. https://doi.org/10.1016/0031-9384(92)90117-K

Vertes, R.P., 2004. Differential projections of the infralimbic and prelimbic cortex in the rat. Synapse 51, 32–58. https://doi.org/10.1002/syn.10279

Vranjkovic, O., Gasser, P.J., Gerndt, C.H., Baker, D.A., Mantsch, J.R., 2014. Stress-Induced Cocaine Seeking Requires a Beta-2 Adrenergic Receptor-Regulated Pathway from the Ventral Bed Nucleus of the Stria Terminalis That Regulates CRF Actions in the Ventral Tegmental Area. J. Neurosci. 34, 12504–12514. https://doi.org/10.1523/JNEUROSCI.0680-14.2014

Vranjkovic, O., Hang, S., Baker, D.A., Mantsch, J.R., 2012. β-Adrenergic Receptor Mediation of Stress-Induced Reinstatement of Extinguished Cocaine-Induced Conditioned Place Preference in Mice: Roles for β_1 and β_2 Adrenergic Receptors. J. Pharmacol. Exp. Ther. 342, 541–551. https://doi.org/10.1124/jpet.112.193615

Vranjkovic, O., Pina, M., Kash, T.L., Winder, D.G., 2017. The bed nucleus of the stria terminalis in drug-associated behavior and affect: A circuit-based perspective. Neuropharmacology 122, 100–106. https://doi.org/10.1016/j.neuropharm.2017.03.028

Walker, B.M., Rasmussen, D.D., Raskind, M.A., Koob, G.F., 2008. α1-noradrenergic receptor antagonism blocks dependence-induced increases in responding for ethanol. Alcohol 42, 91–97. https://doi.org/10.1016/j.alcohol.2007.12.002

Walker, D.L., Davis, M., 2008. Role of the extended amygdala in short-duration versus sustained fear: a tribute to Dr. Lennart Heimer. Brain Struct. Funct. 213, 29–42. https://doi.org/10.1007/s00429-008-0183-3

Walker, J.R., Ahmed, S.H., Gracy, K.N., Koob, G.F., 2000. Microinjections of an opiate receptor antagonist into the bed nucleus of the stria terminalis suppress heroin self-administration in dependent rats. Brain Res. 854, 85–92. https://doi.org/10.1016/S0006-8993(99)02288-X

Wang, M., Ramos, B.P., Paspalas, C.D., Shu, Y., Simen, A., Duque, A., Vijayraghavan, S., Brennan, A., Dudley, A., Nou, E., Mazer, J.A., McCormick, D.A., Arnsten, A.F.T., 2007. α2A-Adrenoceptors Strengthen Working Memory Networks by Inhibiting cAMP-HCN Channel Signaling in Prefrontal Cortex. Cell 129, 397–410. https://doi.org/10.1016/j.cell.2007.03.015

Wayne, Pa., 2010. Intuniv (guanfacine extended-release oral tablets), product information.

Wee, S., Mandyam, C.D., Lekic, D.M., Koob, G.F., 2008. α1-Noradrenergic system role in increased motivation for cocaine intake in rats with prolonged access. Eur. Neuropsychopharmacol. 18, 303–311. https://doi.org/10.1016/j.euroneuro.2007.08.003

Weinshenker, D., Schroeder, J.P., 2007. There and Back Again: A Tale of Norepinephrine and Drug Addiction. Neuropsychopharmacology 32, 1433–1451. https://doi.org/10.1038/sj.npp.1301263

Weitlauf, C., 2004. High-Frequency Stimulation Induces Ethanol-Sensitive Long-Term Potentiation at Glutamatergic Synapses in the Dorsolateral Bed Nucleus of the Stria Terminalis. J. Neurosci. 24, 5741–5747. https://doi.org/10.1523/JNEUROSCI.1181-04.2004

Wenzel, J.M., Cotten, S.W., Dominguez, H.M., Lane, J.E., Shelton, K., Su, Z.-I., Ettenberg, A., 2014. Noradrenergic β-Receptor Antagonism within the Central Nucleus of the Amygdala or Bed Nucleus of the Stria Terminalis Attenuates the Negative/Anxiogenic Effects of Cocaine. J. Neurosci. 34, 3467–3474. https://doi.org/10.1523/JNEUROSCI.3861-13.2014

Wilens, T.E., Bukstein, O., Brams, M., Cutler, A.J., Childress, A., Rugino, T., Lyne, A., Grannis, K., Youcha, S., 2012. A Controlled Trial of Extended-Release Guanfacine and Psychostimulants for Attention-Deficit/Hyperactivity Disorder. J. Am. Acad. Child Adolesc. Psychiatry 51, 74-85.e2. https://doi.org/10.1016/j.jaac.2011.10.012

Wilens, T.E., McBurnett, K., Turnbow, J., Rugino, T., White, C., Youcha, S., 2017. Morning and Evening Effects of Guanfacine Extended Release Adjunctive to Psychostimulants in Pediatric ADHD: Results From a Phase III Multicenter Trial. J. Atten. Disord. 21, 110–119. https://doi.org/10.1177/1087054713500144

William Tank, A., Lee Wong, D., 2014. Peripheral and Central Effects of Circulating Catecholamines, in: Terjung, R. (Ed.), Comprehensive Physiology. John Wiley & Sons, Inc., Hoboken, NJ, USA, pp. 1–15. https://doi.org/10.1002/cphy.c140007

Wills, T.A., Klug, J.R., Silberman, Y., Baucum, A.J., Weitlauf, C., Colbran, R.J., Delpire, E., Winder, D.G., 2012. GluN2B subunit deletion reveals key role in acute and chronic ethanol sensitivity of glutamate synapses in bed nucleus of the stria terminalis. Proc. Natl. Acad. Sci. 109, E278–E287. https://doi.org/10.1073/pnas.1113820109

Wills, T.A., Vaccaro, D., McNamara, G., 1992. The role of life events, family support, and competence in adolescent substance use: A test of vulnerability and protective factors. Am. J. Community Psychol. 20, 349–374. https://doi.org/10.1007/BF00937914

Wills, T.A., Winder, D.G., 2013. Ethanol Effects on N-Methyl-D-Aspartate Receptors in the Bed Nucleus of the Stria Terminalis. Cold Spring Harb. Perspect. Med. 3, a012161–a012161. https://doi.org/10.1101/cshperspect.a012161

Wilson, D.A., Kadohisa, M., Fletcher, M.L., 2006. Cortical contributions to olfaction: Plasticity and perception. Semin. Cell Dev. Biol. 17, 462–470. https://doi.org/10.1016/j.semcdb.2006.04.008

Wu, P.Y., Yang, X., Wright, D.E., Christianson, J.A., 2020. Foot shock stress generates persistent widespread hypersensitivity and anhedonic behavior in an anxiety-prone strain of mice. Pain 161, 211–219. https://doi.org/10.1097/j.pain.0000000000001703

Xing, B., Mack, N.R., Guo, K.-M., Zhang, Y.-X., Ramirez, B., Yang, S.-S., Lin, L., Wang, D.V., Li, Y.-C., Gao, W.-J., 2021. A Subpopulation of Prefrontal Cortical Neurons Is Required for Social Memory. Biol. Psychiatry 89, 521–531. https://doi.org/10.1016/j.biopsych.2020.08.023

Ye, J., Veinante, P., 2019. Cell-type specific parallel circuits in the bed nucleus of the stria terminalis and the central nucleus of the amygdala of the mouse. Brain Struct. Funct. 224, 1067–1095. https://doi.org/10.1007/s00429-018-01825-1

Zhang, Z.-M., Chen, S., Liang, Y.-Z., 2010. Baseline correction using adaptive iteratively reweighted penalized least squares. The Analyst 135, 1138. https://doi.org/10.1039/b922045c

Zhou, P., Resendez, S.L., Rodriguez-Romaguera, J., Jimenez, J.C., Neufeld, S.Q., Giovannucci, A., Friedrich, J., Pnevmatikakis, E.A., Stuber, G.D., Hen, R., Kheirbek, M.A., Sabatini, B.L., Kass, R.E., Paninski, L., 2018. Efficient and accurate extraction of in vivo calcium signals from microendoscopic video data. eLife 7, e28728. https://doi.org/10.7554/eLife.28728

Zislis, G., Desai, T.V., Prado, M., Shah, H.P., Bruijnzeel, A.W., 2007. Effects of the CRF receptor antagonist d-Phe CRF(12–41) and the α2-adrenergic receptor agonist clonidine on stress-induced reinstatement of nicotine-seeking behavior in rats. Neuropharmacology 53, 958–966. https://doi.org/10.1016/j.neuropharm.2007.09.007

Zorrilla, E.P., Logrip, M.L., Koob, G.F., 2014. Corticotropin releasing factor: A key role in the neurobiology of addiction. Front. Neuroendocrinol., CRH/Stress in Honor of Wylie Vale 35, 234–244. https://doi.org/10.1016/j.yfrne.2014.01.001